Hydrological Modelling of River Basin and Strategic Management of Watershed under Different Anthropogenic and Climate Change Scenarios: A Case Study of Genale Catchment, Ethiopia.

A thesis submitted in partial fulfilment of the requirements for the award of degree of

Doctor of Philosophy (Ph.D.)

In

Civil Engineering

By

Tufa Feyissa Negewo

(Roll No.: 186104032)

Supervisor: Prof. **Arup Kumar Sarma**

Department of Civil Engineering, Indian Institute of Technology Guwahati, Guwahati-781039, India, Assam

December 2022

Declaration of Authorship

I hereby declare that the work presented in the thesis entitled "**Hydrological Modelling of River Basin and Strategic Management of Watershed under Different Anthropogenic and Climate Change Scenarios: A Case of Genale Catchment, Ethiopia**" is my work and done under the guidance of Prof. Arup Kumar Sarma of the Department of Civil Engineering, Indian Institute of Technology Guwahati, Assam, India. This work has not been submitted anywhere for the award of any degree. To the best of my knowledge, it contains no materials previously published or written by another person or substantial properties of the material which has been accepted for the award of any other degree or diploma at Indian Institute of Technology Guwahati or any other educational institution, except where due acknowledgment is made in the thesis. Any contribution made to this research by others, with whom I have worked at Indian Institute of Technology Guwahati or elsewhere, explicitly acknowledged in the thesis. I declare that the intellectual content of this thesis represents my own work and words. I have adequately cited and referred to the original work where others' ideas, work, and words have been included. I also declare that I have adhered to all principals of academic honesty and integrity and not misrepresented or fabricated or falsified any idea/ data/ fact/ source in my submission.

Place: IIT Guwahati

December 2022

Tufa Feyissa Negewo
(Roll No. 186104032)
Department of Civil Engineering
Indian Institute of Technology
Guwahati -781039, India, Assam

Prof. A. K. Sarma, PhD
Professor
Department of Civil Engg.
B.P.C.Chair Prof.(2009-18)

Indian Institute of Technology
Guwahati,
Guwahati-781 039

Phones: 0361- 2582409 (O)
0361- 2584409 (R)
9435732225 (m)
Fax: 0361- 2690762
0361- 2582440
E-mail: aks@iitg.ac.in

DEPARTMENT OF CIVIL ENGINEERING

CERTIFICATE

This is to certify that the work contained in this thesis entitled "**Hydrological Modelling of River Basin and Strategic Management of Watershed under Different Anthropogenic and Climate Change Scenarios: A Case of Genale Catchment, Ethiopia**" submitted by Mr. Tufa Feyissa Negewo (Roll No. 186104032) to the Indian Institute of Technology Guwahati, for the award of the degree of Doctor of Philosophy (Ph.D.) in Civil Engineering (Water Resources Engineering and Management) has been carried out under my supervision and guidance. This work (the results contained in this thesis) has not been submitted elsewhere in part or full for the award of any other degree or diploma at any other institutions.

Sincerely yours,

(Arup Kumar Sarma)
Supervisor of Mr. Tufa

Place: IIT Guwahati
December 2022

Department of Civil Engineering
Indian Institute of Technology
Guwahati, Guwahati-781039, India,
Assam

ACKNOWLEDGMENTS

I hereby take the opportunity to express my profound sense of gratitude and reverence to all those who have helped and encouraged me towards the successful completion of the Ph.D. thesis. It has been a great experience working on the broad research topic entitled “Hydrological Modeling of Genale Basin, Ethiopia”. It gives me a complete insight of Hydrological modelling and its application. I would like to thank my supervisor, Prof. Arup.Kr. Sarma, for his immense guidance, constructive recommendations and encouraging words, valuable help, and the opportunity provided to me to complete the Ph.D. thesis under his guidance. My gratitude to the chairperson on my doctoral committee, Prof. Sudip Talukdar for the decisive suggestions and support during the research. His insights for technical aspects are invaluable in the progress of the thesis work. I am profoundly grateful to all my committee members for reviewing an earlier draft of this thesis, and for providing me with their valuable comments.

I am deeply indebted to Ministry of Science and Higher Education, Ethiopia, for the scholarship and financial support during my PhD work. I would like to thank all faculty members of Civil Engineering Department - IIT Guwahati, for guiding and supporting me in the completion of PhD from time to time.

This acknowledgment will not be complete without expressing my love and gratitude for my family without whose concerned and devoted support to the completion of PhD would not have been the way it is today.

I express my sincere thanks to the entire research team of Water Resources Lab at IIT Guwahati for being very warm and welcoming and for creating a constructive work environment and for their support and assistance for my Ph.D work during my stay in India.

Finally, I would like to extend my very great appreciation to my classmates and all my close friends inside and outside India for their unconditional and necessary emotional support throughout my project.

Tufa Feyissa Negewo

Executive Summary of the thesis

It is important to estimate the quantity and quality of water resources in terms of spatial and temporal variability to utilize it sustainably. Change in future climate conditions affects the availability of water resources by modifying the magnitude of precipitation, groundwater recharge, surface runoff, actual evapotranspiration, lateral flow, water yield, the river flows, and provoke water stress in the downstream. Local government authority around the globe is also emphasizing water resources project exploration, design, planning, and management aspect within the river basin.

Erosion of the topsoil is a serious environmental problem worldwide that critically alarms agricultural and upland areas. Most of the wetlands, rivers, and reservoirs are losing their capacity because of sediment deposition into the water body from the upstream of watersheds, as they were not managed.

Land, water and air are the most essential resources blessed by nature to humankind, conserved and maintained with steadfast efforts. This study applies the Modified Universal Soil Loss Equation (MUSLE) to identify critically degraded sub-basins and a non-linear optimization algorithm to determine the optimal area combination of Ecological Management Practices (EMPs) to control sediment and water yield within permissible limits at a minimum cost.

Change in land use land-cover (LULC) is a paramount dynamic of present-day challenging landscape process and is capable of altering the hydrological responses in the catchment and can bring positive changes on water resources system through watershed management. As the land use planners require updated and high-resolution land resources information, understanding land cover change-induced status due to anthropogenic activities is significant.

Soil and Water Assessment Tool (SWAT) model is used to simulate streamflow, sediment load, & identify spatiotemporal variability of the sediment yield and sediment delivery ratio (SDR), point out erosion-prone area, and prioritize sub-basins/hydrologic response units (HRUs) for management.

The model is implemented by utilizing a digital elevation model, land use, soil type, and slope of the Genale basin; a total of isolated 464 HRUs were created, spreading over 25 sub-basins within the drainage area 54,942Km^2. SUFI 2 algorithm of SWAT Calibration & Uncertainty Programs (SWAT_CUP) is used to calibrate (1990 – 2005) and validated (2006 – 2013) streamflow & sediment on monthly scale and found to show satisfactory performance in both the cases.

Hydrological analysis of the Genale watershed has revealed a high potential value of water yield at the sub-basin-8 and sub-basin-12 under all climate change scenarios. The assessment was done for the whole watershed, and the variation ranges from 7mm to 2124mm. The average value of 421.17 mm, 543.5mm, and 358.1mm under baseline condition, RCP4.5, & RCP8.5 respectively. Under bias-corrected of Regional Climate Model (RCM)-CORDEX data, the result shows there is a decline in precipitation and an increase in future temperature under representative concentration pathways-RCP8.5, and likely to reduce the future production of water yield in the basin, which shows RCP8.5 projection is warmer than RCP4.5.

Among the total 25 sub-basins, three sub-basins produced a very high sediment rate (21-31 ton/ha/year), one produced high (16-20 ton/ha/year), one is moderate (11-15 ton/ha/year), three were low (6-10 ton/ha/year), and the rest 16 sub-basins were under very low categories. In the case of SDR, three sub-basins have very high SDR (>0.452), two sub-basins resulted in high SDR (0.326-0.451), which are located at the upland basin. Based on the model results, sub-basins 6, 8,12, 10, and 7 were identified as sediment-prone areas. Further investigation at the HRUs scale is taken up to understand critical erosion areas and minimize the cost of management practice, time & human resources. HRU analysis has revealed the immense scope of minimizing cost by concentrating management measures only in the critical HRUs. For example, Sub-basin-6 has 31 HRUs, of which only seven are assessed to have the high rates of sediment yield and thus prioritized as; HRU-159, HRU-160, HRU-161, HRU-168, HRU-170, and HRU-171, which are located on agricultural and arable lands of steep slopes.

The model is practiced for critical sub-basins in the Genale watershed to assess the effectiveness of five EMPs individually and as a combination in controlling sediment yields and peak flow. A relative assessment revealed that terracing as an individual (61.8%) and EMPs combinations (78.5%) are better in reducing sediment yield at the sub-basin scale. Considering the environmental and economic viewpoint, the total cost of EMPs (for five critical sub-basins), applied to reduce sediment yield, is 46.101 million USD or (1.844 billion Ethiopian birr). EMPs are environment-friendly and cost-effective measures to reduce sediment yield.

The analysis of LULC change patterns for the area under study over 24 years showed that most parts of the green forest, barren land, and range shrubs were changed into agriculture, built up, wetlands, and water body with an increase of agriculture by 60%, built up 68%, pasture 37%, range shrubs 9%, and water body 57% during the study period (1990 to 2013), which increased surface runoff, water yield, and sediment yield in the catchment. Significant changes in hydrological elements were observed at the sub-catchment scale, mainly associated with the uneven spatial distribution of LULC changes compared to the whole watershed.

Based on this estimate, the regional governmental authority can prioritize projects to solve water and land degradation related problems of the community.

Table of Contents **Page No**

Declaration of Authorship.......i
CERTIFICATE.......ii
ACKNOWLEDGMENTS.......iii
Executive Summary of the thesis.......iv
List of Figures.......x
List of Tables.......xii
Abbreviations.......xiv
Chapter 1.......1
Introduction.......1
1.1 General/Background.......1
1.2 Motivation and Scope.......4
1.3 Literature Survey/Review.......5
1.3.1 Hydrologic Modelling.......5
1.4 Short-Summary of Literature Survey/Review.......15
1.5 Technological Research Gap.......16
1.6 Objectives and Research Plan.......17
1.7 Description of the Study Area.......17
1.8 Framework of the thesis/Thesis organizations.......19
Chapter 2.......21
Estimation of Water Yield under Baseline & Future Climate Change Scenarios in Genale Watershed, Ethiopia using SWAT Model.......21
2.0 Introduction.......21
2.1 Materials and Methodology.......24
2.1.1 Study area description.......24
2.1.2 Model description.......27
2.1.3 Future climate change data and bias-correction for regional climate model (RCM)31
2.1.4 Description of SWAT-CUP (SUFI-2).......31
2.1.5 Assessment of Performance criteria for the model.......32
2.2 Results and Discussions.......34

2.2.1 Model parameter sensitivity analysis 34
2.2.2 Calibration/validation 36
2.2.3 Water yield and water balance components prediction in the Genale watershed 39
2.2.4 Impacts of baseline condition and future climate change scenarios on water yield 41
2.3 Conclusions 46
Chapter 3 47
Spatial and Temporal Variability Estimation of Sediment Yield and Sub-basins/Hydrologic Response Units Prioritization on Genale Basin, Ethiopia 47
3.0. Introduction 47
3.1 Materials and Methodology 50
3.1.1 Meteorological Data Analysis, Processing, and Sources 53
3.1.2 Developing Sediment Rating Curve (SRC) 54
3.1.2 Sediment Delivery Ratio (SDR) 56
3.1.2.1 Identification of critical/erosion-prone sub-basins 56
3. 2 Results 57
3.2.1 Uncertainty analysis for streamflow and Sediment 57
3.2.2 Model calibration and validation 59
3.2.3 Spatial and Temporal Variation of Sediment Delivery Ratio (SDR) at Watershed-Scale 61
3.2.4 Comparing SDR values Using SWAT-MUSLE Versus Area-Based (Empirical) Methods 64
3.2.5 Spatial and temporal variability of sediment yield at sub-basins scale 64
3.2.6 Spatial and temporal variability of sediment yield at HRUs level 67
3.3. Discussions 70
3.4. Conclusions 73
Chapter 4 75
Sustainable and Cost-Effective Management of Degraded Sub-Watersheds Using Ecological Management Practices (EMPs) for Genale Basin, Ethiopia 75
4.0 Introduction 75
4.1 Materials and methodology 79
4.1.1 Estimation of Surface runoff ($Q_{Surface}$) 82

4.1.2 Determination of maximum and minimum peak discharge of watershed 83
4.1.3 Selection of Potential Ecological Management Practices (EMPs) 87
4.1.4 Simulation of EMPs 88
4.1.5 Optimization and Cost analysis for different EMPs scenarios 89
4.2 Results and discussions 92
4.1 Uncertainty analysis for streamflow and sediment 93
4.2.1 Model calibration and validation 94
4.2.2 Identification of critical sub-basins in the study area 95
4.2.3 Impacts of EMPs on sediment yield reduction at sub-basins scale 97
4.2.4 Optimal Combination of EMPs areas and Cost-effectiveness analysis 99
4.3 Conclusions 101
Chapter 5 103
Anthropogenic Land Use/Cover Change Detection and Its Impacts on Hydrological Responses of Genale Catchment, Ethiopia 103
5.0 Introduction 103
5.1 Materials and methodology 107
5.1.1 Data sources, preparation, and image processing 108
5.1.2 Land-Use/Land-Cover Supervised Classification System 109
5.2 Results and Discussions 113
5.2.1 Land Use Land Cover Change Analysis 113
5.3 Conclusions 126
Chapter 6 127
Contribution, Findings and Novelty of the Research, Limitations, Conclusions and Recommendations 127
6.1 Contributions 127
6.2 Findings and Novelty of the Research 128
6.3 Limitations 129
6.4 Conclusions and Recommendations 129
7. References 131
8. List of publications 147

List of Figures

Figure 1. 1 SWAT Model summary of input data required 3
Figure 1. 2 Location of Genale River Basin, Ethiopia 18
Figure 1. 3 Flow of thesis organizations 20

Figure 2. 1 Location of the study area and Digital Terrain 25
Figure 2. 2 Mean Monthly Temperature & Rainfall for the selected stations in the study area respectively 26
Figure 2. 3 Steps of the SWAT model for the study area (Methodology) 28
Figure 2. 4 Meteorological and hydrological gauging station distribution sub-basin wise for Genale River 30
Figure 2. 5 Monthly calibration and validation from (1990-2013) for Genale River Basin flow at Genale Halwen 37
Figure 2. 6 Correlation of Monthly observed and simulated flow in calibration/validation process 38
Figure 2. 7 Annual predicted water balance components in the Genale watershed (1990-2013) 40
Figure 2. 8 Spatial distribution of water yield in each sub-basin of the Genale watershed under baseline condition and future climate scenarios 42
Figure 2. 9 Components of water yield distribution in the Genale River Basin based on baseline condition (1990-2013) and future climate change scenarios RCP4.5 & RCP8.5 (2022-2080) 43
Figure 2. 10 Relationship between water yield components and rainfall monthly over the entire watershed under baseline condition (1990-2013) and future climate change (2022-2080) 44

Figure 3. 1 Flow chart of the study area 52
Figure 3. 2 The double mass curve of different selected stations 54
Figure 3. 3 Developed sediment-rating curve for Genale River @ Halwen gauge station 55
Figure 3. 4 Graphical representation of the normalized parameter sensitivity rank for flow and sediment yielded 59
Figure 3. 5 Monthly observed and simulated sediment load plot for the calibration (1990-2005) and validation (2006-2013) 61
Figure 3. 6 Spatial variability of SDR superimposed with sediment yield and gross erosion .. 62
Figure 3. 7 Genale watershed sediment yield superimposed with SDR monthly 63
Figure 3. 8 Spatial variability of sediment yield with precipitation, runoff, and slope in Genale watershed at sub-basin level 65
Figure 3. 9 Spatial plot of sediment yield against a gradient sub-basin wise from 1990-2013 66

Figure 3. 10 Temporal variability of sediment yield with runoff, precipitation, observed and simulated flow monthly 67
Figure 3. 11 Spatial variability of sediment yield for the Genale watershed at the HRU scale for subbasin-6 68
Figure 3. 12 Effects of Land use/cover and gradient on sediment yield at HRUs level for subbasin-6 69
Figure 3. 13 Temporal variation of sediment yield at HRU scale for selected sub-6 from 1990-2013 70

Figure 4. 1 SWAT- land use/cover, soil type, and slope classes of the study area (1990-2013) 79
Figure 4. 2 Work flow chart of the study methodology (steps required to flourish the activities of SWAT model........ 80
Figure 4. 3 Identified critical reaches for EMPs implementation within the Genale watershed 86
Figure 4. 4 Cross-section detail for the selected critical reach at sub-basin outlet to estimate channel carrying capacity 86
Figure 4. 5 Impacts of EMPs scenarios on changing soil erosion class in the study area over 1990-2013........ 96
Figure 4. 6 Sediment yield reduction at treated sub-basins under five scenarios and mean slope over 1990-2013........ 98
Figure 4. 7 The relationship/variation between the cost of EMPs combinations and area availability over critical sub-basins 100

Figure 5. 1 Flow chart and methodology of the study area 108
Figure 5. 2 Image accuracy assessment points (ground truth points) over 1990, 2002, and 2013 114
Figure 5. 3 Land use/cover classification of Genale watershed for the period 1990, 2002, and 2013 116
Figure 5. 4 The dynamics pattern of LULC changes for the years 1990, 2002, and 2013 117
Figure 5. 5 Change in area of LULC between 1990 and 2013 for Genale Basin 118
Figure 5. 6 Average annual hydrological response of for three years LULC map of Genale catchment........ 120
Figure 5. 7 Spatial variability of hydrological responses at the sub-basin level between LULC maps 1990, 2002, and 2013 in Genale watershed 121
Figure 5. 8 Monthly average (1990–2013) hydrological components in the different LULC periods (1990, 2002, and 2013) of the Genale watershed 122
Figure 5. 9 Hydrological responses relative change under a different period of LULC map (1990 – 2013)........ 123

Figure 5. 10 Qualitative pictorial heat map showing correlation matrixes of LULC and hydrological components....125

List of Tables

Table 2. 1 Fitted values and rank of parameters used in the SWAT model calibration/validation on Monthly step (1990-2013)....35
Table 2. 2 Model Performance and acceptable range assessment during calibration and validation period....36
Table 2. 3 The actual statistical properties' index value of Genale catchment for the calibration and validation process....37
Table 2. 4 Performance evaluation of the model for overestimated flood event using peak percent threshold statistics (PPTS)....38
Table 2. 5 Changes in water balance components under baseline and future climate change . 41

Table 3. 1 Soil erosion classes based on the erosion rates (Uniyal et al. 2020)....57
Table 3. 2 SWAT statistical performance index acceptable range (Abbaspour et al.,2011; Moriasi et al.,2007)....60
Table 3. 3 Actual index value for SWAT output during calibration/validation process....60
Table 3. 4 Classification of Genale watershed based on SDR value (Woznicki & Nejadhashemi (2013); Gelagay (2016); Mutua & Klik (2006); Lu et al., (2006))....62
Table 3. 5 Comparisons between various sediment delivery ratio (SDR) estimation methods 64

Table 4. 1 Properties of the Genale watershed for soil erodibility factor (K)....81
Table 4. 2 Summary of model discharge for each prioritized sub-basin....85
Table 4. 3 Model parameters' value used to represent EMPs/BMPs in the SWAT model....88
Table 4. 4 Summary of maximum and minimum sediment yields over the critical sub-basins & EMPs....91
Table 4. 5 Fitted values and rank of parameters used in the SWAT model calibration/validation (1990-2013)....93
Table 4. 6 Actual ranges of performance criteria for SWAT output during calibration and validation action....94
Table 4. 7 Effectiveness of five EMPs on sediment reduction for selected critical sub-basins over 1990-2013....97
Table 4. 8 Optimal area available and total Cost analysis of EMPs for the critical sub-basins (5-Sub-basins)....99

Table 5. 1 Detail sources of satellite imageries used in this study with the output file are in GeoTIFF format.. 109
Table 5. 2 Description of the different LULC classification systems of the Genale watershed 110
Table 5. 3 Rating criteria of kappa statistics efficiency (Rwanga and Ndambuki, 2017) 112
Table 5. 4 How to summarize and quantify accuracy assessment using confusion matrix for the LULC-2013 114
Table 5. 5 Summary of the area and relative changes statistics in LULC over 1990 to 2013 116
Table 5. 6 Correlation matrix for changes in LULC and hydrological responses between 1990 and 2013 124

Abbreviations

HRU – Hydrologic Response Units

IPCC – Intergovernmental Panel on Climate Change

LULC – Land use land cover

CN – Curve Number

FAO – Food and Agricultural Organization

GCM – Global Climate Model

GIS – Global Information System

RS - Remote sensing

SWAT – Soil and Water Assessment Tool

SWAT – CUP - SWAT Calibration Uncertainty Program

MUSLE - Modified Universal Soil Loss Equation

USLE - Universal Soil Loss Equation

SUFI-2 - Sequential Uncertainty Fitting – 2

GLUE - Generalized Likelihood Uncertainty Estimation

ParaSol - Parameter Solution

MCMC - Markov Chain Monte Carlo

PSO - Particle Swarm Optimization

RSR - standard deviation ratio of the observations

R^2 - correlation coefficient

time LHS-OAT - Latin Hypercube Sampling and one-factor-at-a-

NSE – Nash – Satcliff Efficiency

SDR – Sediment Delivery Ratio

PCP – Precipitation

SRC - Developing Sediment Rating Curve

RCM – Regional Climate Model

RCP – Representation Concentration Pathways

SCS – Soil Conservation Services

PPTS - Peak percent threshold statistics

PBIAS - Percent Bias

GHGs - Greenhouse gases

USD – United States Dollar

RC - Runoff coefficients

MATLAB programming

USGS - United States Geological Survey

NPS - Point and non-point sources

DEM - Digital Elevation Model

CORDEX - Coordinated Regional Climate Downscaling Experiment

RMSE – Root mean square error

SRTM – Shuttle Radar Topographic Missions

RNGB - Range shrubs

AGRL - Agriculture

FRST - Forest

URBN - Built up

PAST - Pasture

BARR - Barren land

WATR - Water body

WET - Wetlands

GW_Q - Groundwater contribution to streamflow

TL- Transmission Loss

SW- Soil water content

SURQ - Surface runoff

LAT_Q - Lateral flow

PERC - Percolation

GW_RCHG - Groundwater Recharge

DA_RCHG - Deep aquifer recharge

WYLD - Water Yield;

ET - Evapotranspiration

SYLD - Sediment Yield

QSED - Sediment Load (metric-tons)

SSC - Suspended Sediment Cconcentration/load

CMIP5 – Coupled Model Inter-comparision Project Phase 5

EMPs - Ecological Manaagement Practices

GMS – Gridded Meteorological Stations

95 PPU – 95 Percent Prediction Uncertainity

WDSM - World Digital Soil Map

CMhyd - Climate model data for hydrological modeling

Chapter 1
Introduction

1.1 General/Background

Knowledge of spatiotemporal variability of available water within a basin is crucial for deciding sustainable water resources conservation projects. Water resources planning and management is now becoming essential in Ethiopia and many other countries over the globe (Loi, & Liem 2012). The recent changes in climate have significantly affected the natural phenomenon globally (IPCC 2014). Change in precipitation patterns and variability of temperature would affect the hydrological characteristics of catchments leading to floods, long-term drought, and amplifying extended water scarcity.

Inappropriate land use, uncontrolled runoff, lack of suitable soil conservation measures, unfavorable physiographic characteristics (topography, vegetation cover, soil type, slope), increased population pressure leading to land degradation, urbanization, deforestation, erroneous tillage, and use of chemical fertilizers are the primary causes of soil erosion/degradation and sedimentation problems in a watershed (Adeogun et al. 2018; Markhi et al. 2019).

The land is one of the non-renewable/dynamic resources, and mapping of land-use land-cover (LULC) is fundamental for designing and developing land, water resources with appropriate tools (Manjunatha and Basavarajappa 2020). Erosion of soil is a worldwide significant social and environmental challenges that degrades the productivity of watershed, river flow, reservoir water quality, a discontinuous breeding system of the aquatic ecosystem, and deposition of eroded sediment decreases reservoir storage capacity and increases the risk of flooding. Human induced land-use modifications like agricultural practice, overgrazing, deforestation etc. are responsible, as they accelerate erosion rates above natural level (Adeogun et al. 2018).

Nowadays, the impacts of sedimentation have been a subject of discussion among the researchers due to its negative effect on the available water capacity of hydropower reservoirs all over the world. In most of developing countries, the storage capacity of the reservoir is lost annually because of sedimentation, approximately about 1 percent of the storage capacity of reservoirs every year. The cost of replacing this lost capacity is a very massive amount for restoration options, and it is better to construct new reservoirs instead. With high sediment inflow to the dam site, because of decrease in velocities of water, change in slope, increase in flow depth, sediment deposition starts and it disturbes the river morphology and reduces their ability to trap sediment and eventually leads to silting up of the dams (Adeogun et al. 2018; Briak et al. 2016).

In recent years, applying the Modified Universal Soil Loss Equation (MUSLE) available in the Soil and Water Assessment Tool (SWAT) model for simulating impacts of management practices on sediment yield, water yield, and NPS pollution, has attracted researchers' attention (Arnold et al. 1998, Bieger et al. 2015, Epelde et al. 2015, Ma, D et al. 2020, Winchell et al. 2015). The hydrological model, SWAT is a physically-based, continuous time step model that has been used extensively to assess watershed streamflow generation, sediment yield , response of sustainable agricultural management practices at sub-basin/HRU level and water quality and quantity changes. Erosion of soil and water from cropland into nearby streams can be a significant source of sediment, nutrients, and pesticides in watersheds dominated by agricultural land (Babaei 2019).

Therefore, it is suggestible to envision soil conservation management strategies which mimic effectively the spatial disparity of sediment loss rates, and sustainable sediment management strategies should be in place to arrest soil erosion at the source in general to achieve diverse benefits. This approach is not only sustainable but also provides an effective platform for the management of sediment yield at the watershed level (Duru et al. 2018; Singh et al. 2012). Indeed, soil erosion due to water is a crucial problem in Genale River Basin, Ethiopia and the main causes for this erosion is uncontrolled runoff which occurrs due to rainfall, geological condition, bio-physiographic characteristics (topography, vegetation cover, soil type, slope used etc.), increased population, groundwater exploitation, deforestation, and chemical fertilizers.

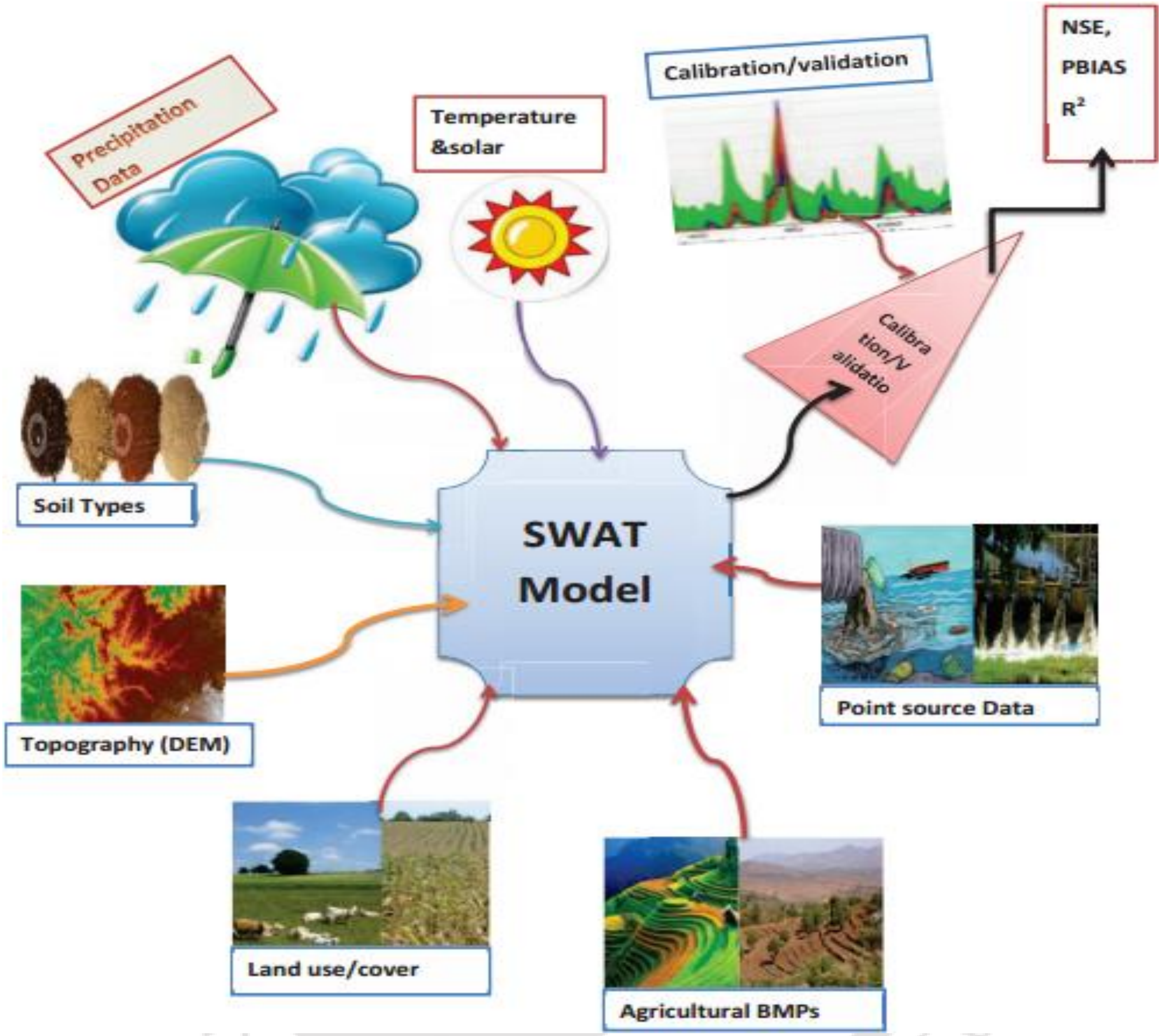

Figure 1. 1 SWAT Model summary of input data required

The SWAT model has the ability to effectively evaluate several Best Management Practices (BMPs) for reducing Non-Point Sources (NPS) pollution (sediment and nutrient load) based on watershed characteristics (size, shape,soil type, LULC etc.) and can use combinations of BMPs and therefore, the model can simulate management processes realistically in dominant agricultural watershed areas (Adeogun et al. 2018).

In this study, the main target is to assess the suitability of Soil and Water Assessment Tool (SWAT) model in simulating the performance of Genale River Basin, Ethiopia for generating streamflow, predicting sediment yield, sediment spatial variability/distribution in sub-basin, identifying areas of vulnerable to soil erosion, prioritizing the sub-basin and propose desirable sustainable cost-effective Ecological Management Practices (EMPs) for soil and water conservation. The study will assist the Governmental Authority in providing relevant decision making on how best to manage sediment loss by using SWAT model incorporated with the Modified Universal Sediment Loss Equation (MUSLE).

1.2 Motivation and Scope

Literature survey has revealed that soil erosion by the action of water is one of the main problems negatively affecting agricultural productivity, which is mainly caused by heavy precipitation, low vegetation cover, topography, urbanization, animal grazing/settlement, deforestation and intensive agriculture practices. Most of the watersheds, ponds, streams, rivers, and reservoirs are getting impaired all over the world because of sediment delivering into the water body due to inadequate management of the upstream watershed.

The scope of sediment aspect of this study is limited to prioritizing sub-basins with more sediment yield and propose the sustainable, cost-effective optimal ecological management practices (EMPs) in the degraded watershed up to HRUs level in order to reduce the erosion impact and thus to provide a relevant decision making tool that will assist the Governmental Authority to decide how best to manage soil erosion/sediment yield.

Indeed, the SWAT model is getting more attention in the research of hydraulic and water resources and has been adopted widely because of its robust algorithms for simulation of the hydrological systems, sediment yield, and NPS pollutant transport, as well as its advantages of having comprehensive database on agricultural management practices.

Furthermore, it is evident from the literature review that there is lack of identifying erosion critical area till HRUs scale in the watershed and cost optimization for management of degradable sub-basins/HRUs. Thus, this research work contributes to fill research gaps existing in the identification of suitable and socio-economically viable management measures to renovate the critically degraded portions in the catchment.

1.3 Literature Survey/Review

This section reports the relevant literature of the studies, which are already conducted across the globe, in relation to hydrological modelling, anthropogenic and climate change impacts on water resources potential, sediment management and implementation of ecological management practices in the affected region of watershed. As this research work output will primally depend on the hydrological modelling, the available literatures on the previous studies on hydrological modelling are reviewed extensively in addition to other relevant topics.

1.3.1 Hydrologic Modelling

Watershed studies have a wide application of hydrological model software that uses various watershed physiographic characteristics input information (soil properties, land use/cover, slope types, weather data). The availability, resolution, and choice of input data has significant impact on the output of the model and spatial heterogeneity on hydrologic parameters is essential to identify potential water yield in sub-basins and suggesting government and other agencies of water sectors to address community problems related to water and prioritize accordingly. Hydrological model, Soil and Water Assessment Tool (SWAT), is a physically based continuous time step model that has been used extensively to assess watershed stream flow generation, sediment yield estimation, responding to sustainable agricultural management practices at sub-basin/HRU level and evaluating water quality and quantity changes. Erosion of a soil and water runoff from cropland into nearby streams can be a major source of sediment, nutrients, and pesticides in watersheds dominated by agricultural land (Duru et al., 2018; Mtibaa et al, 2018; Hallouz et al, 2018). Therefore, sustainable strategies for managing sediment at source effectively to reduce the spatial disparity of sediment loss rates should be in place to minimize adverse impacts at downstream such as siltation potential of the hydropower dams and to optimally improve the generating capacities of hydropower plant, making sufficient water to drive the turbines for effective hydropower generation throughout the year. This approach is not only sustainable but also provides the effective platform for management of sediment yield at watershed level (Adeogun et al, 2020; Abbaspour et al; Hussain et al, 2019).

The concept of Ecological Management Practices (EMPs) is an Eco-friendly sustainable management practices that are used for maintaining and enhancing land uses in a natural way. The combination of different structural and non-structural vegetative measures like tree/grass plantation, detention and retention ponds, contour terracing, buffer zone with vegetation strip, sediment trap, mulching, rainwater harvesting systems, vegetated water passageway, sediment trap, permeable surface cover with pebble and stone, etc., which can be used for reducing ecological disturbances by controlling the sediment yield and peak runoff volume from a degraded watershed/land surface (Patowary et al, 2019;Adeogun et al, 2020). The accumulation of greenhouse gases (GHG) in the environment is a major issue for nowadays global climate changes and these climate variabilities due to increase in CO2 concentration have a remarkable influence on natural water resources, agricultural product and evaporation specially in developing countries. According to the Intergovernmental Panel on Climate Change (IPCC) report, increase in temperature and variability of precipitation will behave significantly to water-related risks such as flood, watershed degradation, abruptly decline in water level of River Basins and drought. As per the IPCC report, the global temperature may increase by 1^0 C to 5^0 C by the end of the century (Zhou et al, 2017; Nilawar and Waikar, 2019).

The IPCC defines a series of Representative concentration pathway (RCP) scenarios (2.6, 4.5, 6 and 8.5) for future climate projection based on Coupled Model Inter comparison Project (CMIP5).These pathways are identified by their approximate total (accumulated) radiative forcing at 2100 relative to 1750 and incorporate one alleviation scenarios priming a low driving level (low emission scenarios) (RCP2.6), two stabilization (medium) scenarios (RCP4.5 and RCP6), and high emissions scenarios (GHG) without stabilization (RCP8.5). These scenarios are evolved based on the driving force such as the growth of population, GHG, industrialization/urbanization, socio-economic development and increase in CO2 concentration (Zhou et al, 2017; Nilawar and Waikar, 2019).

Indeed, soil erosion due to water and water quality degradation is a crucial problem in Genale River Basin, Ethiopia and the main causes for this erosion is uncontrolled runoff which has occurred due to rainfall, geological condition, bio-physiographic characteristics (topography, vegetation cover, soil type, slope used etc.) increased population, urbanization (industrialization), ground water exploitation, deforestation and chemical fertilizers.

Therefore, the watershed modeling plays a vital role in the early management planning and local resources development to propose the Ecological management practices (EMPs) scenarios to reduce the erosion impact (Hallouz et al, 2018; Yesuf et al, 2015; Babaei et al, 2019). Sources of pollution are majorly classified into two categories as point and non-point sources. Point sources are contaminants that are generated from single identifiable sources of pollution, such as discharge from waste-water treatment plants (Yesuf et al, 2015; Babaei et al, 2019), whereas non-point sources refer to contaminants that do not have a specific point of sources and originates from agricultural activities such as sediment yields due to tillage, excess fertilizers, herbicides, and insecticides that comes from agricultural land and residential watershed areas to water bodies through runoff. This requires specific Ecological Management Practices (EMPs) implementation within watersheds as an effective and sustainable techniques to safe watershed from impairment of soil erosion and water quality (Babaei et al, 2019). EMPs includes all ecologically sound Best Management Practices (BMPs), which are effective and efficient ways not only to improve agricultural productivity, but also to limit soil erosion impacts and to reduce nutrients, pesticides, animal wastes and other pollutant loads from their source area at the reception of water bodies. However, to minimize the intensity of soil erosion rate , it is important first to determine the areas of sources for sediment yield where soil conservation practice works have to focus on. However, the approach of actual field monitoring is time consuming and cost intensive, and therefore, distributed watershed models are often used for evaluating the effectiveness of various best management practices (BMPs) (Briak et al, 2019) and to prioritize planning. Soil erosion by the action of water is one of the main factors negatively affecting agricultural productivity, which is mainly caused by heavy precipitation, low vegetation cover, topography, urbanization, animal grazing/settlement, deforestation, intensive agriculture practices etc. (Pimentel and Burgess, 2013). This erosion process has a number of onsite and offsite negative consequences that impair the socioeconomic, environmental, social and sustainable development of many developing countries (Ananda and Herath, 2003). Onsite problems includes reduction in soil fertility, crop productivity, and nutrients while Offsite negative impact includes reduction in reservoir storage capacity, increased flood risk, water quality degradation because of the discharge of sediments and other pollutant loads (Mtibaa et al, 2018; Moss,2007). Best management practices (BMPs) have been widely practiced to limit soil erosion problems, control non-point source (NPS) pollution and improve agricultural productivity and it can be structural, such as contour terracing, check dam, guide bank, hill ponds and grassed waterways; or non-structural/agronomic, such as no-till farming systems, afforestation, residue management, crop rotation, and strip cropping (Mtibaa et al, 2018; Hallouz et al, 2018). The environmental effectiveness of BMPs in terms of sediment yield/loss or non-point sources of pollution load reduction can be assessed by different methods of watershed models (Xie et al, 2015), such as Agricultural Policy Environmental ex-tender (APEX) (Gassman et al, 2009), Hydrological Simulation Program FORTRAN (HSPF) (Al-Abed & Al-Sharif, 2008), Soil and Water Assessment Tool (SWAT) (Arnold et al, 1998). Among from these models, SWAT has been selected and adopted widely for simulation of hydrological system, because of its robust algorithms in figuring out sediment transport, and NPS pollutant transport, as well as its comprehensive database on agricultural management practices (Arabi 2008). SWAT has higher model efficiency, acceptable uncertainty and consider the watershed properties as the major sources of soil erosion and sediment yield to the reservoir compared with other models (Dutta and Sen, 2018; Arnold and Fohrer, 2005).

Proper sediment management and control strategies are required at the watersheds level, located at upstream of the reservoirs to reduce the erosion processes and other activities that may lead to sediment yield production. For this, the GIS interfaced applicable watershed model SWAT is the platform frequently used (Adeogun et al, 2018).

Researchers have used hydrological model SWAT for modelling flow and sediment yield processes in diverse watersheds, however, limited studies are found on determining optimal combination of management measures for managing land and water. Some of such studies are presented below.

Zalaki et al, 2017 performed the simulation of runoff and sediment yield by using SWAT2005, and calibrated/validated the model based on Monthly step basis data for flow and Yearly step data for sediment flow with SWAT-CUP(SUFI-2) from 1994 to 2006 for flow calibration and validation, from 1995 to 2006 for sediment yield calibration /validation with model performance of R2=0.75, NSE=0.7 and R2=0.98, NSE=0.6 for flow and sediment respectively.

Djebou et al, 2018 Assessed sediment inflow to the reservoir watershed for the simulation of flow data by using SWAT model and calibrated at three (3) gauging stations G3 and G2 at upstream of watershed and G1 at Reservoir outlet under un-dammed condition. Hence, the out flowing water and the rate of sediment loss were addressed at the catchment level. The model was developed with multi-site calibrated and validated by targeting the outflow of two major tributaries located at the upstream side of the reservoir. Evaluation of their SWAT model performance yielded satisfactory values of efficiency criteria ranging as $0.69 < NSE < 0.75$, $0.66 < R2 < 0.81$ and $0.85 < D < 0.93$ during the calibration and validation. Monthly flow data from 2008 to 2011 were used for calibration and data from 2012 to 2016 were used for validation. From the visual perspective, the spatial patterns of sediment yields/losses seem to reveal variation among the upstream, the midstream and the downstream sub-basins. The spatial distribution of the soil erosion with in watershed at sub-basin level is identified and classified in to 5 categories ranged from 0 to 4 t/ha/year. The sub-basins with higher soil loss rates (3.0-4.0 and > 4.0 t/ha/year) are remarkably represented at the downstream of the watershed and need special soil conservation practices, while the midstream sub-basins are particularly characterized by a low soil loss rates and the upstream sub-basins seems to show a moderate configuration of sediment loss rate.

Hallouz et al, 2018, evaluated the performance of SWAT2009 model, SWAT-CUP(SUFI-2) in the determination of discharge and sediment transport with in the basin and calibrated/validated the model using Monthly data of discharge from 2004-2007 and obtained P-factor=0.55, D-factor=0.88 and NSE=0.82, for calibration and for validation from 2008-2009, P-factor=0.64, D-factor=0.78 and NSE=0.77 . Also, they have predicted the sediment yield yearly over the period of 2011 to 2020 and obtained the year that displays an important value of maximum degradation to be in 2008 which is equal to 92.21 t/ha and the evolution of the average total annual sediment loading from the watershed was estimated as 54.24 t/ha/year.

Using OPTEMP-LS model, the Linear Model Solver Tool in Microsoft Excel application, Patowary et al, 2019, showed that the implementation of the considered EMPs makes possible to manage the peak runoff and sediment yield from the watershed within the permissible limits satisfying all given constraints. Due to the consideration of soil loss from steep hill cuts, the EMP cost per unit settlement area is found to be higher for the hilly portion than that in the plain area of the watershed; with consideration of owners' choice constraint, the EMP cost per unit settlement area in the hilly portion becomes 4.77 times the unit cost for the plain portion of the watershed and it is 1.55 times without consideration of owners' choice constraint.

Sarma et al, in 2015 applied the linear programming optimization model to a hilly watershed of a rapidly developing city for determining the best combination of EMP that control sediment and peak discharge within permissible limits at a minimum cost. The best combination of three possible ecological management practices, namely, grass, garden, and detention pond were then established. In this study, owner's choice plays an important role in deciding the most optimal EMP combination and the total cost increases with consideration of the owner's choice constraint.

Soil and Water Assessment Tool (SWAT, version 2012) model integrated with Geographic Information System (GIS, version10.1) was used to simulate the discharge flow and sediment concentration of the study area catchment situated in north of Morocco for the period from 1971 to 1993 (Briak et al, 2016). Model calibration and validation for streamflow and sediment concentration were performed for monthly time periods using Sequential Uncertainty Fitting-2 (SUFI−2, version2) within SWAT-CUP using 16 parameters and the calibration outputs for monthly simulation was presented for the period from 1976 to 1984. From the analysis, the effective hydraulic conductivity in main channel alluvium (CH−K2), USLE support practice factor (USLE−P) and mannings roughness parameter value for the main channel (CH−N2) were found to be the most sensitive parameters during different iterations with different number of simulation but with the same inputs. The total estimated soil erosion/degradation in spatial distribution within watershed at sub-basin level is identified and classified in to 5 categories ranging from 20 to 120 t/ha/yr with average rate of around 55 t/ha/yr.

Duru et al, 2018, exploredthe applicability of SWAT2012 Model and SWAT-CUP (SUFI−2) in modeling stream flow and sediment yield/loss by using Monthly basis data from 1989-1996. The spatial distribution of the soil erosion within watershed at sub-basin level was identified and classified in to 7 categories ranged from 0 to 41.6 t/ha and indicates that significant portions of urbanized and highly agricultural cultivated areas near the stream/reach are more vulnerable to soil erosion by existing condition in the studied basin and suggested SWAT model can be used as a tool in decision-making in water resources planning and management practices in a basin with hydrologically and meteorologically similar/homogeneous characteristics.

Zhou et al, 2017 applied calibrated and validated SWAT model to evaluate changes in runoff and sediment yield under two future climate change scenarios, i.e.,stabilization projection (RCP4.5) and a projection without stabilization (RCP8.5). They combined a calibrated hydrological model and a runoff-sediment yield rating curve for the purpose. The results from model shows that for climate change projections of 2021-2050 both annual surface runoff and sediment yield would increase compared with the baseline period (1981-2010). Sediment yield were increase by 237 percent under RCP4.5 and 133 percent for RCP8.5 and the annual runoff in the headwaters would increase by 88 percent for RCP4.5 and by 48 percent for RCP8.5 which is primarily caused by precipitation changes and the increase seemed to be prevalent in summer and autumn during warm climate.

The SWAT model coupled with the SUFI-2 algorithm was used by Nilawar et al, 2019 for the calibration, validation, sensitivity and uncertainty analysis. Two future climate projections RCP 4.5 and RCP 8.5 are selected for the period from 2009 t0 2099. The tmax projected for future period ranges from 0.390.68 C and 0.521.32 C, under RCP 4.5 and RCP 8.5 respectively. Similarly, average projected precipitation (PCP) for future periods are increased by 1.286.90 percent (11.37mm to 61.59 mm) and 4.9010.61 percent (59.68mmto 161.91mm), under RCP 4.5 and RCP 8.5 respectively. Monthly variations indicate that increase in flow rate and sediment concentration is more predominant in the wet season June, July, August and September.

Bajracharya et al, 2018 usedSoil and Water Assessment Tool (SWAT) for a future projection of changes in the hydrological regime of the basin based on Representative Concentration Pathways Scenarios (RCP 4.5 and RCP 8.5) of ensemble downscaled General Circulation Model (GCM) outputs. The hydrological regime of the region is vulnerable to climatic variations, especially precipitation and temperature. It is predicted to increase the annual temperature of over 4 C, and Compared to the baseline period (1990), the average annual precipitation in the basin will increase by about 20 percent, during the 2090 under RCP 4.5, about 26 percent under RCP 8.5 scenarios by the end of the 21st century. Water yield would increase during the 2090s, by 41 percent and 51 percent under RCP 4.5 and RCP 8.5, respectively at the outlet of the basin.

Applying SWAT model on a daily time step, Hussain et al, 2019 simulated stream flow and soil erosion for specific storm events, and four small sub-catchments, i.e., sub-catchments- 25 31 were characterized by incised/created gullies while sub-catchments-27 and 32 consist of terraced land-use systems. The performance of the SWAT model was satisfactory with R2 values _ 0.674 and NSE_ 0.53 for both surface runoff and sediment yield during the calibration (2009-2010) and validation year (2011). It was estimated that in 2009, the gully sub-catchments (25 and 31) produced annual sediment yield that ranged from 13.19 t/ha to 20.60 t/ha in response to rainfall events that were between 230.76-399.95 mm and surface runoff amounts that ranged from 49.34 mm to 95.59 mm. In comparison, the terraced sub-catchments (27 and 32) produced 1.90-3.77 t/ha sediment yield for the same rainfall levels and surface runoff that was measured from 10.17 mm to 54.0 mm. It was found that the sediment yield generated by the terraced sub-catchments was 4-5 times lower than the sediment yields that were exported from the gully sub-catchments. Thus, there is a huge potential for terraces to reduce the soil erosion in the catchment.

O'Donnell et al, 2008 used the Soil and Water Assessment Tool (SWAT), a deterministic hydrologic model, to predict the reduction of sediment erosion and transport over a 30-years period due to grass and woody-riparian establishment on cropland in the La Moine River Basin, U.S.A. Mean annual sediment reduction due to BMPs was predicted to be 3.6 percent at the downstream watershed gaging station. Identification of sediment sources in this watershed based on predicted hill-slope erosion indicated a cost-effective strategy to reduce sediment load.

Babaei et al, 2019 established applicability of SWAT model in a river basin based on calibrated/validated value and achieved good performance criteria by using SWAT Model and SWAT-CUP (SUFI-2). The model washen used for the identification of critical sources area based on the amount of non-point source pollution produced in each sub-basin. After identifying, the CSAs, the BMPs were implemented in the model to evaluate their applicability in reducing pollution loads. Then by using several BMPs, including source elimination, filter strips (5m and 10m), livestock grazing management, and river channel management were implemented to evaluate their applicability in reducing the entry of pollutants to the river. The highest reduction in pollution load was achieved by implementing filter strips in the agricultural areas. Under this BMP, the highest reduction in pollutants was observed for nitrate (58.92 percent).

Sood et al, 2010 developed five management scenarios for implementation, one at a time, to measure its effectiveness in reducing the non-point source nutrient loading in the watershed using a hydrological model, calibrated and validated by SWAT2000, SWAT-CUP(SUFI-2). Among the Best Management Practices (BMPs), planting winter cover crops on the agriculture land was the most effective method in reducing the nutrient loads. The second most effective method was to provide grassland riparian zones. When all of the agriculture land in the watershed were converted to forest, it led to significant reduction in nutrient loading, i.e. the TN loading reduced by approximately 46 percent and the TP loading reduced by approximately 54 percent.

Notably, the total sediment yield in the watershed was estimated by Adeogun et al, 2018 as 31,757 t/ha while average annual sediment yield was estimated at 35.29 t/ha/year and Average annual sediment concentration in the river reaches within the basin was predicted as 11903.7 mg/l(ppm). Erosion prone area of the watershed showed that 11 sub-basins are in low erosion prone category, 23 sub-basins in moderate zone, 12 sub-basins in severe erosion category while 8 sub-basins are in the extreme erosion category [4]. The results of sediment yield after implementation of BMPs-filter strips and stone bundsin the watershed showed both methods are capable of reducing the sediment production within the watershed. Application of filter strip on the erosion prone area showed that sediment yield and concentration could be reduced up to 37 percent and 34 percent respectively. On the other hand, application of stone bund can reduce sediment yield and concentrations in the watershed up to 89 percent and 84 percent respectively as compared with the existing scenario.

Briak et al, 2019 in their research finding, different soil conservation practice scenarios were simulated and tested with respect to sediment yield/loss using SWAT model. Furthermore, the simulation of effective best management practices (BMPs) by the SWAT model provides us to have an idea in reducing sediment yield in the watershed. Among the applied BMP based on the existing scenarios/basic conditions are parallel terracing, contouring and strip-cropping. From this, terracing is applied on the agricultural land effectively to reduce the sediment yield/losses to manage the soil erosion intensity particularly at steep slopes with significant improvement of 28 percent sediment yield reduction at the outlet of watershed compared to existing scenario.

Mtibaa et al, 2018 in their paper, analysed the suitability of SWAT model for benefit-cost analysis (CBA) to investigate the effectiveness of different BMPs in reducing sediment yield. They found that sediment yield dependends mainly on the slope angle of the target location area; e.g. strip cropping and contour ridges practices were more effective when implemented in gentle slope areas than in steep slope location. At the level of watershed, contour ridges were considered to be the most effective BMPs in terms of sediment yield/loss reduction. Implementing contour ridge alone reduced sediment yield by 59.09 percent. Combinations of BMPs scenario were found to be more effective and efficient than individual BMPs and contour ridges, strip cropping, 5m-buffer strip and no-till farming with residue management practice is the highest efficiency in terms of sediment yield reduction by 61.84 percent.

Himanshu et al, 2019,on the basis of simulated results found that the annual average sediment yield from the watershed at the outlet is 12.2 ton/ha/year and adaptation of agricultural field cultivator tillage practice and conservation practices with contour farming and filter strips, could reduce the sediment yield and nutrient losses in the critical sub-watersheds of the study area. The application of BMPs, like Contour farming reduced the sediment yield by 9.3 to 38.3 percent, while filter strips reduced sediment yield from 25.4 to 43.3 percent.

Ozcan et al, 2017, using SWAT, analyzed application of 11 scenarios in the watershed area, where 1-9 scenarios are single BMPs and the Scenarios 10 and 11 are the combination of scenarios. Therefore, combination of BMPs application is about two times effective than the single BMPs applications, with 11 percent reduction of average annual sediment yield.

, After successful calibration/ validation, SWAT model is used in watershed for predicting SDR at the sub-watershed scale to minimize sediment yield at the respective sub basin area by Dutta et al, 2018. The total sediment yields from the whole watershed is classified into three classes (_ 5, 520 and _ 20 t/ha/year) to prioritize the sub-basin. The highest value of yearly sediment yield at the sub-watershed level is 102.20 t/ha/year, which is from the agricultural lands.

1.4 Short-Summary of Literature Survey/Review

It is important to estimate the quantity and quality of water resources in terms of spatial and temporal variability to utilize sustainably. Change in future climate conditions affects the availability of water resources by modifying the magnitude of precipitation, groundwater recharge, surface runoff, actual evapotranspiration, lateral flow, water yield, the river flows, and provoke water stress in the downstream. Local government authority around the globe is also emphasizing water resources project exploration, design, planning, and management aspect within the river basin. To assist such decision, knowledge and understanding of water yield and water balance at basin and sub-basin level are extremely important.

Erosion of the topsoil is a serious environmental problem worldwide that critically alarms agricultural and upland areas. Most wetlands, rivers, and reservoirs are losing their capacity because of sediment deposition into the water body from the upstream of watersheds, as they were not managed.

Change in land use land-cover (LULC) is a paramount dynamic present-day challenging landscape process capable of altering the hydrological responses in the catchment. As the land use planners require updated and high-resolution land resources information, understanding land cover change-induced status due to anthropogenic activities is significant.

Based on the different researchers SWAT model has been implemented/adopted widely because of its robust algorithms for simulation of the hydrological model system, sediment transport, and NPS pollutant transport, as well as its comprehensive database on agricultural management practices.

The calibrated and validated SWAT model was applied to evaluate changes in runoff and sediment yield under two future climate change scenarios as a stabilization projection (RCP4.5) and a projection without stabilization (RCP8.5). A combined approach of a calibrated hydrological model and a runoff-sediment yield-rating curve are used. The results from model shows that both climate change projections for 2021-2050 would increase annual surface runoff and sediment yield compared with the baseline period (Zhou et al. 2017; Nilawar & Waikar, 2019).

Ecological Management Practices (EMPs) assign nature-based solutions described as "eco-friendly sustainable management practices used for preserving and enhancing land uses naturally" and limits sediment yield and peak surface runoff to its natural condition in a sustainable and economically viable manner. Selection of an optimal combination of EMPs need to be done with due consideration to constraints like space availability, financial constraint and land ownership (Singh et al. 2020, Sarma et al. 2015, Dolowitz et al. 2018).

The linear programming optimization model was applied to a hilly watershed of a rapidly developing city for determining the best combination of EMP that control sediment and peak discharge within permissible limits at a minimum cost (Sarma et al. 2015; Patowary et al. 2019).

1.5 Technological Research Gap

The following points are worth noting from the literature Survey as a technological/research gaps;

- ✓ The SWAT model though is capable enough, still needs site specific performance evaluation in hydrological modeling system in hydraulic and water resources engineering.
- ✓ Suggestion and direction have not been given by different Authors on sustainable agricultural management for Governmental Authority to facilitate relevant decision making on what combinations and what extent of EMPs application are the robust and most environment friendly to reduce soil erosion/ sediment yield.

- ✓ The cost-effectiveness of EMPs were not considered for large basin by different researchers, it is needed.
- ✓ Limited work has been reported in prioritizing the degraded sub-basins of a watershed and climate change impacts analysis on hydrological response.
- ✓ So far, there is no reported literature about identification of the sediment yield prone sub-basin using SDR

1.6 Objectives and Research Plan

The overall objective of the research is to analyze the applicability, advantages and limitations of SWAT model integrated with Geographical Information System (GIS) and SWAT-CUP (SUFI-2) in estimating water and sediment yield from Genale River basin in Ethiopia and their spatio-temporal variability in the present and future climate impacted scenarios to identify degraded areas prone to sediment generation and hence to suggest ecologically sustainable optimal management measures.

The specific objectives to be conducted in the present research study are as follows:

- ✓ Estimation of water yield under baseline & future climate change scenarios in Genale watershed, Ethiopia using SWAT model
- ✓ Spatial and Temporal Variability Evaluation of Sediment Yield and Sub-basins/HRUs Prioritization on Genale Basin, Ethiopia
- ✓ Land Use/Cover Change Detection and Its Impacts on Hydrological Responses of Genale Catchment, Ethiopia
- ✓ Sustainable and Cost-Effective Management of Degraded Sub-Watersheds Using Ecological Management Practices (EMPs) for Genale Basin, Ethiopia

1.7 Description of the Study Area

The Genale watershed (54,942 Km^2) is located in Ethiopia, covering Oromia, South Nation Nationalities and People, and the Somali region. The Genale River joins the Dawa River at the Dolo Ado border, which is geographically located between 4° 08' to 7° 02' North and 39° 00' to

42° 00' East. The basin gets its first maximum rainfall during spring (March to May) and secondary maximum rainfall during autumn (September to November) from the Indian Ocean easterlies, but the basin receives little rainfall in summer compared to the spring season. In the Genale watershed, a total of isolated 464 HRUs were created, spreading over 25 sub-basins. The mean annual precipitation experienced in the area is 810 mm, and the distribution of precipitation in a watershed is from 300 to 1303 mm within a year. The Monthly temperature ranges from 14.5 ℃ to 24.6 ℃, with an average of 19.5 ℃. The maximum and minimum elevation of the area is 4280 and 176 m, respectively.

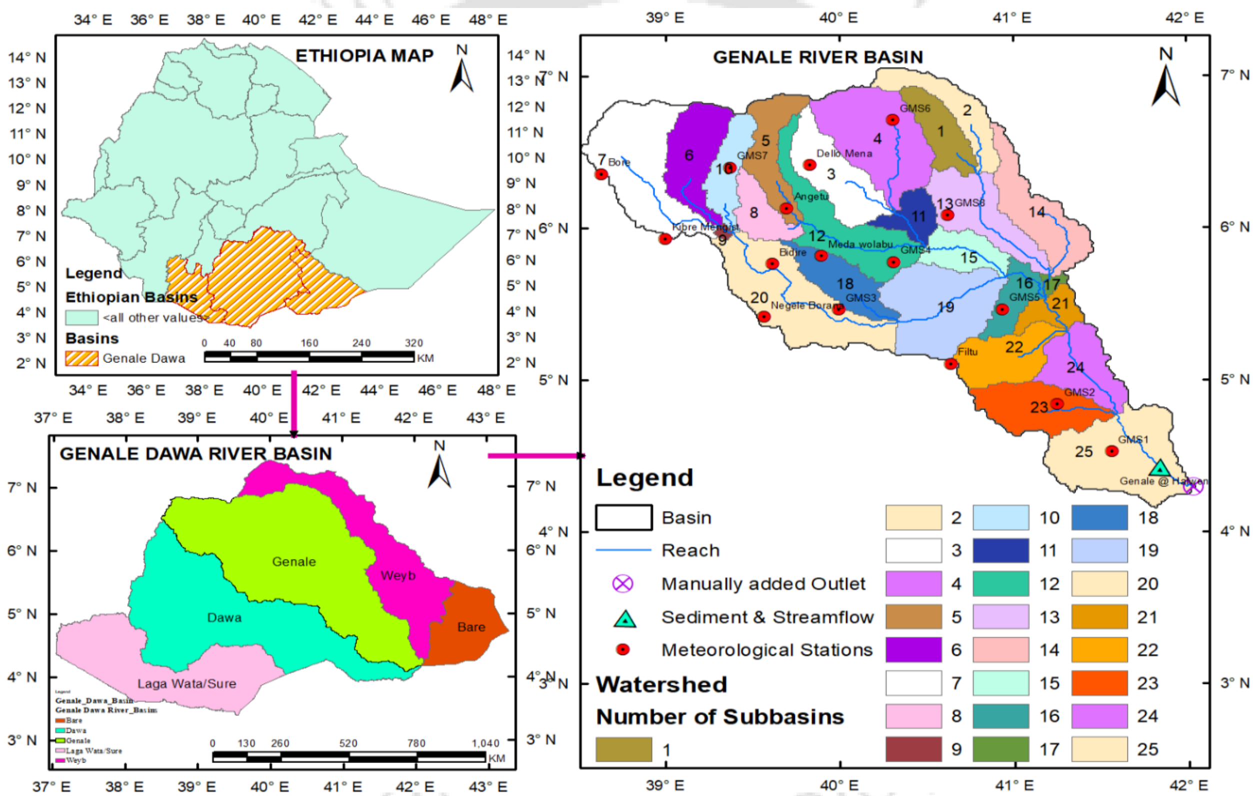

Figure 1. 2 Location of Genale River Basin, Ethiopia

Figure 1.2 shows the study area's location in Ethiopia, Africa, and the Genale watershed delineated using Arc SWAT embedded in ArcGIS. The Genale catchment contains 25 sub-basins in the delineated watershed, labeled as 1, 2, 3…up to 25. The study area contained the marked monitoring streamflow, meteorological, and sediment concentration gauging stations and GMS1-8- Global Metrological Stations 1, 2, 3 …8.

1.8 Framework of the thesis/Thesis organizations

Based on the case study workflow, the thesis report is divided into five chapters. Figure 1.3 illustrates a brief plan. The overview of the research questions, objectives, and hypotheses addressed in the individual chapters, is depicted in Figure 1.3, which presents the summary of each chapter in the thesis.

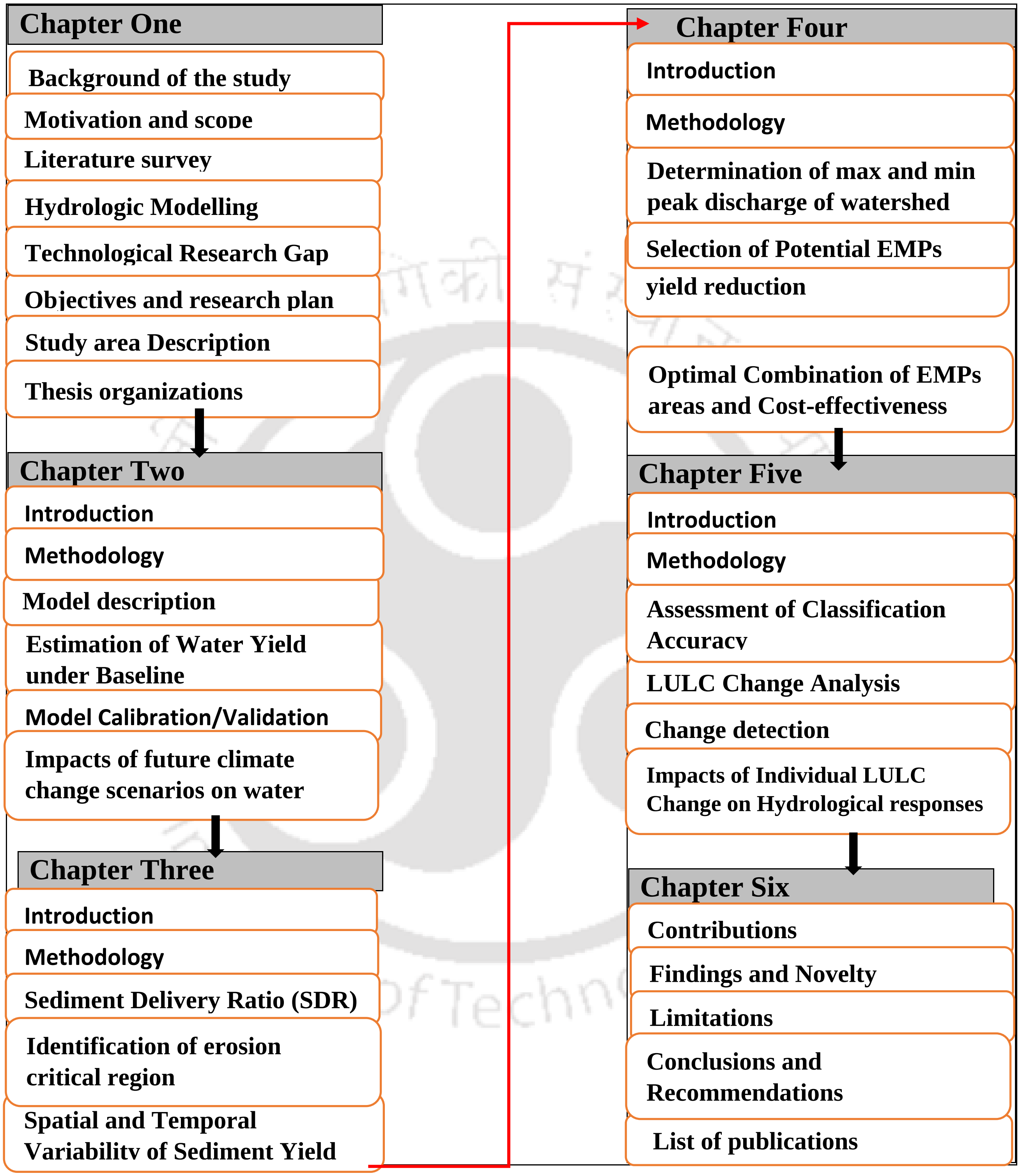

Figure 1. 3 Flow of thesis organizations

Chapter 2

Estimation of Water Yield under Baseline & Future Climate Change Scenarios in Genale Watershed, Ethiopia using SWAT Model

2.0 Introduction

Knowledge of spatiotemporal variability of available water within a basin is crucial for deciding sustainable water resources conservation projects. Water resources planning and management is now becoming essential in Ethiopia and many other countries over the globe (Loi, & Liem 2012). The recent changes in climate have significantly affected the natural phenomenon globally (IPCC 2014). Change in precipitation patterns and variability of temperature would affect the hydrological characteristics of catchments leading to floods, long-term drought, and amplifying extended water scarcity. Water is the most fundamental for living among the resources on the earth and sometimes getting scarce. Hydrological diagnostic studies in river basins are vital because they help to understand the system that controls water movement and impacts both quantity and quality of water. In this context, the quantitative understanding of hydrological framework (precipitation and surface runoff) and its spatial and temporal variability in the watershed is essential for planning and management of water resources (Arai et al. 2012; Kumar et al. 2015). For the comprehensive sustainable development of any country, improvement and utilization of its water resources in a planned manner is essential. The increase in water demand due to population growth, productive activities, environmental deterioration of water bodies, and scanty rainfall have contributed to the extent of water scarcity and food insecurity in several regions of the planet (Tram 2014; Wei et al. 2018; Kirby et al. 2007).

The effect of land use/cover (LULC) and climatic change on stream hydrology and surface water availability is studied by the application of temporally and spatially referenced hydrologic models. Nowadays, hydrological models have been widely used by modelers to assess the impact of climate variability on hydrological regimes. Indeed, the models are used to quantify different hydrological parameters such as streamflow, lateral flow, runoff, actual evapotranspiration, and water yield (Touseef et al. 2020). Estimation of these hydrological parameters by choosing appropriate hydrological models is essential for assessing the present water scenario and possible future impacts of climate change on it (Thrasher & Nemani 2015; Dibaba et al. 2020). SWAT model was selected to simulate hydrological components under current and future climate scenarios at a basin and sub-basin level, as it has a broader application in the areas of water resources. The reasons are its convenience to evaluate the present and future water quantity and quality, sediment yield up to hydrologic response units (HRUs) level with flexibility and capability (Arnold et al. 1999; Muleta et al. 2007). In the SWAT, a watershed is divided into different sub-watersheds, which are then further subdivided into HRUs that are composed of similar LULC, slope, and soil types. Different hydrological models use precipitation and temperature in the form of input, and after accounting for intermediate processes like actual evapotranspiration, groundwater, and runoff within the watershed, they give water yield in the way of output (Healy et al. 2007; Pathak et al. 2019). Climate change impacted precipitation, and temperature patterns could have a significant impact on the hydrological systems/components, which in turn affects water yield, runoff, and streamflow characteristics. These rapid alterations could be seen as the results of socio-economic development, deforestation, population growth, urbanization/ industrialization, and land use/cover changes, which are contributing to global warming (emissions of greenhouse gases (GHGs)) (IPCC 2014; Touseef et al. 2020; Thrasher & Nemani 2015).

Climate change and anthropogenic activities have played a major role in increasing stress over the water resources of the Genale Basin. Groundwater is a key and dominant water resources among the water balance components in Sub-Saharan African countries, as surface water is not often sufficient to fulfill water demands. Therefore, groundwater is becoming the principal source of clean domestic, commercial, and irrigation water for most rural and urban communities (Rwanga and Ndambuki 2017; Gebru & Tesfahunegn 2020; Aish 2014). Assessment of water resources and utilization systems are also vital to design and introduce appropriate water management practices that can reduce the demand-supply gap of water for a community. In Ethiopia, precipitation varies immensely both spatially and temporally all over the country, but such variability is more amplified in Southern Ethiopia. This has a significant influence on water resources availability that is important to support the life of local communities as rainfall is inadequate to supply the water demanded their socio-economic development (Gebru & Tesfahunegn 2020). Finally, the odd spatiotemporal distribution of the rainfall, together with poor management and harvesting of water resources, has led the country to face repeated food insecurity and prolonged drought. In response to such an argument, there are different attempts to suggest catchment-based assessment studies, including estimation of hydrological components at the sub-basins scale. Some of the techniques expressed in the existing literature to compute the water yield & water balance components are lumped or empirical approaches. However, the processes of the water balance elements are natural and are difficult to sustainably manage and fully explain the hydrologic processes by such models (Aish 2014; Frenken 2005). Advances in computing approach combined with bigger and wider data handling efforts have now permitted the development of physically-based hydrological simulation models. Subsequently, the long-term average water balance components such as groundwater recharge, actual evapotranspiration, surface runoff, and water yield can be estimated using the SWAT model that is integrated with Arc GIS (Muleta et al. 2007; Pathak et al. 2019). The use of physically-based SWAT model is the most widely applied method for simulating water balance components in areas where there is a lack of available data and where the input parameters are limited to assess water resources in the entire basin (Arnold et al. 1999; Wei et al. 2018; Kirby et al. 2007). To apply effective management practices for water resources enhancement, a detailed understanding of local water yield at a sub-basins level is important. Water yield is the average annual streamflow produced in a nested watershed that could able to move in interconnectivity (cavities, pores, and cracks) under the control of gravity, or it is the summation of all water balance components going into the main channel. Water yield is the most significant and essential component of the water budget for continuous water resources management and decision-making processes.

In this study, the SWAT model is first calibrated and validated using available flow data. The validated model is then applied to evaluate the spatial variability of water yield, water balance components and to identify areas of high potential water yield under different future climate scenarios so that the decision-maker can look for water resources project, explore planning and management in the Genale River Basin for sustainable use of water resources. Regional Climate Model (RCM) in the coordinated regional climate downscaling experiment (CORDEX)-Africa/Ethiopia was used for the impact of future climate scenarios on water yield production.

2.1 Materials and Methodology

2.1.1 Study area description

Ethiopia is located in Africa between 30° 30'and 180° 12' North latitude and 32°0 42'and 480° 12' East longitude. Genale River Basin (54,942 Km^2) lies in the southern part of Ethiopia, covering Oromia, SNNP, and Somali regions. It is geographically located between 4° 08' to 7° 02' North and 39° 00' to 42° 00' East. The basin gets its first maximum rainfall during spring (March to May) and secondary maximum rainfall during autumn (September to November) from the Indian Ocean easterlies, but the basin receives little rainfall in summer compared to the spring season. It is because Southerly Indian Ocean air currents lie in the lee side of the highlands in summer, and Atlantic westerlies reach the southeastern lowlands (Genale Dawa) after losing their moisture on the highlands to the west. In the Genale watershed, a total of 464 HRUs were created, spreading among 25 sub-basins. The mean annual precipitation experienced in the area is 810mm, and the distribution of rainfall in the watershed ranges from 300mm to 1303mm per year. The Monthly temperature ranges from 14.5^0C to 24.6^0C, with an average of 19.5^0C. The maximum and minimum elevation of the area is 4280 and 176 m, respectively. Figure 2.1 shows the location of the study area with the Digital Elevation Model (DEM), Genale River basin, stream reach, high and low elevation clipped from Ethiopian map using Arc GIS.

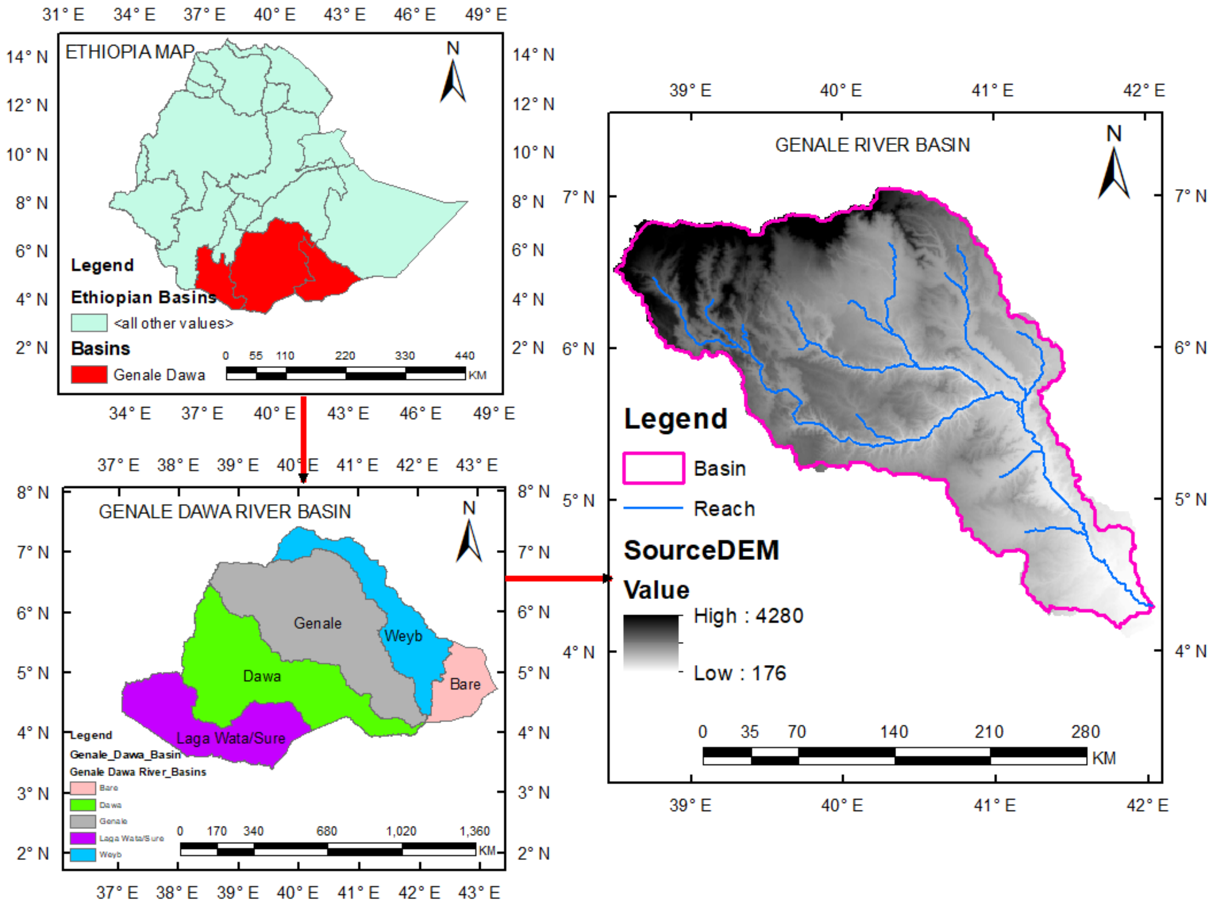

Figure 2. 1 Location of the study area and Digital Terrain

Figure 2. 2a & b shows Monthly temperature and precipitation of the Genale River Basin for the selected stations. The study area has two rainfall seasons, which are in spring (March to May) and autumn (September to November).

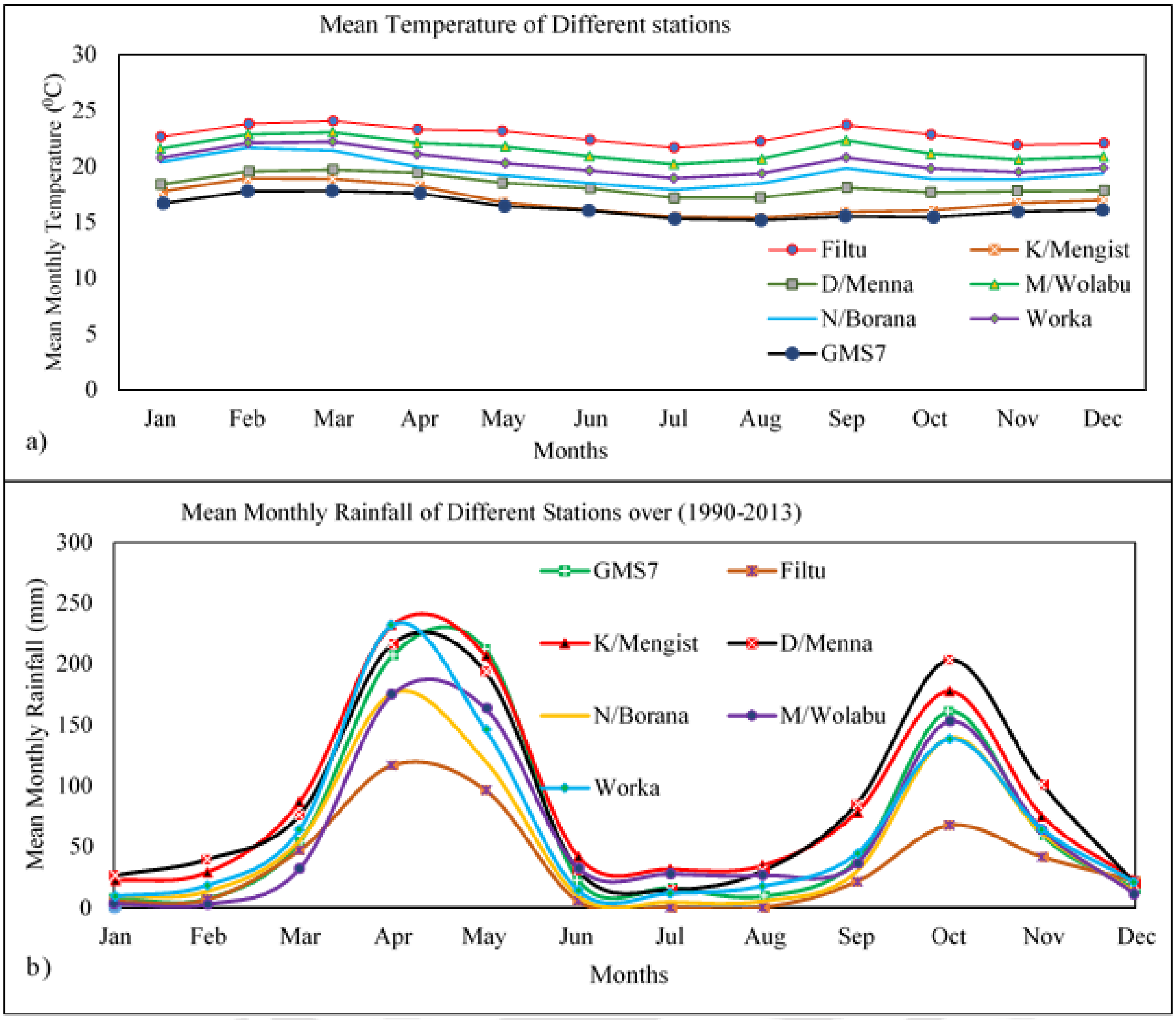

Figure 2. 2 Mean Monthly Temperature & Rainfall for the selected stations in the study area respectively

From Figure 2.2a, the Filtu station has a maximum temperature, while the gridded meteorological station (GMS7) has a low temperature in the area. In the first rainfall season, station K/Mengist has high rainfall, and station Filtu has low rainfall, while in the second rainfall season, station D/Mena has high rainfall, and station Filtu again has low rainfall for the Genale watershed as shown on Figure 2. 2b.

2.1.2 Model description

The SWAT (Soil and Water Assessment Tool) (Arnold et al. 1999) developed by the United States Department of Agriculture (USDA) in the 1990s is a semi-distributed, physically-based hydrological model developed to simulate water flow, sediment yield, nutrient (non-point sources of pollution) and the effects resulting from changes in land use/cover in the river basins. The model took into consideration for assessing infiltration, surface runoff, percolation, actual evaporation, evapotranspiration, and lateral and recharge into deep aquifer flows of hydrological processes.

The SWAT simulates the water balance in the basin using the equation:

$$SW_t = SW_o + \sum_{i=1}^{t} \left(R_{day} - Q_{sur} - E_a - W_{seep} - Q_{gw} \right) \tag{2.1}$$

Where; SW_t = Final soil water content on a day i (mm/day), SW_o = Initial soil water content on day i (mm/day), t = time in days, R_{day} = amount of precipitation on day i (mm/day) ,Q_{sur} = amount of surface runoff on day i (mm/day), E_a = amount of evapotranspiration on day i (mm/day), W_{seep} = amount of water entering the vadose zone from the soil profile on day i (mm/day), Q_{gw} = amount of return flow on day i (mm/day).

The model also estimates the streamflow in the sub-basins as a result of the total daily rainfall using the Soil Conservation Service (SCS) curve number (CN) method as follows:

$$Q_{Surface} = \frac{\{R_{Day-0.2S}\}^2}{\{R_{Day}+0.8S\}} \tag{2.2}$$

The retention parameter(S) and prediction of lateral flow by the SWAT model is expressed as;

$$S = 25.4(1000/CN - 10) \tag{2.3}$$

Where; S=drainable volume of soil water per unit area of a saturated thickness(mm/day), CN= curve number.

One of the demanding parameters that was figured out for sustainable water resources management of the study area is the water yield. Water yield is the cumulative sum of water leaving the HRU and getting into the principle channel during the time step (Neitsch et al.,2011). SWAT evaluates the components of water yield and water balance, which are crucial parameters for the planning & management of water resources in a River Basin (Ouallali et al.,2020; Ayivi & Jha, 2018). Water yield within a catchment is estimated by the model based on the equation;

$$W_{YLD} = Q_{Surface} + Q_{GW} + Q_{LAT} - TL \quad (2.4)$$

Where, W_{YLD} = a measure of water yield (mm), $Q_{Surface}$ - surface runoff (mm), Q_{LAT} - lateral flow contribution to stream(mm), Q_{GW} - groundwater contribution to streamflow (mm), and TL-transmission losses (mm) from tributary in the HRU. Water yield and water balance components are the main active force behind each process in the SWAT model and have effects on plant development and the movement of water yield in the watershed region (Neitsch et al.,2011). Typically, the application of the SWAT model contained different main steps starting from watershed delineation to creating Hydrological Response Unit (HRUs) and then the simulation.

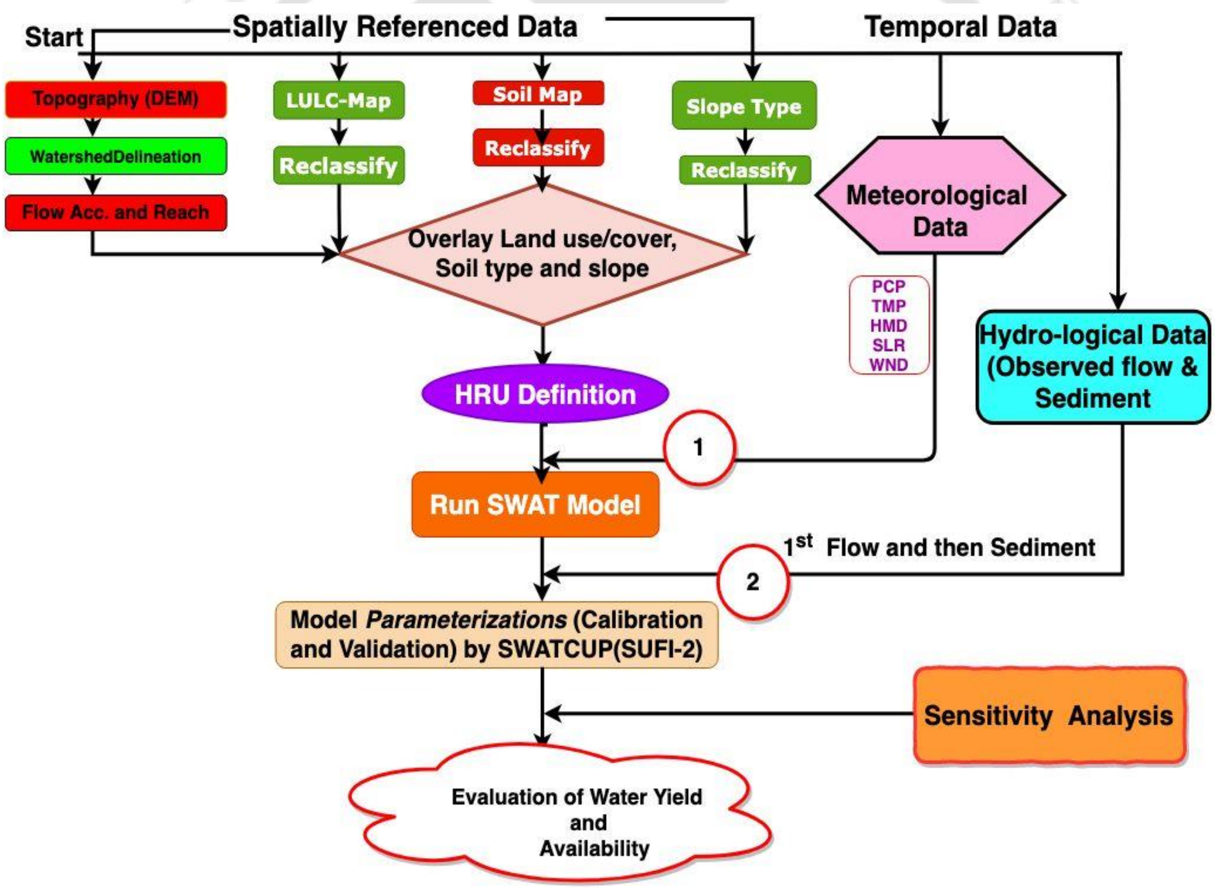

Figure 2. 3 Steps of the SWAT model for the study area (Methodology)

Figure 2.3 shows the input data required for SWAT, steps to be followed, and methodology to be applied in the study area.

Analysis of SWAT input data and sources

The DEM was downloaded from USGS Earth Explorer(http://earthexplorer.usgs.gov/) SRTM (Shuttle Radar Topography Mission) 90m and used for watershed discretization, sub-basin formation, slope calculation/ classification, and extracting stream networks with flow accumulation. The slope contained five classes, of which 5-20% was dominating the study area. The geospatial land cover data collected from the GIS department of the Ethiopian Ministry of water, irrigation, and electricity (MoWIE) for the year 2014 is used for SWAT input. The dominant land use/cover is range brushland (RNGB), which accounts for about 71% of the area. The soil map/type used in this study is from the Food and Agricultural Organization (FAO), the World Digital Soil Map (http://www.fao.org/geonetwork/srv/en/metadata) at the scale 1/5000000 for 2007. The soil data integrated into the SWAT model are the available water content, the texture, the hydraulic conductivity, the apparent density of the different soil layers. The dominant soil type in the study watershed is Rc19-bc-204 (Calcaric Regosols), and it accounts for about 40% of the catchment. The weather data required for this study has been taken from 'National Meteorological Agency of Ethiopia; http://www.ethiomet.gov.et/etms. These data consist of precipitation, maximum and minimum temperatures, wind energy, solar radiation, and relative humidity on a daily time basis. It covered from 1987 to 2013 period for 16 stations, of which eight are Gridded meteorological stations (GMS), and the other eight are installed gauging stations. The discharge data was taken from the Ethiopian Ministry of water, irrigation, and electricity (MoWIE) Hydrology department. The flow data of Genale River was recorded at Halwen gauging station, which is about 25km upstream of the outlet.

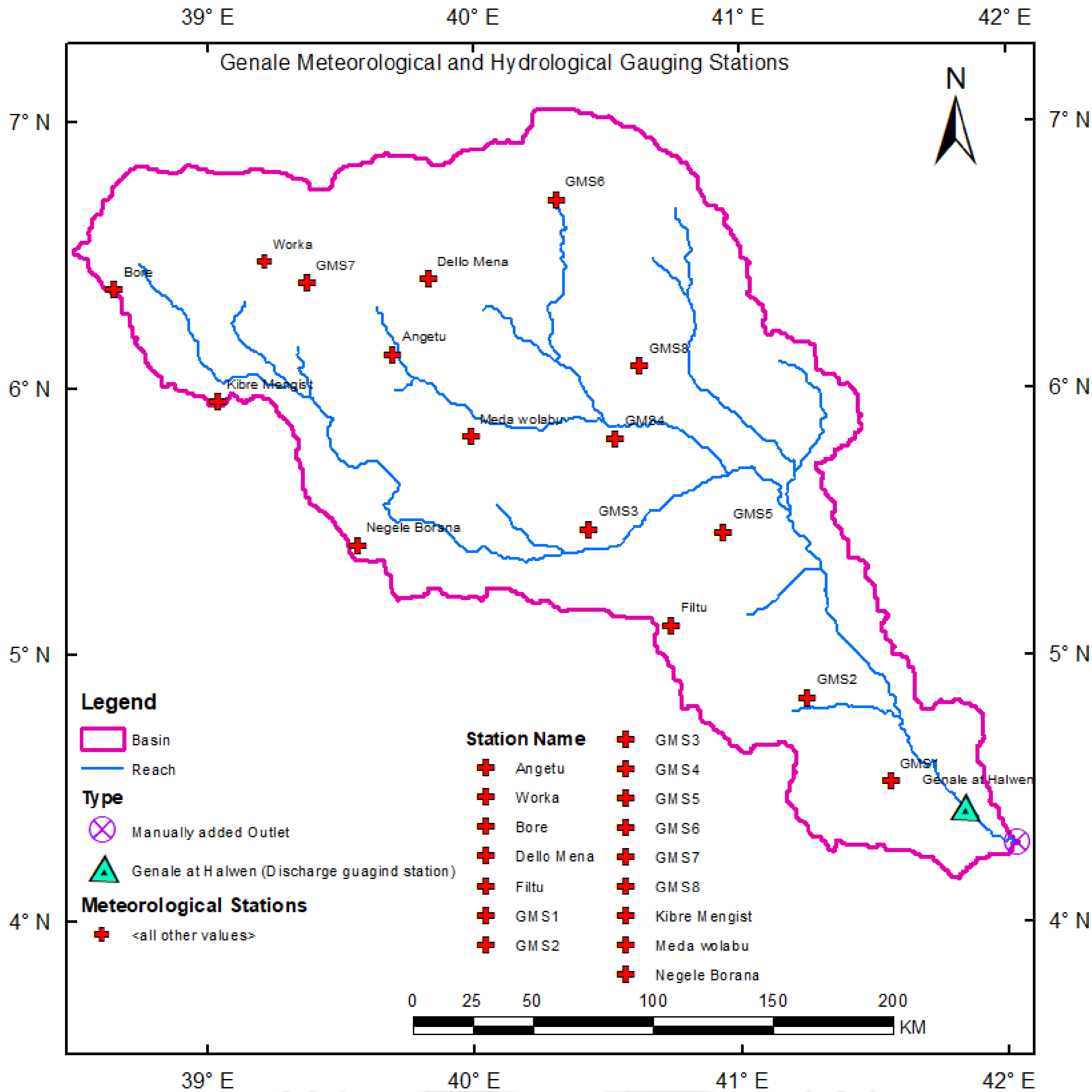

Figure 2. 4 Meteorological and hydrological gauging station distribution sub-basin wise for Genale River

Figure 2.4 shows different 16 (sixteen) meteorological stations were scattered in the catchment, one hydrological gauging station, watershed outlet, stream reach, and basin of the study area. The stations which were designated as; GMS1-Gridded Meteorological station-1, GMS2-Gridded Meteorological station-2, GMS3- Gridded Meteorological station-3, 4,5,6,7, & 8 respectively (Figure 2.4).

2.1.3 Future climate change data and bias-correction for regional climate model (RCM)

The statistically downscaled Regional Climate Model (RCM) in Coordinated Regional Climate Downscaling Experiment (CORDEX) for Ethiopia was downloaded from (https://dataservices.gfzpotsdam.de/pik/showshort.php? id=escidoc:3124935) and is used as an input data for hydrological modeling. This dataset provides downscaled data for different projections in a spatial resolution of 0.25degree x 0.25degree (about 25 km x 25 km) for use in any kind of climate impact modeling (Thrasher & Nemani 2015); (Ndhlovu & Woyessa 2020). The climate model data for hydrological modeling (CMhyd) tool, obtained from https://swat.tamu.edu/software/cmhyd/, was used to process bias correction of the climate model data for both precipitation and temperature (Dibaba et al. 2020). Accordingly, all precipitation and temperature data of CORDEX-RCM outputs were processed and improved through bias correction before using in climate impact modeling. We have used CMhyd for extraction of CORDEX-NetCDF, and bias correction of precipitation, minimum and maximum temperature to predict climate change-induced temperature changes in the Genale catchment. The Soil and Water Assessment Tool (SWAT) model was used to simulate water yield using the RCM under the future emission scenarios of two representative concentration pathways (RCPs) (medium emission scenario (RCP4.5), and high emission scenario (RCP-8.5)).

2.1.4 Description of SWAT-CUP (SUFI-2)

SWAT-CUP (SWAT-calibration uncertainty program) is a tool that interfaced with Arc-SWAT to perform the automatic calibration, validation, and sensitivity/uncertainty analysis in the SWAT model. For both calibration and validation analysis in the automatic SWAT-CUP optimization, the agreement between observed and simulated streamflow was determined using subjective and quantitative measures for recommended parameter thresholds (Abbaspour et al.,2007). During sensitivity analysis, propagation of the uncertainties in the parameters leads to uncertainties in the model output, which is expressed as 95 percent prediction uncertainty (95PPU). Using SWAT-CUP, the sensitivity analysis is carried out, which combines the Latin

Hypercube Sampling and one-factor-at-a-time (LHS-OAT) sampling (van Griensven & Meixner, 2006). In the LHS-OAT technique, one parameter value is changed at a time while keeping others constant. A global sensitivity analysis approach was used where all the parameters were granted to modify simultaneously. In the case of global sensitivity analysis, it performs the sensitivity of one parameter while the values of other related parameters are also changing. Global sensitivity analysis uses t-stat and p-value to determine the sensitivity and rank of each parameter. The SWAT-CUP is interfaced with five algorithms: (1) sequential uncertainty fitting (SUFI-2), (2) generalized likelihood uncertainty estimation (GLUE), (3) Markov chain Monte Carlo (MCMC), (4) parameter solution (ParaSol), and (5) particle swarm optimization (PSO) (Moriasi et al.,2007).

In this study, the SUFI-2 algorithm was implemented for uncertainty analysis, model calibration, and validation in the SWAT-CUP because of its high potential and efficiency for large-scale models, which are time-consuming, require a smaller number of simulations for several basins in the semi-arid region like that of the Genale River Basin. It also accounts for all sources of uncertainties, including climate data, selected model parameters, and observed flow.

2.1.5 Assessment of Performance criteria for the model

In this study, the goodness of fit was estimated based on the visual comparisons and statistical criteria suggested by previous studies (Moriasi et al., 2007). NSE (Nash-Sutcliffe coefficient of efficiency), R^2 (correlation coefficient), PBIAS, and Root Mean Squared Error (RMSE), and standard deviation ratio of the observations (RSR), are the most common evaluation criteria. RSR varies from 0 (perfect prediction) to a significant positive value. To this end, the lower the value of RSR, the lower the RMSE, and the better the model simulation efficiency in the Genale watershed. The following functions are mainly used for daily, monthly, and yearly streamflow; Calibration/validation uncertainty analysis.

Coefficient of Determination (R^2), $$R^2 = \frac{\left[\sum_{i=1}^{n}(Q_{si}-Q_{sm})(Q_{oi}-Q_{om})\right]^2}{\sum_{i=1}^{n}(Q_{si}-Q_{sm})^2\sum_{i=1}^{n}(Q_{oi}-Q_{om})^2} \quad (2.5)$$

Where, Q_{si} is the simulated value, Q_{oi} is the measured value, Q_{om} is the average observed value and Q_{sm} -average simulated value.

Nash Sutcliffe Efficiency (NSE), $NSE = 1 - \frac{\sum_{i=1}^{n}(Q_{oi}-Q_{si})^2}{\sum_{i=1}^{n}(Q_{oi}-Q_{om})^2}$ (2.6)

where, Q_{oi} is the observed, Q_{si} is the simulated and Q_{om}- observed average values of discharge.

Percent Bias (PBIAS), $PBIAS = \frac{\sum_{i=1}^{n}(Q_{oi}-Q_{si})}{\sum_{i=1}^{n}Q_{oi}} * 100\%$ (2.7)

For streamflow evaluation, a value of ±25% can be considered as satisfactory for the model performance. If the value is positive, the bias represents an underestimation of the simulated flow, while negative value suggests a model bias overestimated, where zero value shows the optimal value.

Peak percent threshold statistics (PPTS) (Lohani et al. 2014) were used to assess the extreme flow prediction ability of the model. It is a performance criterion of prediction between top U% and L% of the given data ($PPTS_{(L,U)}$). It is the mean absolute relative error value in the prediction of flows placed in the band of top U% and L% data. For the estimation of the $PPTS_{(L,U)}$, the observed/simulated data should be arranged in descending series using the following equation (Equation 2.8).

$PPTS_{(L,U)} = \frac{1}{(K_L-K_U+1)}\sum_{i=K_L}^{K_U}\left|\frac{(Q_{oi}-Q_{si})}{Q_{si}}\right| * 100\%$ (2.8)

Where, $K_L = \frac{L*N}{100\%}, K_U = \frac{U*N}{100\%}$, L & U are lower and upper bound in percentage, N is the number of data involved. When the value of U=100%, it represents $PPTS_{(L,100)}$ or simply $PPTS_{(L)}$, which in turn shows that $PPTS_{(L)}$, peak percent threshold statistics of top L% data. In this study, we use $PPTS_{(L)}$ to show the peak percent threshold statistics of top L% data. The lower value (L) illustrates, the better the statistical performance of the model.

2.2 Results and Discussions

The SWAT model used spatial geo-referenced data (DEM, soil type, land use, and slope classes) as input and built up 25 sub-basins, 464 HRUs with the drainage area of 54,942Km^2 in the Genale River Basin.

2.2.1 Model parameter sensitivity analysis

The model was calibrated and validated for monthly flow at the catchment outlet. Seven iterations with 500 number of simulations were used in the SUFI-2 program. In each iteration, the parameter's value ranges closer to the reasonable region were transferred to the next iteration, which provided better results in the next iteration. As the upper and lower bound ranges of parameters become smaller, the 95% prediction uncertainty distribution envelope gets smaller, implying that the targeted objective function gets better in the subsequent iterations. Initially, 20 numbers of parameters were selected for sensitivity analysis and then, based on the values of t-stat, and p-value ten (10) parameters revealed a meaningful effect on streamflow. In the calibration and uncertainty procedures, the final value of each model parameter that revealed optimal model efficiency during calibration was used for model validation without further modification. The simulation of the model was carried out for twenty-seven (27) years of recorded data from 1987-2013, of which the first three years data were used as a warm-up period, and the sensitivity analysis of hydrologic parameters was done on a monthly basis. Among the ten revealed parameters involved in monthly parameterization, the most sensitive parameters were curve number (CN2), followed by available water capacity of the soil layer (mm H2O/mm soil) (Sol_AWC), saturated hydraulic conductivity (mm/hr) (SOL_K.sol), moist bulk density (g/cm3 @ Mg/m3) SOL_BD.sol and the Baseflow alpha-factor (days) (ALPHA_BF.gw) (Table 2.1).

Table 2. 1 Fitted values and rank of parameters used in the SWAT model calibration/validation on Monthly step (1990-2013)

Parameter Name	Description of the parameter	Range value	Fitted value	p-value	t-stat	Rank
CN2.mgt	SCS runoff curve number	35-98	-0.176	0.0	-42.55	1
SOL_AWC.sol	Available water capacity of the soil layer	0-1	1.0	0.004	2.912	2
SOL_K.sol	Saturated hydraulic conductivity	0-2000	0.566	0.122	-1.548	3
SOL_BD.sol	Moist bulk density (g/cm^3 @ Mg/m^3)	0.9-2.5	0.984	0.20	1.28	4
ALPHA_BF.gw	Baseflow alpha-factor (days).	0-1	0.570	0.21	-1.26	5
REVAPMN.gw	Threshold depth of water in a shallow aquifer for "revap" to occur (mm)	0-500	408.6	0.308	-1.02	6
GW_REVAP.gw	USLE support practice factor	0-1	1.2	0.489	-0.69	7
ESCO.hru	Soil evaporation compensation factor	0-1	0.27	0.65	-0.45	8
HRU_SLP.hru	Average slope steepness	0-1	0.578	0.72	0.354	9
SURLAG.bsn	Surface runoff lag time	0.05-24	0.072	0.96	-0.05	10

The t-Stat is the parameter coefficient divided by its standard error. A parameter with more considered an absolute value of t-stat is more sensitive to flow. The p-value gives the relevance of the sensitivity. Thus, when the p-value close to zero, the sensitivity of the parameter is high.

Parameters adjustment

After pinpointing the sensitive parameters for the Genale watershed, those parameters were adjusted so that they are becoming fit to the local context. SWAT-CUP (SUFI-2) gave us the choice of three methods for advancing the value of the sensitive parameters (N'Dri, 2019). 1. (v_Replace) is to replace the delinquency value of the parameter with a given value (by the user). 2. (r_Relative) is updating the value of the parameter by multiplying the entrenched values (in each HRU) by the same coefficient. 3. (a_Absolute) consists of adding the given value to the fundamental value.

2.2.2 Calibration/validation

Calibration is an endeavor to better parameterize the model to a given set of local circumstances, thus reducing the prediction uncertainty. Calibrated parameters and the fitted values are the final notes for the modeler from the calibration action, which are then used for the required objectives. The visual comparison of the model performance during the calibration and validation period for stream discharge was responded well to the respective rainfall in the given span. The calibration was done from 1990 to 2005, and validation was from 2006 to 2013 on a monthly basis.

Table 2. 2 Model Performance and acceptable range assessment during calibration and validation period

R2	NSE	PBIAS	RSR	Rating	References
0.75-1	0.75-1	<10%	0-0.5	very good	(Abbaspour et al.,2007)
0.65-0.75	0.65-0.75	10-15%	0.5-0.6	good	
0.5-0.65	0.5-0.65	15-25%	0.6-0.7	satisfactory	
<0.5	≤0.5	>25%	>0.7	unsatisfactory	(Moriasi et al.,2007)

Table 2.2 shows the acceptable range of model performance value that we should look during the calibration and validation period.

Figure 2.5 shows, the SWAT model result is found to be in good agreement with the monthly-observed streamflow over both the calibration and validation periods, as shown in hydrograph from 1990 to 2013 years monthly, for 24 years excluding model warm-up periods.

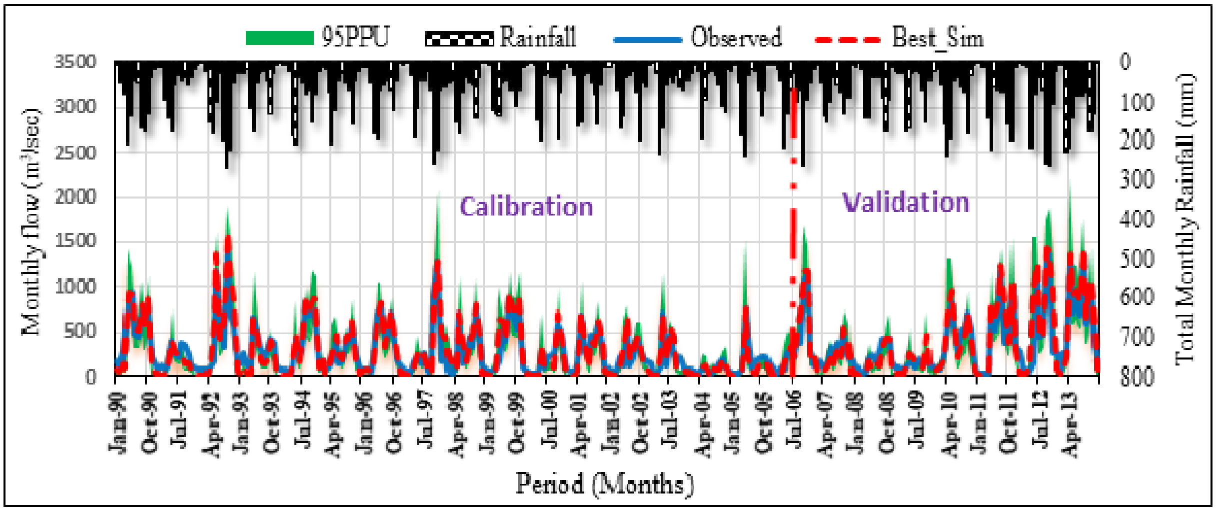

Figure 2. 5 Monthly calibration and validation from (1990-2013) for Genale River Basin flow at Genale Halwen

From Figure 2.5, the hydrograph showed that the highest peak for both simulated and observed flow occurred in September 1992, and the model result was slightly overestimated the peak in most of the year and underestimated in a few years. This disparity between the observed and estimated discharge is due to the effort of representing complex hydrological processes by adjusting values of sensitive SWAT parameters to represent the hydrological system in the semi-arid region of the Genale River Basin in Ethiopia. Difficulty also arises in the fitting between observed and simulated hydrograph due to lack of detailed information about water use, representation of topography by DEM, spatial resolution, scale issue in representing soil type, and land use activity.

Table 2. 3 The actual statistical properties' index value of Genale catchment for the calibration and validation process

For calibration process, Goal type=Nash Sutcliff, No_sims= 500, Best_sim_no=112, Best goal=0.8142875								
Variables	p-factor	r-factor	R^2	NSE	PBIAS	RSR	Mean_sim(Mean_obs)	StdDev_sim(StdDev_obs)
FLOW_OUT_25	0.51	0.78	0.87	0.81	-2.1	0.43	316.91(310.53)	346.79(295.23)
For validation process, Goal type=Nash Sutcliff, No_sims= 500, Best_sim_no=105, Best goal=0.766975								
FLOW_OUT_25	0.51	0.79	0.83	0.77	-2.5	0.48	307.56(300.13)	340.32(290.05)

From Table 2. 3, the calibration and validation of SWAT model performance are found to be in a reasonable range with the monthly observed and simulated streamflow over 1990 to 2013 years.

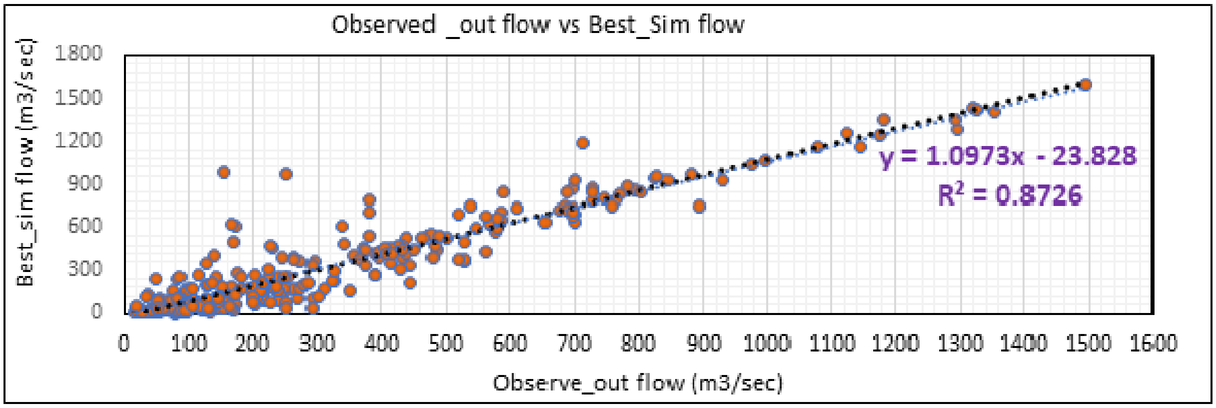

Figure 2. 6 Correlation of Monthly observed and simulated flow in calibration/validation process

From the scattered plot of observed versus simulated flow is agreed, and one can understand that more values are distributed above 45^0 (1:1) line shows that the model slightly overestimated the simulated flows (2.6). Besides, from the calibration/validation point of view, the pbias value is negative (Table 2.3) confirmed that the model is slightly overestimated.

Table 2. 4 Performance evaluation of the model for overestimated flood event using peak percent threshold statistics (PPTS)

Purpose	High flood events	$PPTS_{(5)}$	$PPTS_{(10)}$	$PPTS_{(15)}$	$PPTS_{(20)}$
	May 2005	4.6	4.2	3.5	2.5
	August, 1999	4.75	4.2	3.3	2.2
	November, 1997	3.4	2.5	1.5	0.75
Calibration	June, 1992	3.75	3.2	2.6	1.8
	August, 1994	4.6	3.5	2.41	1.6
	September, 1992	3.5	2.3	1.4	1.2
	May,1990	4.1	3.5	2.4	1.6
	April 2013	2.9	1.5	0.63	0.48
	August, 2013	4.6	2.45	1	0.76

	October, 2012	3.7	2	0.81	0.62
Validation	September, 2012	3.6	2.1	0.8	0.63
	August, 2011	4.2	3.1	2.0	1.1
	November, 2006	5.5	2.94	1.2	0.91

A new model efficiency evaluating criteria as peak percent threshold statistics (PPTS) value computed using equation-8 was used to verify the model performance during high floods event. The lower the values of PPTS better is the simulation during high flows. The values of PPTS statistics, PPTS(5), PPTS(10), PPTS(15), and PPTS(20) confirm the reasonably acceptable performance of the SWAT model during the period when the simulated flow is overestimated to some extent (Table 2.4).

2.2.3 Water yield and water balance components prediction in the Genale watershed

After calibration and validation of the SWAT model, estimation of water yield is found to be the best approach for predicting the availability of water in various components of the hydrological cycle and modification in between these components. Water yield is one of the critical parameters predicted by the model for adequate water management and planning of the study area. Figure 2.7 shows that the percentage of soil water is the highest, having 45% of the total water availability, 27% is the actual evapotranspiration, 24% is groundwater, and 3% surface runoff. As compared to these, other water balance components like deep aquifer recharge and lateral flow are minimal in the sub-basins of the study area.

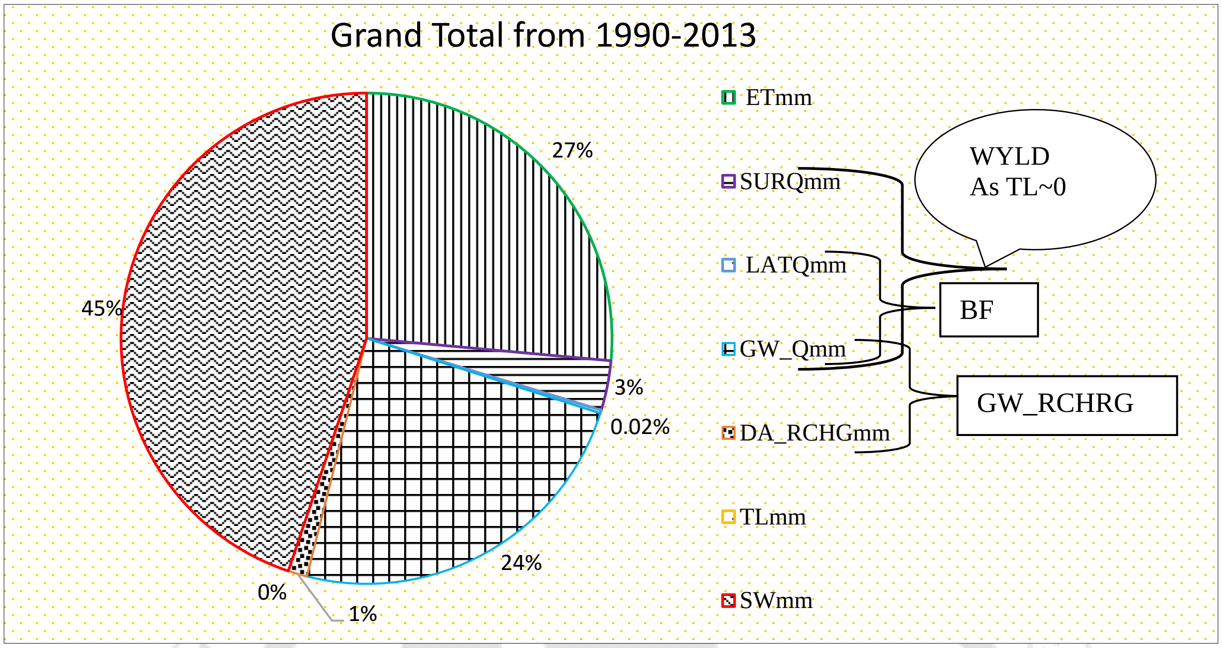

Figure 2. 7 Annual predicted water balance components in the Genale watershed (1990-2013)

Where, ET-Actual evapotranspiration, SURQ-Surface runoff, LATQ-Lateral flow, GWQ-Groundwater contribution to streamflow (mm H2O) from the shallow aquifer(Return flow), DA_RCHG-Deep aquifer recharge (mm H2O), TL-Average daily rate of water loss from reach by transmission through the streambed during a time step, SW- Soil water content (mm H2O) all in mm.

The average daily rate of water loss from the considered river reach by transmission through the streambed during the time step is almost insignificant (Figure 2.7). From the analysis, it can be winded up that evaporation loss is one of the significant loss components in the water balance of the Genale River Basin. It is mainly due to the type of land cover comprising of range brush and scrubland. Scanty rainfall in the study area and rise in temperature, principally in the dry seasons, are also other factors that contribute to the high evaporation loss. As seen from Figure 2.7, groundwater contribution to stream is very high (24%) comparing to surface runoff (3%) in the study area. It is because of an increase in actual evapotranspiration, low rainfall, and a small value of curve number in the study area. Among the water balance components shown in Figure 2.7, four elements, namely surface water contribution (SURQmm), lateral flow contribution (LATQmm), groundwater contribution from the shallow aquifer (GW_Qmm), and transmission loss (TLmm), are incorporated to compute water yield using equation 2.4. However, in this study, the effect of TLmm on water yield is not significant as its value practically approaches to zero.

2.2.4 Impacts of baseline condition and future climate change scenarios on water yield

Climate change impacted rainfall and temperature were used to predict the impacts of climate change on water yield and water balance components within the catchment. Projected annual precipitation and temperature, under the two RCPs (RCP 4.5 & RCP 85), leads to a significant disparity in the projected water yield of the Genale catchment. The changes in magnitudes and spatiotemporal variations of precipitation directly disturbed by the hydrological process, while more indirect effects are expected due to changes in temperature.

Table 2. 5 Changes in water balance components under baseline and future climate change

Scenarios	Water balance components					
	Period	Precip(mm)	ETmm	GW_Qmm	SURQmm	WYLDmm
Baseline condition	1990-2013	67.5	29.4	32.3	4.4	36.7
RCP4.5	2022-2080	86.85	28.5	34.8	5.3	40.1
RCP8.5	2022-2080	64.25	38.6	30.7	4.1	34.8

The RCMs were used to evaluate climate change in two future climate emission scenarios, RCP4.5 and RCP8.5, over 2022–2080 with respect to the baseline condition. Principally, the impacts of the climate changes on the watershed hydrology could be elucidated with the combinations of precipitation, temperature, and evapotranspiration. The decline of rainfall reduces surface runoff, and increasing temperatures amplified the increase in the actual evapotranspiration, which in turn has resulted in decreased runoff and groundwater. The predicted groundwater, surface runoff, and total water yield are relatively higher during 2022–2080 under RCP4.5 as compared to the scenario RCP8.5, as the actual evapotranspiration plays a significant role (Table 2.5). Under future climate change scenarios, the increase in temperature is another dominant factor affecting surface runoff, groundwater, and water yield.

Spatial heterogeneity of the sub-basin characteristics such as soils, land use, and DEM could have a significant effect on the water yield response of Genale watershed. Based on the heterogeneity of catchment characteristics, the simulated value of water yields in individual sub-basin disparate throughout the watershed.

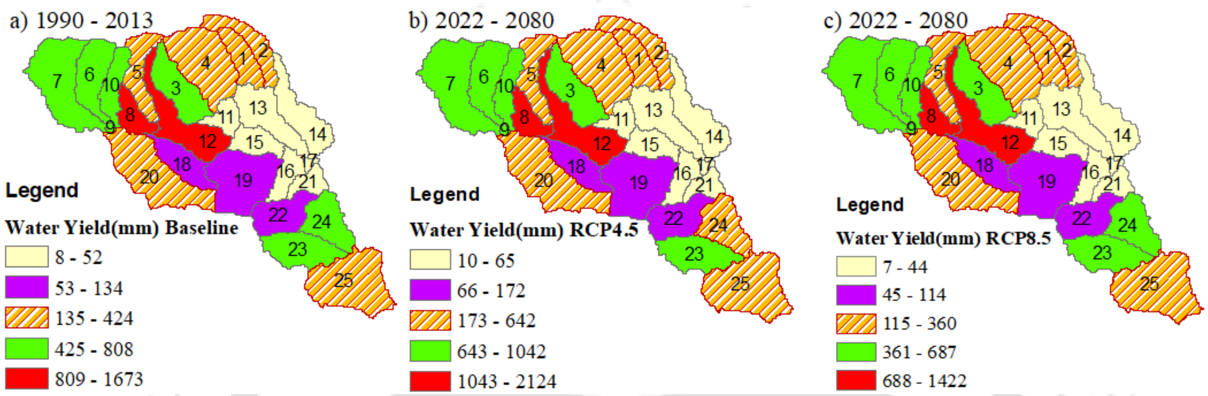

Figure 2. 8 Spatial distribution of water yield in each sub-basin of the Genale watershed under baseline condition and future climate scenarios

From the simulation results (Figure 2.8), sub-8 and sub-12 were revealed to the high production of water yield under all scenarios. The middle of the watershed generally has balanced values between 420 mm and 940 mm. In contrast, the sub-basin located downstream reflects moderate amounts of water yield, and the extreme water yield was noticed at most upstream of the watershed (Figure 2.8). The water yields vary from as low as 7 mm to as high as 2124 mm, with an average equal to 421.17mm, 543.5mm, and 358.1mm under baseline condition, RCP4.5 & RCP8.5 respectively (Figure 2.8). Understanding the effects of spatial heterogeneity on hydrologic parameters is essential to identify potential water yield in sub-basins and suggesting government and other agencies of water sectors to address community problems related to water and prioritize accordingly. Generally, the spatial distribution of water yields increases in areas of high precipitation. For instance, the highest precipitation occurs in the sub-6, 7,8,10,12, and water production also tends to be higher in these regions. In future emission scenarios, water yield will be likely decreased by 15% under RCP8.5 and is likely to increase by 28% under RCP4.5 (Figure 2.8) as compared to the baseline condition.

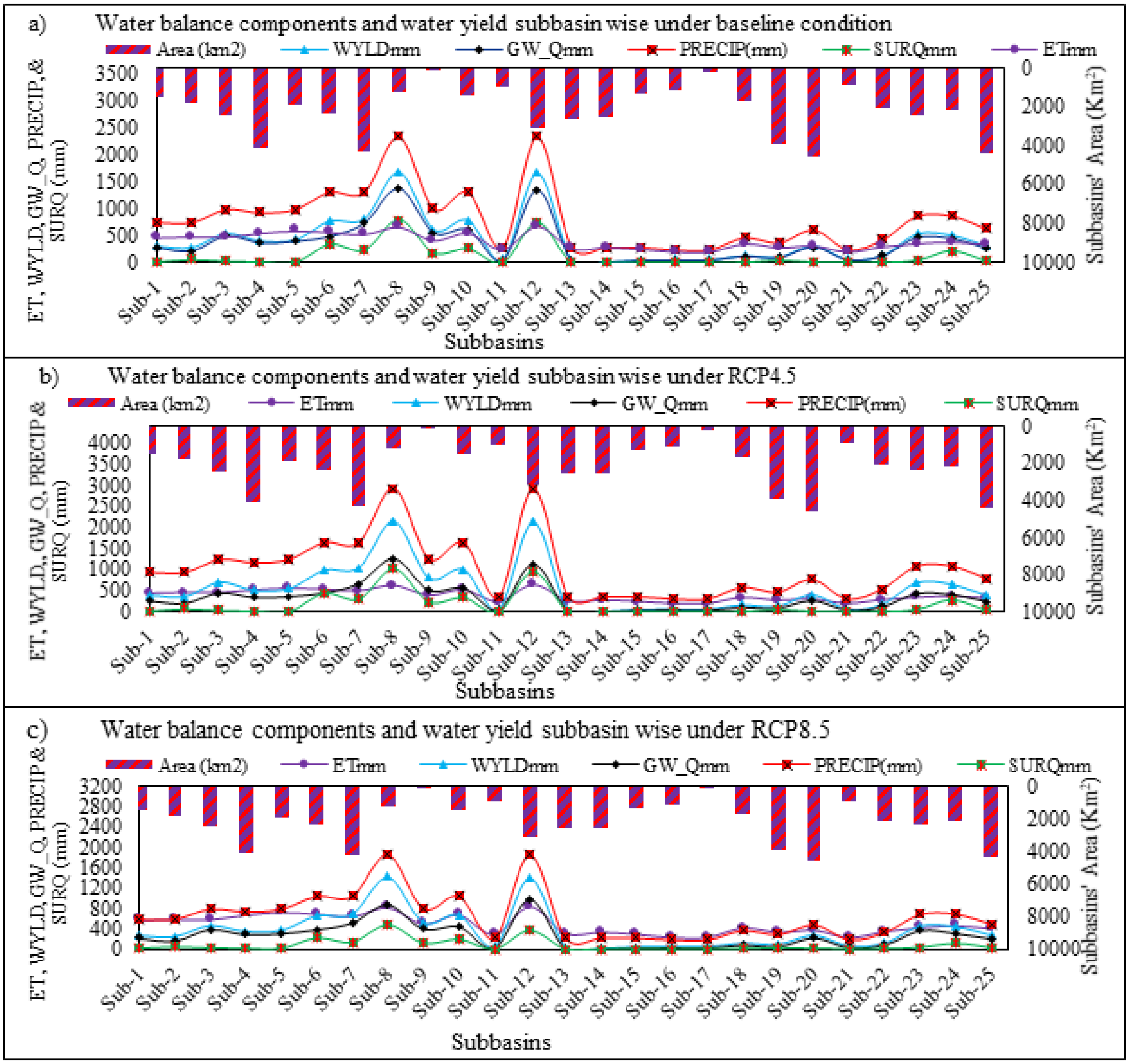

Figure 2. 9 Components of water yield distribution in the Genale River Basin based on baseline condition (1990-2013) and future climate change scenarios RCP4.5 & RCP8.5 (2022-2080)

Figure 2.9 shows the annual mean of the distinctive water yield with other water balance components in each sub-basin from 1990 to 2013 and from 2022-2080. It showed that sub-8 and sub-12 were the most water yielded sub-basin irrespective of the sub-basin area under all scenarios. Therefore, the regional state government might explore the water resources project site mostly at sub-8 and sub-12 in the catchment. However, the precipitation, runoff, groundwater, and water yield will likely be reduced under future emission scenario RCP8.5 as the temperature and evapotranspiration will probably be increasing (Figure 2.9). In relation to surface runoff, groundwater has more contribution to water yield in the basin. It is because of actual evapotranspiration is dominant, an increase in temperature, and the occurrence of scanty precipitation in the study area.

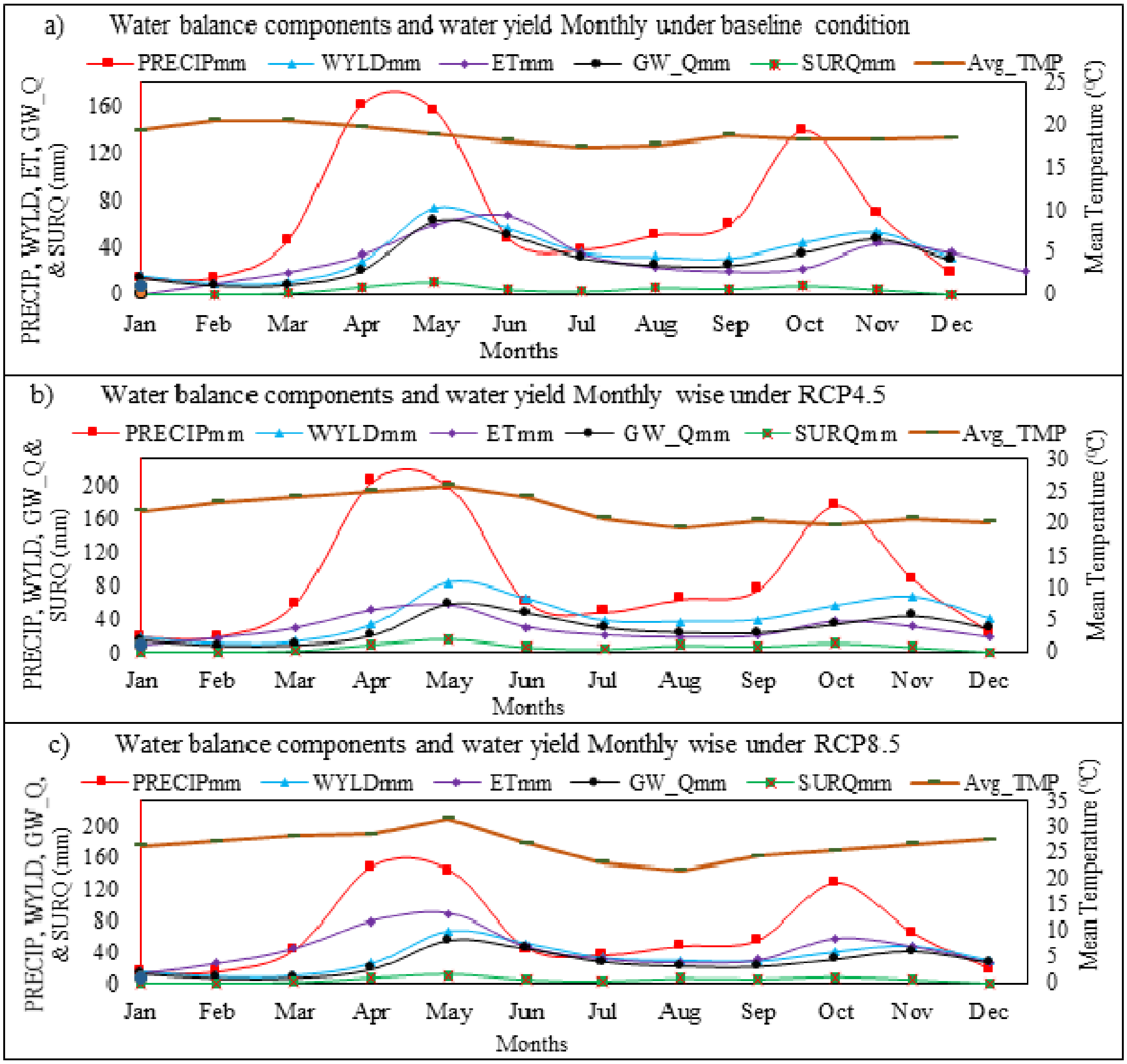

Figure 2. 10 Relationship between water yield components and rainfall monthly over the entire watershed under baseline condition (1990-2013) and future climate change (2022-2080)

In June and December, that the water yield graph was showing slightly above the precipitation, confirms that though the scanty amount of rainfall occurred during those months in the area, groundwater contributed significantly to water yield soon after rainfall stopped (Figure 2.10). For exploring water resources projects, March to May and September to November has a high potential of water yield under all scenarios. The projected precipitation shows an increasing trend in all Months under emission scenario RCP4.5, while decrease trends were observed under the RCP8.5 scenario compared to the baseline condition. As the exact scenario to be realized is not known; therefore, more flexible design is necessary for any water resources project to cater to the need both for possible high and low water yield. Accordingly, the suggestion is given to the regional state government to address possible community problems related to water resources in the Genale River Basin during these months.

2.3 Conclusions

The SWAT model is applied successfully in the Genale River Basin, Ethiopia, for determining water availability at the sub-basin level to identify sub-basins with high water yield potential both under present and climate impacted future scenarios. Identification of sensitive parameters and estimation of streamflow, water yield, and water balance components has given insight into the hydrological processes of the basin, providing useful information for water management at the basin level yet addressing water-related problems of the local community. The curve number (CN2.mgt), available water capacity of the soil layer (SOL_AWC.sol), saturated hydraulic conductivity (SOL_K.sol), and baseflow alpha-factor (days) (ALPHA_BF.gw) are identified as the most sensitive parameters to flow. Model validation statistics like NSE and R2 revealed the acceptable performance of the model in Genale Basin, and PPTS values were confirmed its satisfactory performance even in simulating peak flow.

Water yield in different sub-basins ranges from 7.00 mm to 2124.00 mm with an average equal to 421.17mm, 543.50mm, 358.10mm under baseline condition, RCP4.5 & RCP8.5 scenarios respectively. Such high spatial variation in water yield is of significant concern. Therefore, the local government authority, in general, should give priority in looking for water resources project exploring, design, planning, and management practice in the basin to solve problems related to water. As the sub-basin 8 and sub-basin12 are identified to have maximum in water yield in all scenarios and are located towards the upstream of the Ganale Basin, water resources project planned in these basins can play a pivotal role in meeting the water demand of the Genale Basin during a crucial period. Also, water yield under RCP4.5 and RCP8.5 differs significantly. As the actual realization of the scenario is uncertain, more flexible project design and climate-resilient water management policies will be imperative to manage the risks. This study, therefore, also showed the need for monitoring hydrological parameters continuously to have informed water management in the Genale Basin. The study has also revealed the need for further research on the scope of augmenting basin storage/yield by adopting ecological management practices (EMPs) in the sub-watersheds of the Genale River Basin.

Chapter 3

Spatial and Temporal Variability Estimation of Sediment Yield and Sub-basins/Hydrologic Response Units Prioritization on Genale Basin, Ethiopia

3.0. Introduction

Inappropriate land use, uncontrolled runoff, lack of suitable soil conservation measures, unfavorable physiographic characteristics (topography, vegetation cover, soil type, slope), increased population pressure leading to land degradation, urbanization, deforestation, erroneous tillage, and use of chemical fertilizers are the primary causes of soil erosion and sedimentation problems in a watershed (Adeogun et al. 2018; Markhi et al. 2019). Sediment yield and land degradation have strong interaction with land use/cover, soil type, and slope classes in the watershed (Gizaw & Kebede 2019). Effects of soil erosion in the upper catchments can be of many folds in the form of onsite and offsite negative consequences. While the onsite effect includes a reduction in cultivable soil depth, soil fertility, crop productivity, and nutrient, offsite negative impacts include reduced reservoir storage capacity, increased flood risk, and water quality degradation because of excess release of sediment and other pollutant loads (Moss 2008). In addition to these direct impacts, all these factors' combined effect can finally lead to potentially widespread food insecurity (Ayele & Gebremariam 2020; Namomsa & Adugna 2019). Runoff water flowing over an erosion-prone agriculture-dominated watershed degrades the land productivity and becomes a source of sediment, nutrients, and pesticides for the nearby stream (Duru et al. 2018; Singh et al. 2012), and their presence in excess quantity can adversely affect the aquatic biota. Sources of pollution for aquatic systems are primarily classified into a point and non-point sources (NPS). Point sources are contaminants generated from single identifiable sources of pollution such as discharge from waste-water treatment plants, and therefore relatively easy to handle. However, non-point sources refer to pollutants that do not have a specific point of sources and include sediment yields, excess fertilizers, herbicides, and insecticides from agricultural and residential watershed areas (Dong et al., 2018; Babaei 2019). Sediment yield, being an NPS pollutant, controlling sediment loss at the source, i.e., in the upper catchment itself, using suitable soil conservation practices is ideal for eliminating all sediment-related problems stated above. However, many a time, it becomes challenging to take management measures in the entire watershed/sub-basin because of financial constraints, particularly for a developing country. Identifying critical soil loss areas in a river basin/watershed is fundamental to better soil loss control through land use prioritization and soil conservation (Mahoney et al., 2018). Hydrological model having provision of sediment assessment can help identify such critical sediment contributing areas logically to prioritized management measures. Soil and Water Assessment Tool (SWAT), one of the widely used physically based semi-distributed hydrological model, has a physical representation for spatiotemporal variability and are adequate for simulating the impacts of climate change & anthropogenic activities on hydrological cycle & environment. SWAT can be used in a nearly continuous time domain to assess streamflow generation, sediment yield, water quality, and quantity, and thus facilitates studying the response of management practices at the sub-basin/HRU level (Liu et al. 2019; Samimi et al. 2020; Xu et al., 2009).

Change in socio-economic condition and increased anthropogenic activities have increased stress on the water resources & watershed management challenge in Ethiopia, particularly in the Genale catchment. In Ethiopia, the spatial and temporal distribution of precipitation & surface runoff varies all over the country, causing significant spatial variation in soil erosion & sediment yield. Such variability is more prominent in southern Ethiopia in the Genale River basin. Thus, it can provide a better opportunity for taking soil and water conservation measures in sub-catchment/HRUs scale to yield effective solutions with optimal funds and human resources to support local communities' lives.

To prioritize critical sediment contributing areas, one needs to assess soil erosion characteristics of a watershed from different angles. Gross Erosion means the sum of all particles leaving the various erodible surface in the watershed. The gross soil erosion in each HRUs cell was calculated using the Modified Universal Soil Loss Equation (MUSLE) in SWAT (Daggupati et al., 2011). The required model parameters for the MUSLE can be calculated using the digital elevation model, soil type, and land use/cover information on a cell basis (Jain & Das 2010). However, all the eroded sediment particles within the catchment are not transported to the watershed outlet as they are trapped and deposited in the upstream reaches. The eroded sediment particles transported to the watershed outlet constitute the Sediment Yield. Sediment Yield can also be defined as the amount of sediment that leaves a boundary, reaching or passing a point of interest in a given period & expressed in mass per unit area (Bhattarai, & Dutta 2007). Sediment Delivery Ratio (SDR) is defined as the ratio of sediment yield at the watershed outlet to the concerned watershed area's gross erosion. The SDR has multi-fold environmental significance in estimating the soil and water losses and the efficacy of control measures in watersheds (Wang et al., 2018). The variations in ranges of SDR between sub-basins are likely due to different physiographic characteristics such as land use, soil type, climate, drainage area, channel density, slope gradient, rainfall-runoff factors, and sediment transport processes (both overland flow and channel), and nearness to the mainstream. In the catchment sub-basins, large SDR also indicates high erosion rates. Watersheds with large drainage areas will generally have a lower SDR than small watersheds, as large areas within a watershed will have more chances to trap soil particles, so the possibility of soil particles reaching the water channel system is low (Wu et al. 2018). SDR represents the efficiency of the watershed in transporting soil particles/ sediment from areas of erosion to the point where sediment yield is measured. Therefore, identifying sub-basins with a high value of SDR will help minimize sediment yield at the watershed outlet (Woznicki & Nejadhashemi 2013; Walling 1983; Bartholic 2004).

The sedimentation problem is also becoming a subject of discussion among researchers due to its negative effect on the available water capacity, design, and operation of hydropower reservoirs worldwide (Ebtehaj et al., 2020). Water shortage for different purposes, backwater flooding, and approximately one percent of reservoir storage capacity are being lost every year because sedimentation is becoming a major concern in most developing countries (Briak et al. 2016; Zarris et al., 2011). The cost of reviving this lost capacity requires a very massive amount of restoration work, and it is somewhat better to construct new reservoirs instead. Therefore, watershed modeling and management play a vital role in the early management planning and local resources development by identifying critical erosion zone (Adeogun et al. 2018; Liu et al. 2019; Markhi et al. 2019). To reduce the peak rate of surface runoff causing soil erosion and sedimentation, comprehensive understanding and estimation of hydrological processes, land management, soil types, slope class, and climatic conditions of different parts of the watersheds are fundamental.

In recent years, the SWAT model is gaining popularity in hydrology and water resources research and has been adopted widely because of its robust algorithms for simulation of the hydrological system, estimating sediment yield, SDR, and calculating NPS pollutant transport. In addition, the scope of incorporating a comprehensive database on agricultural management practices is another advantage of the SWAT Model.

This study presents a systematic procedure of prioritizing the implementation of soil and water conservation measures in limited critical areas of a watershed to manage sediment-related problems of the entire watershed, including its stream network. The procedure presented is implemented using the SWAT model integrated with Geographic Information System (GIS). The criticality of an area, the minimum extent being the HRU level, is assessed based on the severity of soil erosion, sediment yield, and sediment delivery ratio (SDR). To evaluate its implementation suitability, the proposed method is applied in the Genale Basin of Ethiopia, where soil erosion was identified as a major problem, and its severity varies widely within the basin. Spatiotemporal variability of soil erosion, sediment yield, & SDR at sub-basin/HRU scale in the watersheds of Genale catchment is predicted and systematically analyzed to prioritize erosion hotspot area at the sub-basin and HRU level for implementation of soil & and water conservation measures in a socially acceptable and economically viable manner.

3.1 Materials and Methodology

The digital elevation model (DEM) was downloaded from USGS Earth Explorer (https://gisgeography.com/usgs-earth-explorer-download-free-landsat-imagery/) SRTM (Shuttle Radar Topography Mission) 90 m*90 m and used for watershed delineation, hydrologic response unit formation, slope calculation/ classification, and extracting stream networks with flow accumulation. The land cover data were collected from water, irrigation, and electricity (MoWIE), Ethiopia, for 2013. The dominant land use/cover is range brushland/shrubs (RNGB), accounting for about 71% of the area. The soil map/type used in this study is obtained from the Food and Agricultural Organization (FAO), the World Digital Soil Map (http://www.fao.org/geonetwork/srv/en/metadata) at the scale of 1/5000000 for 2007. The dominant soil type in the study watershed is Rc19-bc-204 (Calcaric Regosols), and it accounts for about 40% of the catchment. The weather data required for this study has been taken from 'National Meteorological Agency of Ethiopia; http://www.ethiomet.gov.et/etms. It covered from 1987 to 2013 period for different stations. The streamflow and sediment data were taken from the water, irrigation, and electricity (MoWIE), Ethiopia's hydrology department. The streamflow data of Genale River was recorded at the halwen gauging station from 1990 – 2013, while sediment concentration data ranged from 1987 to 2005, which is about 25km upstream of the outlet. It was then transferred to the outlet and arranged as per the requirement of SWAT-CUP for the period from 1990-2013 on a monthly scale.

Refer Figure 1.2 shows the description of study area's location in Ethiopia, Africa, and the Genale watershed delineated using Arc SWAT embedded in ArcGIS. The Genale catchment contains 25 sub-basins in the delineated watershed, and the stream reach and is labeled as 1, 2, 3…up to 25.

For individual HRU, the sediment losses attributed to the surface runoff were evaluated based on the Modified Universal Soil Loss Equation (MUSLE) (Bonumá et al. 2014). The MUSLE formula of sediment yield in the sub-basin roughly estimates the gross soil erosion caused by sheet, rill, and rain splash but does not include the erosion caused by landslides and gullies.

$$Q_{SED(HRU)} = 11.8*(Q_{Peak}*Q_{Surfac}*A_{hru})^{0.56} * K * C *P* LS *CFRG \quad (3.1)$$

where; $Q_{SED(HRU)}$ = Sediment loss/Sediment yield(ton/ha/day) from individual HRU, $Q_{Surface}$ = surface runoff (mm/ha/day) associated to HRU, A_{hru} = Area(ha) of HRU, Q_{Peak} = peak flow rate(m^3/s), K_{USLE} = soil erodibility factor, C_{USLE} = Cover and management practice factor, P_{USLE} = Conservation support practice factors of land use, LS_{USLE} = Topographic factor, hill slope steepness factor/the length slope factor, CFRG = coarse fragment factor.

The latest version of the SWAT model is used to route and compute peak discharge using equation (5) (Neitsch et al., 2011).

$$Q_{\mathrm{Peak}} = \frac{\mathrm{RC} * \mathrm{i} * \mathrm{A_{Sub}}}{0.36} \tag{3.2}$$

where; Q_{Peak} is peak runoff rate (m^3/s), i is the intensity of rainfall during the time of concentration (cm/hr), A_{sub} is the sub-basin area (km^2), and RC is runoff coefficient. SWAT discretized Genale River Basin in Southeastern Ethiopia to generate streamflow, predict sediment yield, estimate gross erosion, and SDR to identify vulnerable soil erosion areas.

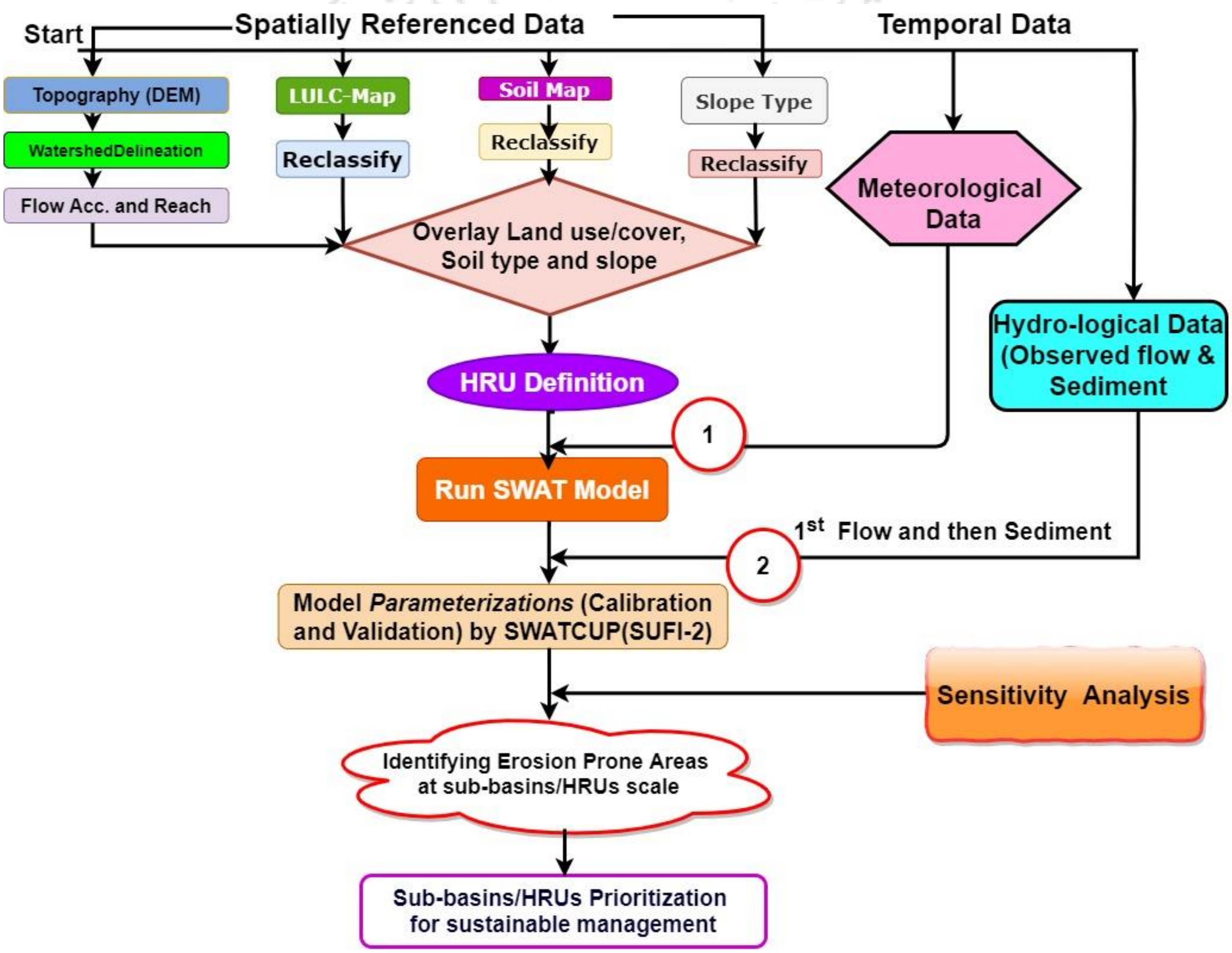

Figure 3. 1 Flow chart of the study area

Figure 3.1 shows the hydrological, meteorological, and geospatial data required for the study and the flow chart depicting the steps to be followed for obtaining the necessary outputs by implementing the SWAT model in the study area. Typically, the application of the SWAT model contains several steps starting from watershed delineation, flow accumulation to creating hydrological response units (HRUs) in the catchment and then the simulation (Figure 3.1). The current SWAT model evaluates surface erosion and sediment yield due to runoff for each HRUs using the modified universal soil loss equation (MUSLE).

3.1.1 Meteorological Data Analysis, Processing, and Sources

After collecting all necessary data, their quality & quantity were analyzed to detect any data inconsistency or missing data, and required adjustments were made to minimize the data uncertainty in the model output.

Double Mass Curve (DMC) analyzes and investigates records in meteorological data, particularly for precipitations at different stations in the catchment. The DMC is used to determine whether the correction is required or not for inconsistency in data, which might occur due to observational error, change in instrumentation, change in gauge location, or surrounding conditions (Owolabi et al., 2021; Gao et al., 2017). DCM is the plot of cumulative rainfall for individual stations against the cumulative of all other stations during the same period. The plot shows as a straight line so long as the data are proportional; the slope of the line will represent the constant of proportionality between the quantities. Following visual observation, we have evaluated the consistency of the data by slope calculation and finding the adjustment (correction) factor at the deviation point (between cumulative plot & linear trend line analysis) and have distributed the adjustment factor by multiplying the data that need to be adjusted. Then the data adjusted using standard procedure are found to be consistent with high values of correlation coefficient (R^2) as indicated in the plot (Figure 3.2).

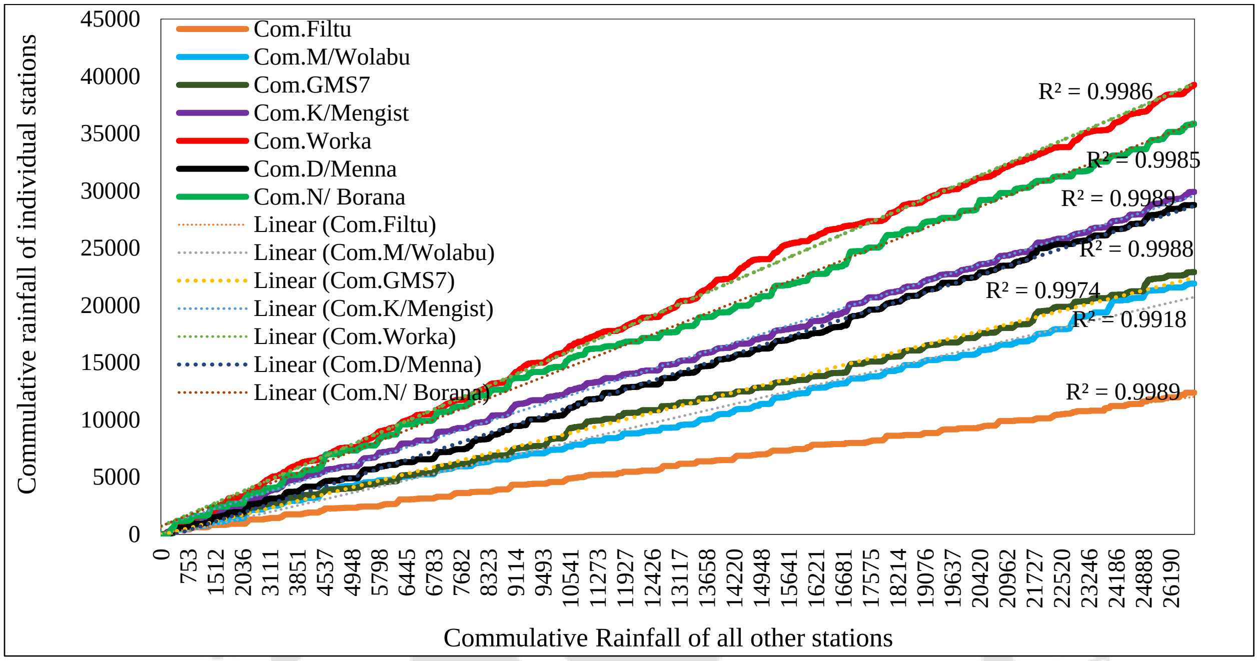

Figure 3. 2 The double mass curve of different selected stations

3.1.2 Developing Sediment Rating Curve (SRC)

Evaluation of sediment yield from watersheds depends on the length of the data series and the reliability of observed records of suspended sediment concentrations. However, some missing estimates are often derived from empirical relations between river discharges and corresponding sediment concentrations/loads (Ulke et al., 2009; Mohammadi et al., 2021). SRC is commonly used to produce a continuous time series of suspended sediment in the river, based on available historical flow and sediment data. SRC thus helps to predict a variable that is difficult to measure continuously from another variable easier to determine. In the present study, historical daily sediment concentration data are available from October 20, 1987, to October 1, 2005. However, streamflow data are available from 1990-2013, i.e., with an overlapping period of 15 years with the sediment. During the non-rainy season, sediment concentration remains almost negligible and generally is not collected by the department. Also, to assess soil erosion due to water, rainy season data are only required. As we have carried out the model study monthly, available daily sediment data for 16 years were converted to monthly data for the monsoon months and used for developing sediment rating curves. This derived equation of SRC (Eq. 6) was used to continuously generate suspended sediment data for the period for which streamflow data are available and facilitate the calibration and validation process of SWAT.

$$SSC = a * Q^b \quad (3.3)$$

where; SSC is suspended sediment concentration/load, Q is streamflow, a and b are constants to be resolved from the measured flow rate and suspended sediment concentrations/loads. Available data of sediment concentration and streamflow were plotted for Genale River. SRC developed from these data and presented in Figure 3.3 shows coefficient, a=3.14, power, b=1.41, with a regression coefficient R2 value of 0.905. Therefore, from the trendline, the developed power scale equation (having the higher correlation coefficient is preferred to fit in this case) to predict the sediment load for the Genale watershed is given as; QSED = 3.14 × Q1.41, where; QSED is sediment load (metric-tons) and Q- streamflow (m3/sec).

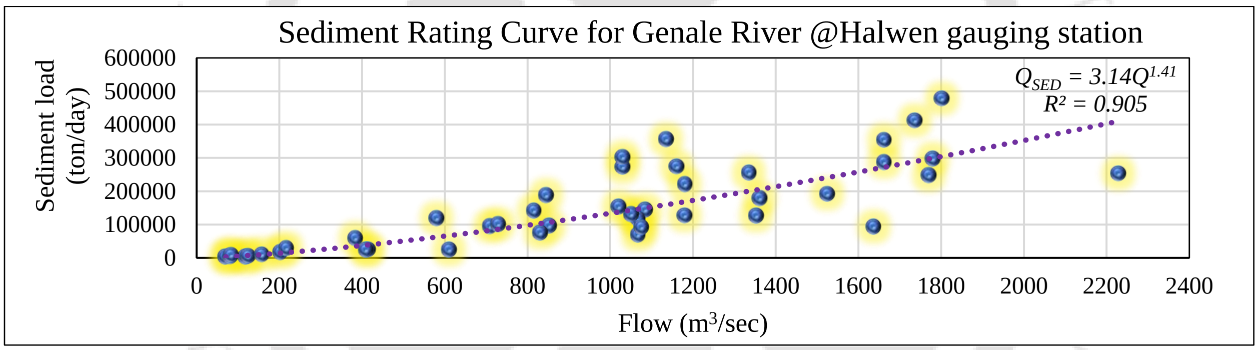

Figure 3. 3 Developed sediment-rating curve for Genale River @ Halwen gauge station

From October 20, 1987, to October 1, 2005, historical daily sediment concentration data were available for the study. Streamflow data were also available from 1990-2013, i.e., with an overlapping period of 16 years with the sediment data. During the non-rainy season, sediment concentration remains almost negligible and generally is not collected by the department. Also, to assess soil erosion from the catchment under the action of water, rainy season data are the relevant data. As we have carried out the model study on a monthly basis, available daily sediment data for 16 years were converted to monthly data for the monsoon months and used for developing the sediment-rating curve. Therefore, the number of points in the curve is appearing to be low. The derived equation of SRC Equation 3.3 was then used to continuously generate suspended sediment data for the period for which streamflow data are available to facilitate the necessary calibration and validation process of SWAT.

3.1.2 Sediment Delivery Ratio (SDR)

In this work, SDR for the sub-basin is described as the ratio of sediment yield at the watershed outlet to the gross erosion (total sediment load generated) from an individual sub-basin. It is a non-dimensional scalar and conventionally expressed as;

$$\mathrm{SDR} = \frac{\mathrm{SYLD}}{\mathrm{E}} \text{ (Walling, 1983).} \quad (3.4)$$

Where; SYLD is the average annual sediment yield (sediment load at the end of slope length) at the endpoint of watershed outlet per unit area, and E is the yearly gross erosion from stream reach over that same area.

SDR is estimated using SWAT with the MUSLE equation and compared with empirical equations.

$$\mathrm{SDR} = 0.5656\mathrm{A}^{-0.11} \text{ (Boyce, 1975)} \quad (3.5)$$

$$\mathrm{SDR} = 0.375\mathrm{A}^{-0.2382} \text{ (USDA-SCS, 1979)} \quad (3.6)$$

$$\mathrm{SDR} = 0.472\mathrm{A}^{-0.125} \text{ (Vanoni, 1975)} \quad (3.7)$$

where A is the drainage area in Km^2. The expected values of SDR are from 0 (floodplains) to 1(in uplands of the basin) because of possible deposition of eroded soil during transport and before reaching the watershed outlet (Walling 1983; Park et al. 2010). However, SDR can also be more extensive than unity in watersheds of very small areas with extremely erosive streams.

3.1.2.1 Identification of critical/erosion-prone sub-basins

Watershed management practice cannot be implemented into the whole/multiple sub-basins because of resource constraints like finances, human resources, time, and land availability in the study area. Identifying erosion-prone areas will draw researchers' attention to the most problematic reach and reduce the involved financial cost required for minimizing sediment yield and NPS pollutant transport for the whole watershed. So, the watershed's critical reach should be identified to implement soil and water conservation management measures by estimating the average annual sediment yield from each sub-basin from 1990 to 2013. The sub-basins were arranged in decreasing the significance of average annual sediment yield and classified as per erosion class specified by Uniyal et al. (2020) (Table 3.1).

Table 3. 1 Soil erosion classes based on the erosion rates (Uniyal et al. 2020)

S.no	Erosion class for soil	Erosion rate ranges (ton/ha/yr)
1	Slight/very low	0-5
2	Low	6-10
3	Moderate	11-15
4	High	16-20
5	Very high	21-40
6	Very severe	≥ 41

3. 2 Results

In the present study, the streamflow and sediment load data used for calibration, parameterization, uncertainty, & validation of the model ranges from 1990-2013, in which, for suspended sediment, the extended data were predicted using sediment rating curve. The model was created with DEM, land use/cover, soil type, and slope characteristics for the Genale basin, which formed 25 sub-basins, 464 HRUs with a drainage area of 54,942 Km2. A hydrological model's capability to adequately simulate streamflow and sediment load typically accounts for the precise calibration/validation of parameters, which are indispensable for the simulation process to minimize uncertainties.

3.2.1 Uncertainty analysis for streamflow and Sediment

Sensitivity analysis helps to determine the relative ranking of parameters depending on how it affects the output variance due to input variability. This helps in reducing uncertainty and provides parameter estimation guidance for the calibration step of the model. Sensitivity analyses were conducted based on the global sensitivity produced by the Sequential Uncertainty Fitting version-2 (SUFI-2) algorithm in SWAT-CUP. Initially16 numbers of parameters were involved in the sensitivity analysis for streamflow. After many iterations based on the p-value & t-stat values, ten parameters revealed a meaningful effect on streamflow to finalize the model parameters as mentioned on Figure 3.4. Six (6) parameters that were not showing sensitivity to streamflow were discarded includes; (GW_DELAY.gw- groundwater delay time; SLSUBBSN.hru-average slope length; OV_N.hru-manning's n value for overland flow; CH_N.rte- manning's "n" value for the main channel; CH_K2-effective hydraulic conductivity in main channel alluvium (mm/h); EPCO-plant uptake compensation factor). For sediment, eight parameters show very sensitivity to the model. Therefore, a sensitivity analysis was conducted to optimize the unknown variables, and the most sensitive parameters which were found to have the most considerable effect on the streamflow and sediment load in the model result were identified. Analysis of sediment sensitivity was carried out for three years warm-up period 1987 to 1989- and 16-years calibration period 1990 to 2005- and 8-years validation period 2006 to 2013. Based on the p-value and t-stat results obtained from sensitivity analysis, the ranks of parameters were assigned. The predicted flow was the most sensitive for the initial SCS curve number II (CN2) belonging to the management class and the soil layer's available water capacity (SOL_AWC.sol). In contrast, the simulated sediment was sensitive to the linear re-entrainment parameter for channel sediment routing (SPCON.bsn), soil layer's available water capacity, & curve number.

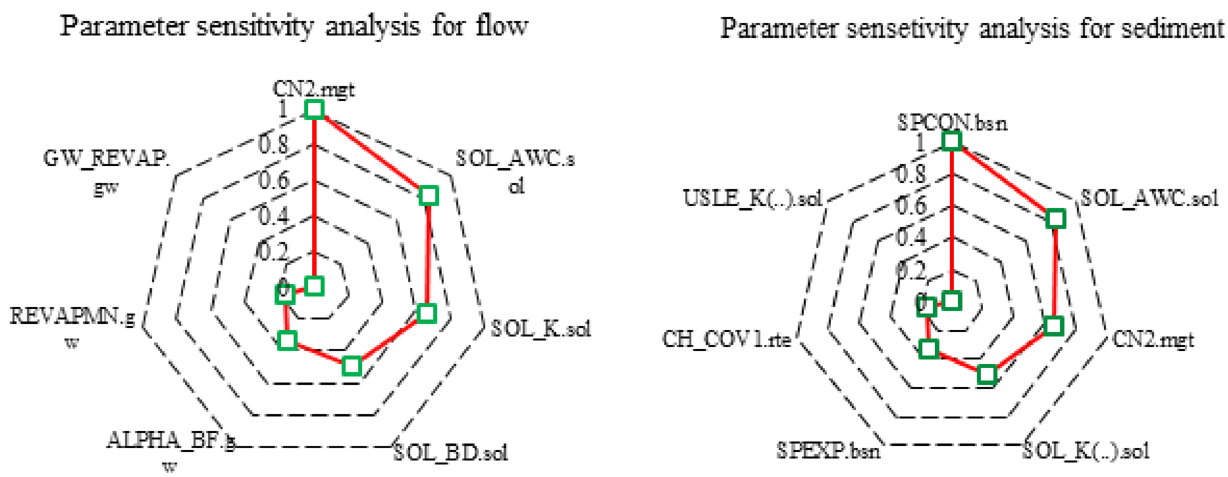

Note: CN2.mgt- curve number for moisture condition II; SOL_AWC.sol- soil layer's available water capacity; SOL_K.sol-saturated hydraulic conductivity; SOL_BD.sol- moist bulk density; ALPHA_BF.gw- baseflow alpha-factor (days); REVAPMN.gw- threshold depth of water in a shallow aquifer for "revap" to occur (mm); GW_REVAP.gw- groundwater revap.or percolation coefficient; SPCON.bsn- linear re-entrainment parameter for channel sediment routing; USLE_K.sol - USLE equation soil erodibility (K) factor; CH_COV1.rte- channel erodibility factor; SPEXP.bsn- exponent of re-entrainment parameter for channel sediment routing

Figure 3. 4 Graphical representation of the normalized parameter sensitivity rank for flow and sediment yielded

Figure 3.4 shows the normalized parameter sensitivity result, which has indicated that a value close to one is more sensitive to streamflow and sediment. The green box shows the magnitude of a parameter and indicates its relative sensitivity. For example, flow estimation is highly sensitive to curve number and has low sensitivity to groundwater revap or percolation coefficient. On the other hand, for sediment modeling, the sensitivity of linear re-entrainment parameter for channel sediment routing to model result is high, and the USLE equation's soil erodibility (K) factor is relatively low.

3.2.2 Model calibration and validation

Calibrated parameters and the fitted values are the modeler's critical notes from the calibration process used for the required objectives. Calibration of streamflow and sediment load was performed with several iterations of 500 simulations number; each was carried out for the calibration period of 1990-2005 monthly. Validation is required to verify whether the calibrated parameters also work for other data of different years within the watershed. Validation involves a model run with continuous flow and sediment parameters, which were already adjusted during the calibration process. Validation period (2006-2013) results showed a satisfactory performance, as statistical measures are in the allowable range for streamflow and sediment. Table 3.2 shows the acceptable ranges of statically performance criteria for the model.

Table 3. 2 SWAT statistical performance index acceptable range (Abbaspour et al.,2011; Moriasi et al.,2007)

P-factor	R-factor	R^2	NSE	PBIAS		RSR	Rating
				Flow	Sediment		
0.7 - 1	<1, (close to 0)	0.75-1	0.75-1	<±10%	<±15%	0-0.5	very good
		0.65-0.75	0.65-0.75	±10-15%	±15-30%	0.5-0.6	good
		0.5-0.65	0.5-0.65	±15-25%	±30-55%	0.6-0.7	satisfactory
Close to 0	>1, (infinite)	<0.5	≤0.5	>±25%	>±55%	>0.7	unsatisfactory

Abbaspour et al.,2011 and Moriasi et al.,2007 stated about the good and satisfactory rating of P-factor & R-factor no fixed numbers exist, but they acknowledge that the results should capture most of the observations with small uncertainty within the range; for P-factor 0-1 and R-factor close to zero but ranges from zero to infinity.

Table 3. 3 Actual index value for SWAT output during calibration/validation process

Types of assessment		p-factor	r-factor	R2	NSE	PBIAS	RSR	Rating
Flow	Calibration	0.51	0.78	0.87	0.81	-2.1%	0.50	good
	Validation	0.54	0.86	0.85	0.78	-0.5%	0.52	good
Sediment	Calibration	0.48	0.37	0.84	0.79	3.8%	0.61	satisfactory
	Validation	0.43	0.39	0.82	0.75	3.9%	0.67	satisfactory

Uncertainty measure of SWAT- CUP (SUFI-2) indicated that P-factor of 0.51 and R-factor of 0.78 for calibration and P-factor of 0.50 and R-factor of 0.86 for validation (Table 3.3). P-factor & R-factor are the two indices calculated to evaluate the model uncertainty. P-factor is the percentage of observed data enveloped/shaded by the 95% of prediction uncertainty (95ppu) in sensitivity analysis represented by green color, while R-factor is the average width/thickness of the 95ppu band/envelop of the observed data. Thus, the P-factor of 1 and R-factor of zero indicates that the simulation exactly/precisely corresponds to the observed data without sources of uncertainty which is not possible in the reality of hydrological modeling. In this study, P-factor for calibration and validation is 0.51 & 0.50, respectively, which means about 51% of calibration and 50% of validation of the observed flow were bracket by 95PPU band. Therefore, the SWAT model is at an acceptable level of uncertainty for analyzing the Genale River Basin's flow.

Refer, Figure 2.5 Monthly observed and simulated hydrograph for the calibration period (1990-2005) and validation (2006-2013).

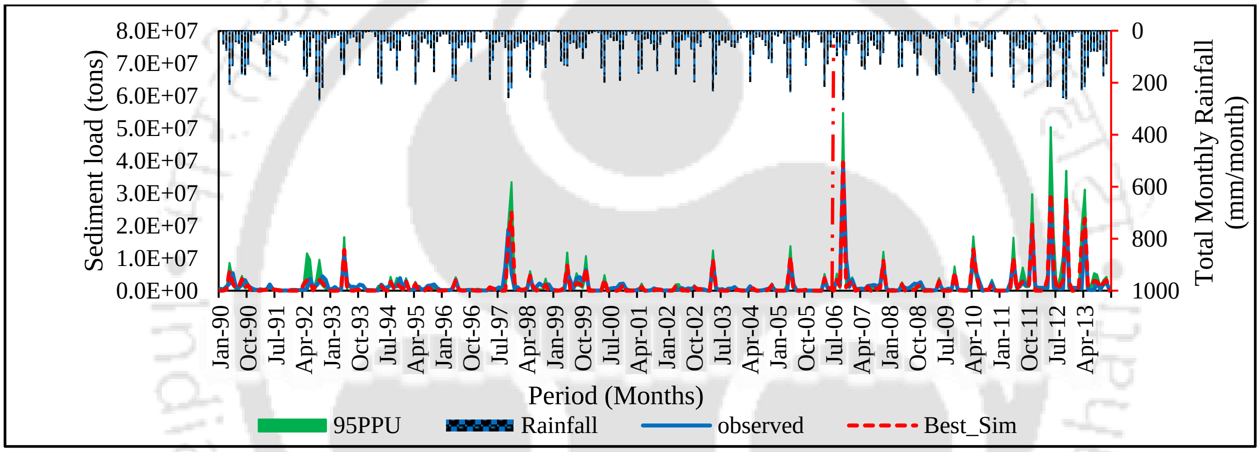

Figure 3. 5 Monthly observed and simulated sediment load plot for the calibration (1990-2005) and validation (2006-2013)

As indicated, the model's simulated and observed sediment load agreed and showed a satisfactory performance during the calibration and validation process (Figure 3.5).

3.2.3 Spatial and Temporal Variation of Sediment Delivery Ratio (SDR) at Watershed-Scale

3.2.3.1 Spatial Variation of SDR

This section aims to resolve each sub-basin sediment contribution to the watershed outlet using SDR and identify erosion-prone areas within the catchment.

Table 3. 4 Classification of Genale watershed based on SDR value (Woznicki & Nejadhashemi (2013); Gelagay (2016); Mutua & Klik (2006); Lu et al., (2006))

Prioritization based on SDR value	SDR Values	Area (Km^2)	Sub-basins number
Very low	<0.036	18,656.97	9, 11, 13, 14, 15, 16, 17, 20, 21 & 25
Low	0.037 to 0.126	8,657.8	3, 18, 22, & 23
Moderate	0.127 to 0.325	15,279.3	1, 2, 4, 5, 19 & 24
High	0.326 to 0.451	4,575.8	10 & 12
Very high	>0.452	7,771.8	6, 7, & 8

From Table 3.4, the average sub-basins SDR dispersed in the Genale watershed. In this case, the identified area of high priority was covered with 12,347.6km^2 (agricultural and brushland) over a steep upland sub-basin. The disparity of SDR is mainly due to the differences in land use/cover, soil type, sub-basin size, the slope of sub-basins, and stream channel characteristics. Understandably, the value of SDR is higher near the watershed outlet because there is a probability of transporting all eroded sediment loads at the watershed outlet. From Figure 3.6, the spatial variability of SDR ranges from 0.001 (sub-15 and sub-21) to 0.754 (sub-7). Sub-7, 6, 8, 12, and 10 have high SDR values and resulted in high sediment yield within the catchment. So, they should be prioritized for implementing management practice

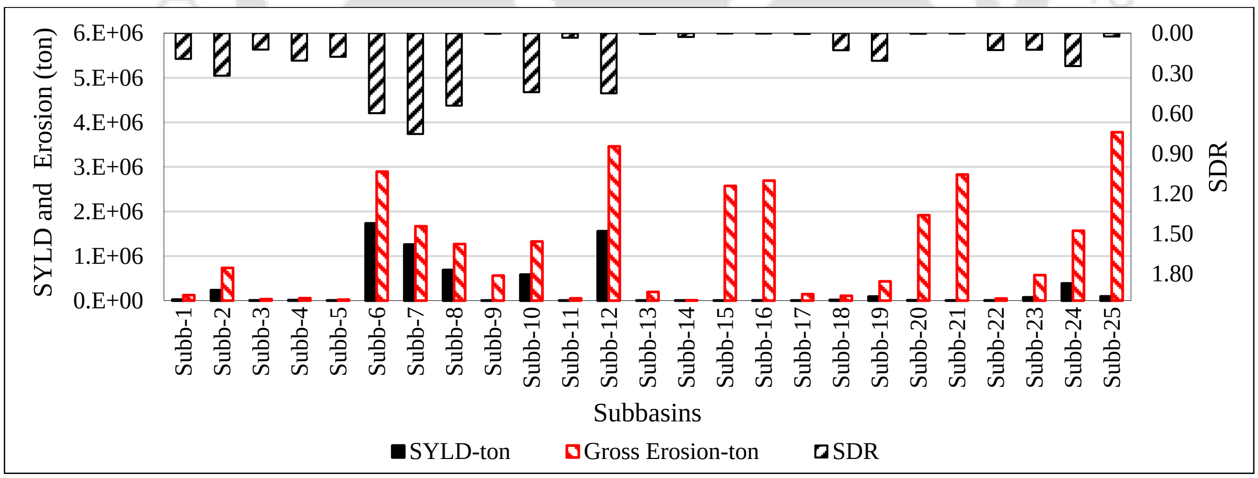

Figure 3. 6 Spatial variability of SDR superimposed with sediment yield and gross erosion

Sub-basins with relatively high gross erosion but low in sediment yield produce a small SDR value, which means SDR has a direct relationship with sediment yield at a sub-watershed outlet (Figure 3.6). For instance, sub-basins 15, 16, 20, 21, & 25 have very high gross erosion but produce very low sediment yield, resulting in small SDR in the sub-basins (Figure 3.6) because of maximum stream transport capacity is reached and a greater proportion of sediment yield deposition effect before reaching into the sub-basins outlet. That is why the generated sub-basin sediment yield is very low compared to gross erosion. Additionally, sediment yield is very low in large sub-basins, and the probability of sediment deposition in a large watershed is higher than in a small watershed under the same circumstances. These sub-basins are relatively large in drainage areas, range shrubs & forest cover, which might curbs/arrest some amounts of sediment yield. Moreover, from Fig. 11c, in the manuscript, based on the spatial distribution, the generated surface runoff from the same sub-basins are still under the category of" very low & low," which also resulted in "very low & low "sediment yield from the respective sub-basins and other physiographic characteristics that dictate erosion potential.

3.2.3.2 Temporal Variation of SDR

Analyzing the temporal variability of SDR at the watershed scale is of significance to understand the sediment transport process. Therefore, management practice in the catchment can be preferred accordingly.

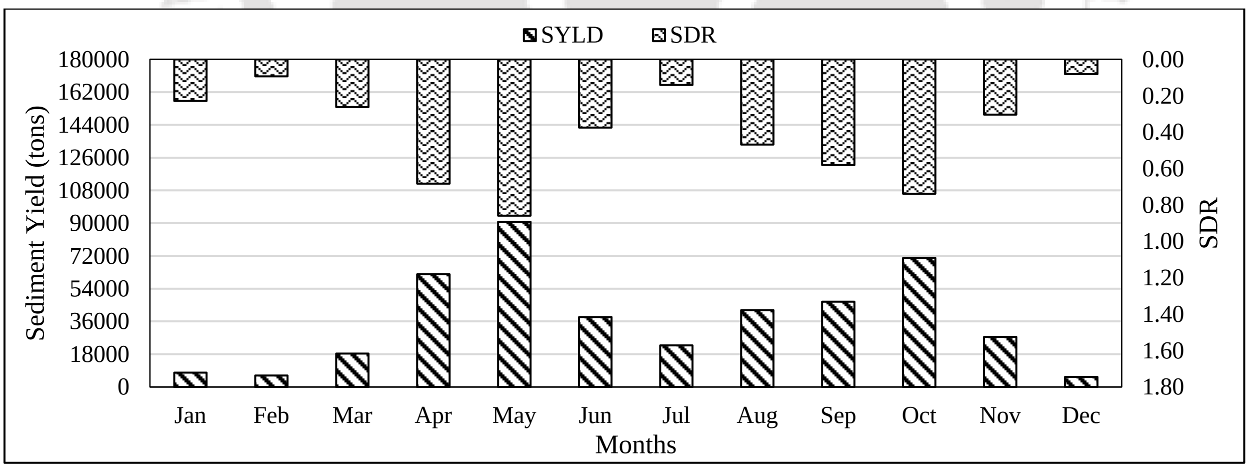

Figure 3. 7 Genale watershed sediment yield superimposed with SDR monthly

From Figure 3.7, the SDR values of the Genale watershed at the outlet varies from 0.08 (December) to 0.86 (May). Gross erosion from all sub-basins and sediment yield at sub-basins outlet is the most significant in May, October, April & September, and similarly, these months have high SDR values.

3.2.4 Comparing SDR values Using SWAT-MUSLE Versus Area-Based (Empirical) Methods

A comparison between the SDR value calculated by the SWAT model and empirical methods was also carried out. Although they produced similar results to the SWAT model, the SDR values vary to some extent in the Genale watershed. The SWAT-MUSLE estimation for the Genale watershed indicated that 19% of all sediment entering a stream reach would be transported to the watershed outlet (Table 3.5).

Table 3. 5 Comparisons between various sediment delivery ratio (SDR) estimation methods

SDR Methods	SDR Values
Vanoni (1975)	0.121
Boyce (1975)	0.170
USDA-SCS (1979)	0.171
SWAT-MUSLE	0.190

From Table 3.5, Vanoni (1975) predicted considerable SDR for the Genale watershed, while the USDA-SCS (1979) method predicted the lowest values. The Boyce (1975) method produced almost similar results to SWAT-MUSLE for the basin. The convenience of using the SWAT-MUSLE model to predict SDR is that it simulates channel transport processes and considers the physiographic characteristics and detailed spatial data over the total watershed. However, other empirical methods lump temporal and spatial data of sediment transport without considering climatic variations, land use/cover, slope class, & soil type.

3.2.5 Spatial and temporal variability of sediment yield at sub-basins scale

The variability of sediment yields spatially and temporally occurred in the watershed due to factors such as the DEM, land use/cover, soil type, rainfall distribution, slope classes, and watershed management practice, which formed uneven sediment yield distribution in each sub-basin. The results obtained from the SWAT model indicate that significant portions of highly gradient, sub-basins near the stream network, urbanized, highly cultivated, & brushland areas are more critical to the rate of sediment yield for the existing conditions in the studied basin.

3.2.5.1 Spatial variability at sub-basins scale

SWAT model was simulated annually for 24 years of sediment data at a sub-basins level. The spatial variability of sediment yield for the entire Genale watershed was estimated, and the average annual sediment yield was found to vary significantly within the catchment, as shown in Figure 3.8.

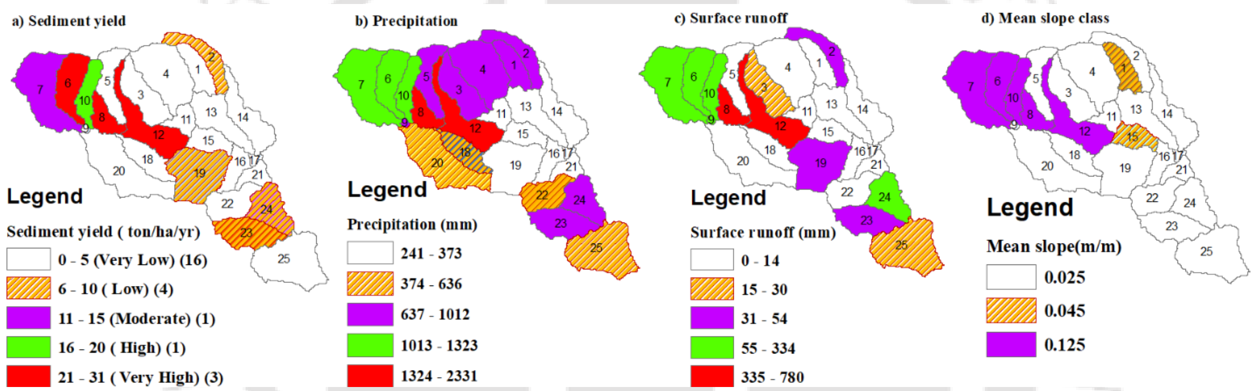

Figure 3. 8 Spatial variability of sediment yield with precipitation, runoff, and slope in Genale watershed at sub-basin level

From Figure 3.8, among the total 25 sub-basins, three sub-basins produced sediment rate at very high (21-31 ton/ha/year), one sub-basin was high (16-20 ton/ha/year), one sub-basin produced moderate (11-15 ton/ha/year), three were low (6-10 ton/ha/year), and the rest 16 sub-basins were under low categories. Sub-basins 6, 8, 12, 10, and 7 were identified as erosions-prone areas. The average sediment yield of five identified sediment hotspot sub-basins was 21.8 ton/ha/year and covered 22.47% of the total watershed area. As shown in Figure 3.8, the spatial variability of sediment yield is remarkably responsive to the precipitation, surface runoff, and mean slope with the respective sub-basins. Critical sub-basins are located in areas with a steep slope, high surface runoff, and high rainfall.

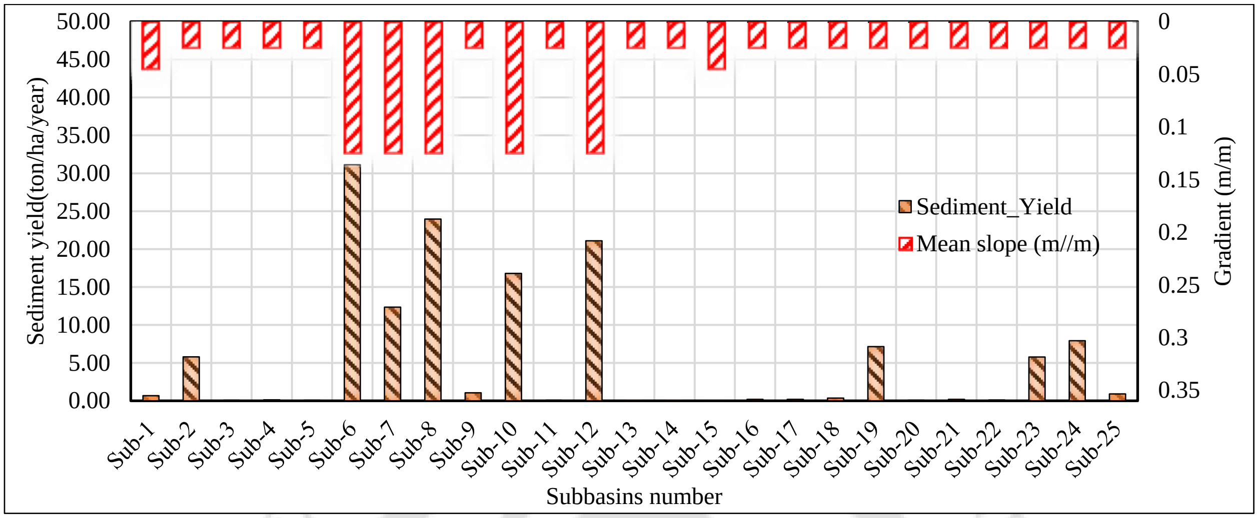

Figure 3. 9 Spatial plot of sediment yield against a gradient sub-basin wise from 1990-2013

From Figure 3.9, sub-basins with a steep slope have high sediment yield (sub-6,8,12,10 & 7) while sub-basins with mild slope produced low sediment yield except that sub-19, 23 & 24, which produced slightly low & moderate sediment rate in which their land use/cover was dominated by range brushland and agricultural area.

For sub-2, 3, 4, 5, 11, 13,14 & 16-25 with mean slope looks the same but slightly different in sediment yield, the effects of other physiographic characteristic factors (land use/cover, shape of sub-basin, area of sub-basins) might be over dominated the visibility of slopes. The slope was taken average/mean; that is why its slope result is approaching each other. Moreover, if we explore the HRUs scale, their slope is also different, as we have seen particularly for HRUs in Sub-6.

3.2.5.2 Temporal variability at sub-basins scale

The temporal variation of sediment yield was evaluated over the entire Genale Basin using the monthly-simulated SWAT model. According to the results, the average sediment yields obtained during May and October are almost double the sediment yields in other months (Figure 3.10).

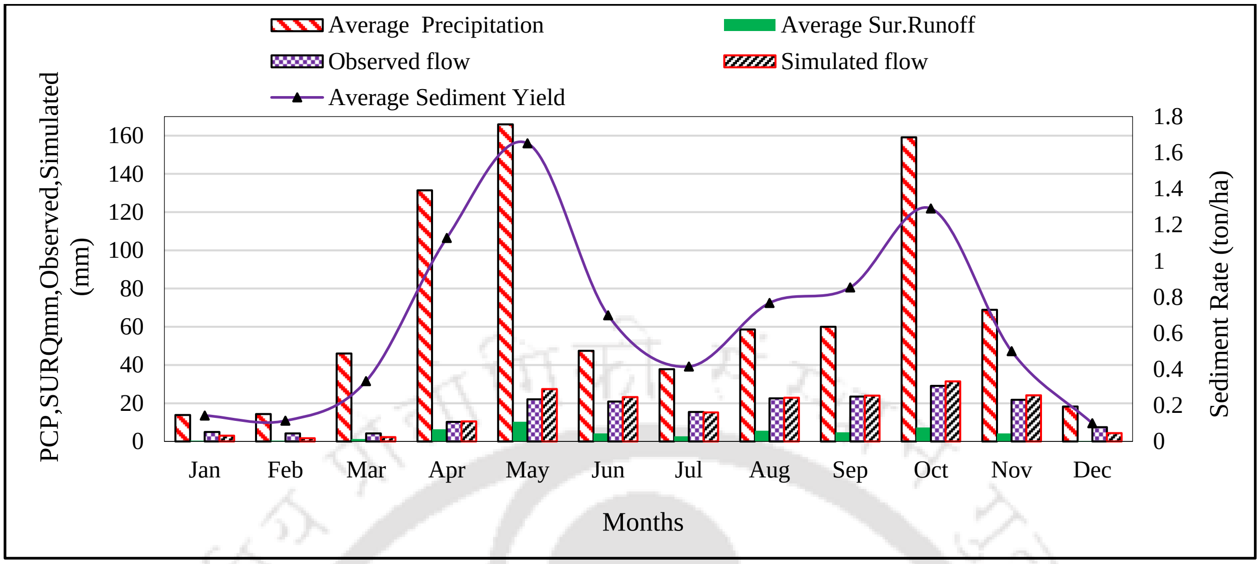

Note: PCP-precipitation; SURQmm-surface runoff

Figure 3. 10 Temporal variability of sediment yield with runoff, precipitation, observed and simulated flow monthly

The temporal variability of sediment yield distribution in the study area is divided into five sediment yield classes; meager erosion time (January, February, and December), low erosion time (March, July, and November), moderate erosion time (June, August & September), high soil erosion time (April) and very severe soil erosion time, which was in May and October (Figure 3.10). It is observed that high sediment yield occurred in May, October, April, September, August, and June, whereas low sediment yield was observed in November, December, January, February, and March. The average temporal variability of sediment yield is 0.667ton/ha. The temporal variability of sediment yield is positively correlated with rainfall distribution, streamflow, and surface runoff (Figure 3.10).

3.2.6 Spatial and temporal variability of sediment yield at HRUs level

To understand in-depth about critical erosion areas, further investigation at the HRUs scale is very important to avoid confusion when land use/cover, slope, and soil type are in doubt. Besides, it helps the stakeholders more when resources like finance, human power, time, and land availability are limited. Furthermore, this investigation allowed us to identify those parts where soil losses are very severe and need prioritization.

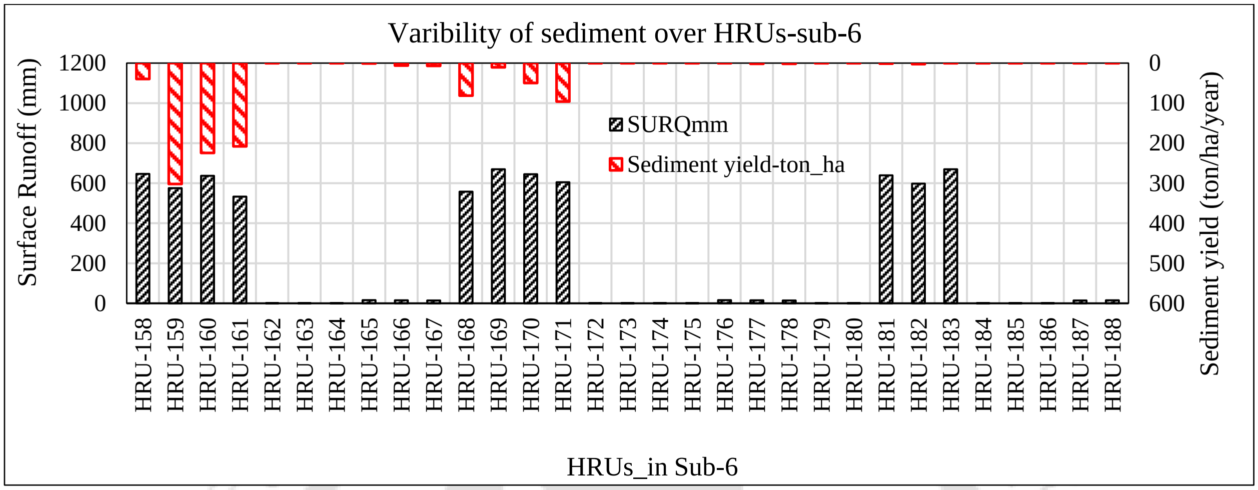

SURQmm-surface runoff, HRUs- hydrologic response units, Sub-6-sub-basin number 6

Figure 3. 11 Spatial variability of sediment yield for the Genale watershed at the HRU scale for subbasin-6

The HRUs with higher surface runoff were intended to generate significant sediment yield, but HRU-181,182 &183 has limited sediment yield because the land use/cover over the areas is mixed forest, which curbs and arrest sediment yield (Figure 3.11). Figure 3.11, among the 31 HRUs scattered in sub-6, only HRU-158, 159, 160,161,168, 169, 170, and 171 are erosion-prone areas in sediment rate while others are insignificant. The erosion-affected HRUs are located in highly agricultural and steep slopes. Economically, to encourage management practice and discouraging catchment mismanagement, identifying soil erosion-prone areas is vital, particularly at the HRUs level. The same steps should be followed for other HRUs in other sub-basins of the Genale watershed.

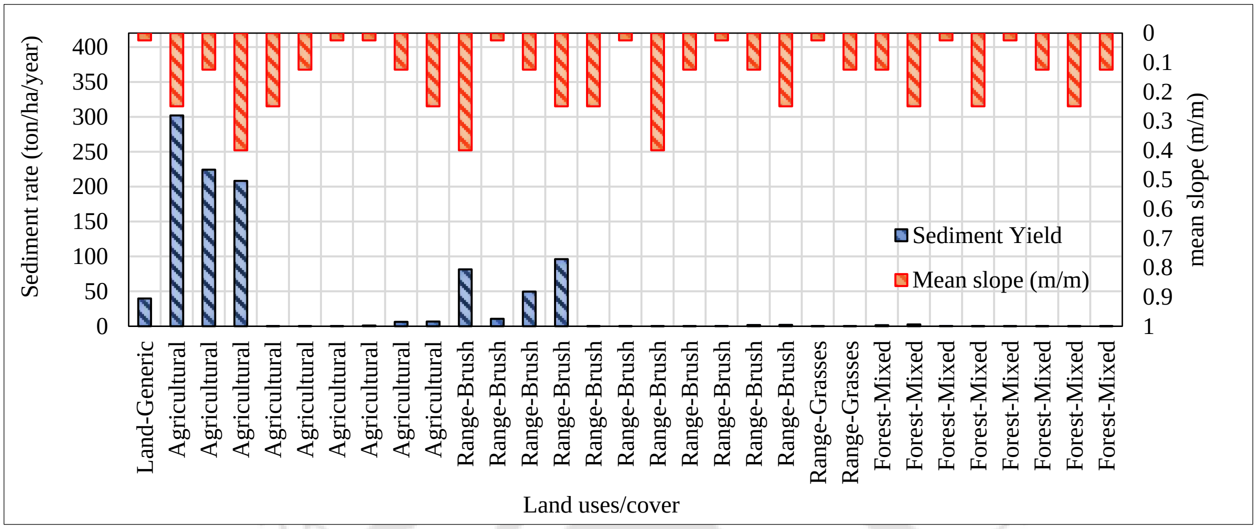

Figure 3. 12 Effects of Land use/cover and gradient on sediment yield at HRUs level for subbasin-6

Figure 3.12 shows the influence of slope/gradient, land use/cover on sediment yield. The HRUs with a steep slope, agricultural, & range brush land cover produced high sediment yield (rate) in the catchment, particularly in sub-6. On the other hand, HRUs (HRU-181, 182, & 183) from Figure 3.11, which exhibits recognizable surface runoff, did not contribute significant sediment yield (Figure 3.12) due to the land use/cover effects (forest mixed) dominated over the influence of surface runoff and slope. Figure 3.12, a particular HRU-174 with a high gradient (steep-slope) produced very low/insignificant sediment yield due to non-recorded surface runoff in that particular hydrologic response unit, as seen in Figure 3.11. Analysis at HRUs level in the subbasin-6 has revealed an interesting fact that the magnitude of sediment yield, precipitation, and surface runoff is relatively higher at the HRU level than at the sub-basin level (Figure 3.11 & 12). This is basically because of the averaging effect at the sub-basin level. From Figure 3.13, a very high sediment yield was recorded in 1996 & 1997 (66.3 and 58.5 ton/ha, respectively), while the lowest sediment yield was obtained in 2005 & 2004 (2 and 9.3 ton/ha, respectively).

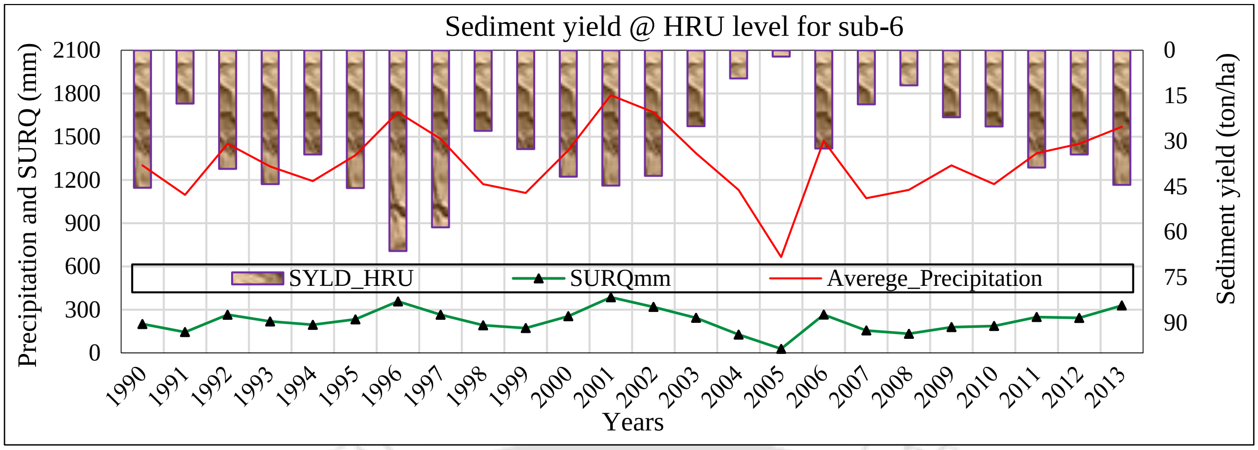

Figure 3. 13 Temporal variation of sediment yield at HRU scale for selected sub-6 from 1990-2013

The temporal variation of sediment yield at the HRU level follows the precipitation and surface runoff graphs in the catchment, i.e., the influence of precipitation and surface runoff is directly proportional to the sediment yield HRU level (Figure 3.13).

3.3. Discussions

Excessive sediment yield from river catchments, particularly in the fast-growing, developing world, is now becoming a global concern. Therefore, identifying sediment contributing areas within the catchment in a more precise manner is necessary to implement management measures at optimal cost and effort. A hydrologic modeling-based approach presented in this chapter has demonstrated its applicability in the Genale Watershed of Ethiopia. Widely used semi-distributed physically-based hydrological model SWAT integrated with ArcGIS is applied after calibration and validation using available streamflow and sediment transport data from 1990-2013. Successful implementation of the model has helped identify the soil erosion critical regions at sub-basins & hydrologic response units (HRUs) scale to prioritize the needful watershed management in the Genale basin, Ethiopia, based on the sediment yield and sediment delivery ratio (SDR). In addition to proposing this generalized modeling-based approach, our effort was also towards the regional importance, as identification of soil erosion critical sub-basins or at HRUs scale providing vital information to help watershed management/decision making for solving the community problem adopting early watershed management measures in the catchment is not yet reported in the study area.

The consistency of precipitation data can always be questioned in such a less explored basin. Therefore, consistency of precipitation data was ensured by using a double mass curve (DMC), evaluating the adjustment (correction) factor at the deviation point (between cumulative plot & linear trend line analysis), and distributing the adjustment factor by multiplying the data that need to be adjusted and then checking the correlation coefficient R2 (Owolabi et al., 2021; Gao et al., 2017).

Historical daily data of sediment concentration was available from October 20, 1987, to October 1, 2005, but since streamflow data was available from 1990-2013, the suspended sediment record was systematically extended to make its length equal with the streamflow period to meet the requirement of calibration and validation process. This is achieved by developing a sediment rating curve (SRC) (Mohammadi et al., 2021) and predicting sediment concentration from 1987 to 2013 continuously monthly to perform the required calibration and validation for 27 years, which is standard practice for the data-scarce region as supported by different report/research (Fig. 4). The previous study by Ulke et al. (2009) used from 1971 to 1985 data range for streamflow & sediment load calibration and validation; the study by Uniyal et al. (2020) used from 1999 to 2003; the study by Markhi et al. (2019) used streamflow and sediment data from 1990 to 2015; the study by Liu et al., 2019 used from 2006 to 2013 for sediment validation; Setegn et al., 2010; Xu et al., 2009; Meshram et al., 2020 also used the data range for sediment calibration & validation from 1984-1993, 1986-1991, 1990-2015 respectively which convinced the validation of the present study on Genale watershed as far as the data range is concerned.

Compared to other empirical models, the convenience of using the SWAT-MUSLE model include better prediction accuracy with less uncertainty, considers watershed physiographic characteristics (land use/cover, soil type, topography, climate, drainage area), and the ability for single storm estimates of sediment yield (Neitsch et al. 2011). Therefore, a physically-based and spatially distributed model that can simulate channel transport processes is more suited to calculating SDR for watershed planning and decision-making.

The prediction of sediment yield is profoundly sensitive to different sub-basins sizes due to the sensitivity of different parameters that mimic the topographic factors. The MUSLE equation is a function of the peak rate of runoff, which is again a function of time of concentration, a variable dependent on the channel length from the remotest point to the sub-basin outlet.

In the Genale catchment, sub-basins with high gross erosion but low sediment yield produce a small value of SDR, which means that SDR is directly related to sediment yield at a sub-watershed outlet (Figure 3.6). This is because the sub-basin SDR is expressed as a ratio of sediment yield from an area to the gross/total soil erosion of individual sub-basin of the same area and represents the efficiency of the sub-basins in transporting soil particles from areas of erosion to the point where sediment yield is measured. For instance, sub-basins 15, 16, 20, 21, & 25 have very high gross erosion but produce very low sediment yield, resulting in low SDR in the sub-basins (Figure 3.6).

The magnitude and change of sediment impacts were significant at a smaller scale whereas relatively small at the sub-basin scale due to compensating effects. Detail analysis of HRUs' response of sub-6 has clearly shown that while some of the HRUs contributed very high towards sediment yield and surface runoff, large numbers of HRUs contribute minimal. This gives a better opportunity to identify the most sensitive area needing treatment. However, sub-basins analysis is still essential to identify priority sub-basin that needs urgent attention.

In general trends, the highest SDR values were produced by sub-basins with high sediment yields and were in proximity to the watershed outlet (in terms of stream distance), but in some watersheds, the same might not have happened (Woznicki & Nejadhashemi 2013; Walling (1983), Bartholic (2004). However, only on few occasions, sub-basins in the Genale watershed located close to the watershed outlet have relatively low SDR because there are limits of sediment transported from sub-basins to the watershed outlet. Therefore, deposition and stream processes are also affecting SDR and physiographic characteristics that dictate erosion potential. The study by Gelagay (2016), Mutua & Klik (2006); Lu et al. (2006); Woznicki & Nejadhashemi (2013), and Walling (1983) used the division range of SDR to identify the critical erosion area for watershed management. Ranges of SDR to indicate a degree of importance to help prioritization are slightly modified in this study based on the evaluated sediment rate and the number of ranges needed to facilitate a sequence of implementation for critical sub-basins prioritization.

Other methods produced almost similar results to SWAT-MUSLE for the Genale basin. The SWAT-MUSLE estimation for the Genale watershed indicated that 19% of all sediment entering a stream reach would be transported to the watershed outlet. Therefore, a physically-based and spatially distributed model that can simulate channel transport processes is more suited to calculating SDR for watershed planning and decision-making.

Identifying the most erosion-critical areas has a regional importance and will help the local government authority and other stakeholders involved in soil and water conservation activities within the Genale catchment.

The present study can be further extended to include estimating other pollutants that may affect the water quality. Data used in this study are up to 2013; therefore, more recent data can be used if actual field implementation is taken up. Also, the result can be compared with that of physically-based distributed SDR & sediment yield calculation, which considers local physiographic characteristics, such as rainfall, topography, vegetation, land use, and soil properties. With the increasing availability of satellite data of high spatiotemporal resolution, using up-to-date weather data range, more detailed study can be taken up to get an idea about delivery of other pollutants in the catchment to address some emerging issues of environmental and ecological concerns.

3.4. Conclusions

The Soil and Water Assessment Tool (SWAT) model used DEM, land use/cover, soil type, and slope characteristics as input for the Genale watershed, which created 25 sub-basins, 464 HRUs, and a drainage area of 54,942Km^2. The model is calibrated/validated for streamflow, and sediment load monthly, and final model parameters were fixed based on acceptable statistical performance and sensitivity analysis. The uncertainty analysis of streamflow and sediment was carried out for three years warm-up period from 1987 to 1989, 16 years calibration period from

1990 to 2005, and 8 years validation period from 2006 to 2013 by using SWAT-CUP (SUFI-2) program.

Identifying spatial and temporal variation of critical erosion-prone areas in the whole Genale watershed was made to adopt management measures, sub-basin prioritization using sediment delivery ratio (SDR) and sediment yield methods at sub-basins/ HRUs scale. Among 25 sub-basins, both ways revealed that the sub-basins 6, 8,12, 10, and 7 are very high erosion-prone areas and need management measures. The output from the Genale watershed indicated that significant portions of the regions known to be highly agricultural, steep slope, poor soil physical properties are more critical to soil erosion and sediment yield. Therefore, prioritizing catchment at sub-basins and HRUs can be a better proposal for integrated soil & water conservation measures.

Economically, to encourage management practice and discouraging catchment mismanagement, identifying soil erosion-prone areas is vital, particularly at the HRUs level. Out of 31 HRUs dispersed in sub-6, only HRU-158, 159, 160,161,168, 169, 170, and 171 were assessed as erosion-prone areas in terms of sediment rate. Application of management practices across the whole watershed/sub-basin is very time-consuming, tedious, laborious, and costly. The magnitude and change of sediment impact from land use, slope & soil type were significant at a smaller scale whereas relatively small at the sub-basin scale due to compensating effects. As we explore analysis further until HRUs scale, the critical area of sediment impacts is more visible, and it becomes easier to address the challenges with low human resources, low cost, and within a short time with a better understanding about the area and acting accordingly. Analysis at the HRUs scale response of sub-6 has given significant insight into the locations needing management practice within the catchment on a priority basis. This approach provides information to recognize the most erosion-critical area facilitating even local bodies to take management measures locally.

This study has demonstrated the SWAT model's adequacy and capability in assessing critical areas needing sediment management in the Genale watershed in Ethiopia, which may inspire other researchers to implement in other watersheds to identify erosion critical area and prioritize at sub-basins HRUs level.

Chapter 4

Sustainable and Cost-Effective Management of Degraded Sub-Watersheds Using Ecological Management Practices (EMPs) for Genale Basin, Ethiopia

4.0 Introduction

Accelerated erosion and increased surface runoff due to the lack of proper management of watersheds have raised global concern. The loss of soil by water action is one of the fundamental factors adversely affecting reservoir capacity, deteriorates surface water quality, reduces agricultural land productivity, and the sustainable use of surface water resources (Kefi et al. 2011, Mtibaa et al. 2018, Song et al. 2018). Excessive precipitation, inadequate vegetation cover, topography, and intensive agriculture practices are the leading causes of watershed degradation and call for management practices (Pimentel and Burgess 2013). The challenge is amplified in developing countries where agricultural practices and urbanization are rapid and unplanned (Patowary et al. 2019, Vijith and Dodge-Wan, 2020). Thus, the modelers and planners need to critically look into the sub-catchment level issues to help developing policies/plans for sustainable management. Land-use land-cover (LULC) management practices play an imperative role in the planning and managing the watershed. Uniyal et al. (2020) advocated that identifying critical erosion-prone areas and selecting best management practices for watershed management is necessary to stop further degradation and reduce sediment yields. In recent years, applying the Modified Universal Soil Loss Equation (MUSLE) available in the Soil and Water Assessment Tool (SWAT) model for simulating impacts of management practices on sediment yield, water yield, and NPS pollution has attracted researchers' attention (Arnold et al. 1998, Bieger et al. 2015, Epelde et al. 2015, Ma, D et al. 2020, Winchell et al. 2015). SWAT is widely accepted because of its powerful algorithms for simulating the hydrologic systems and its comprehensive database on agricultural management practices (Arabi et al., 2008). MUSLE provides an option for incorporating management practices at a catchment level for structural and non-structural/agricultural management practices (Neitsch et al., 2011).

From the beginning of the 21st century, assessing catchment water yield and implications of different management practices at watershed levels is becoming a practical approach before suggesting solutions toward watersheds degradation. Nature-based solutions include soil and landscape approaches in which soil solutions include distinct practices like inter-cropping and mulching on the agricultural fields to improve the soil's health functions, whereas landscape approaches deal with the change of LULC like conversion of agricultural fields to wetlands (Uniyal et al. 2020, Mtibaa et al. 2018, Hunink et al. 2013). In the option of Best Management Practices (BMP) in SWAT, structural management practices include streambank stabilization, grassed waterways, contour farming, terracing, stone bunding and filter strips, and non-structural/agronomic management practices include bio-retention, forest, contour farming crop rotation, and tillage practice (Tuppad et al., 2010, Briak et al. 2019). Strauch et al. (2013) evaluated the performance of terracing, retention basins, and crop rotation towards maintaining the sustainability of an intensively agricultural watershed and established that they could significantly reduce the sediment load by 40% without affecting the catchment's water yield. However, applicability to a particular watershed should be evaluated via watershed modeling as each watershed has its characteristic behavior (Wang et al. 2019, López-Ballesteros et al. 2019). Therefore, watershed modeling is an essential research tool for planning, designing, operating, and managing watersheds at the sub-basins/Hydrologic Response Units (HRUs) level. These can integrate information over large spatiotemporal scales and simulate various watershed processes over a long time, such as surface runoff, soil erosion, transport of nutrients, and NPS pollutants (Wang et al. 2019). With the help of a physically-based semi-distributed watershed model, critical sub-basins areas can be identified to effectively apply management practices to prevent or reduce soil erosion and improve water quality aspects. The MUSLE model has the advantage over other watershed models in incorporating site-specific conditions, basin characteristics, and different extent of agricultural management practices and onsite practices (Mtibaa et al. 2018).

Ecological Management Practices (EMPs) assign nature-based solutions described as "eco-friendly sustainable management practices used for preserving and enhancing land uses naturally" and stabilize sediment yield and peak surface runoff in a sustainable and economically viable manner. Selection of an optimal combination of EMPs needs to be done due to constraints like space availability, financial constraint, and land ownership (Singh et al. 2020, Sarma et al. 2015, Dolowitz et al., 2018). Management of watershed sediment yield must incorporate nature-based solutions for sustainable, pollution-free, and economically viable LULC management. An optimal combination of EMPs resolved by employing the hydrological model and inspecting the performance of different EMPs combinations through a simulation optimization model can sustainably reduce sediment risks and maintain ecological benefits. However, for non-developed countries, the primary challenge is to identify the most critical area, so that maximum benefit can be obtained by implementing EMPs in the minimum area at affordable cost. Unplanned urbanization and unorganized agricultural practices in developing countries result in a very high degree of surface plug and erosion of soil. The non-availability of detailed land-use data in an organized way makes model application difficult.

The application of sustainable land-use allocation and management for ecological and economic benefits requires extensive optimization techniques. Sarma et al. (2015) and Patowary et al. (2019) launched a linear programming model (OPTEMP-LS) for single ownership on a steep area to resolve the optimal combination of EMPs to minimize cost within the constraint of annual sediment yield and peak flow rate. Another study (Singh et al. 2020) used a non-linear programming optimization technique to derive optimal EMPs combination to reduce flood risk in a semi-urban watershed. Another study focused on evaluating and identifying the environmental suitability and cost-effectiveness of various management practices scenarios regarding sediment yield reduction at the sub-basin level (Mtibaa et al. in 2018).

In the current study, an optimization problem is formulated to minimize cost subject to the non-linear constraint of sediment yield, linear constraints of peak discharge and area suitability by utilizing HRUs level study in identifying the most critical erosion-prone area within a prioritized sub-basin.

The present study provides essential information to help decision-makers reduce sediment yield & peak discharge at an affordable cost and give feasible EMPs combinations for future soil and water conservation strategies in the Genale catchment, as the watershed is exposed to excessive degradable/soil erosion due to high precipitation and runoff in the critical region. Applying the OPTEM-LS model and the semi-distributed MUSLE - SWAT model in tandem has helped identify the optimal combination of EMPs and their spatial distribution to help field implementation at minimum cost and without ambiguity. These analyses serve as a powerful tool for the policy and decision-makers to formulate effective management measures for safeguarding vulnerable sub-basins/HRUs against the impacts of degradation/soil erosion at minimum cost.

Refer Figure 1.2 shows the map indicating the location of the study area with the Digital Elevation Model (DEM) extracted from the Ethiopia map.

For this study, the DEM was downloaded from USGS Earth Explorer (http://earthexplorer. usgs.gov) SRTM (Shuttle Radar Topography Mission) 90 m used for catchment delineation, sub-basin creation, and slope classification. The slope consists of five classes, of which 5 - 20% was dominating the study area. The LULC data collected from the GIS department of the Ethiopian Ministry of water, irrigation, and electricity (MoWIE) for the year 2013 is used for MUSLE-SWAT input. The dominant LULC is range brush (RNGB), covering about 71% of the study area. The soil map was downloaded from the World Digital Soil Map of the Food and Agricultural Organization (FAO) (http://www.fao.org/geonetwork/srv/en/metadata) scale 1/5000000 for 2007. The dominant soil type in the study watershed is Rc19-bc-204 (Calcaric Regosols), and it covers about 40% of the study area (Figure 4.1).

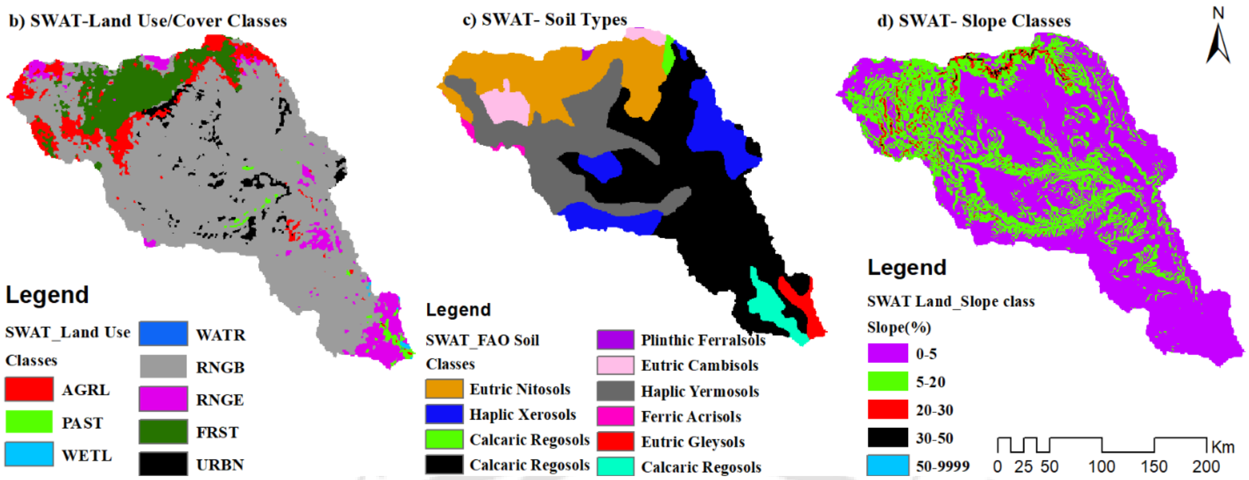

Figure 4. 1 SWAT- land use/cover, soil type, and slope classes of the study area (1990-2013)

4.1 Materials and methodology

The application of land use-based solutions for controlling watershed sediment yield at the sub-basin scale requires dealing with different challenges like the availability of space/area and the suitability of EMPs. Based on the rates of sediment yield estimated over 24 years (1990-2013) using Modified Universal Soil Loss Equation (MUSLE) of Soil and Water Assessment Tool (SWAT) model, the most erosion-prone sub-basins in the Genale watershed was identified for the planning/management. Based on the annual average sediment yield obtained from the model at respective outlets of sub-basins, critical areas were located, and base values for the performance evaluation of selected EMPs were computed. To minimize the cost of EMP implementation using combinations of EMPs as an optimized variable, a non-linear programming method of MATLAB optimization toolbox was used. EMPs application cost differs based on constraints like targeted peak runoff, sediment yield, and area availability for different EMPs.

The MUSLE in SWAT discretized Genale watershed, Ethiopia, to generate streamflow, predict sediment yield, identifying critical erosion areas, and estimate optimal cost and space availability for EMPs combinations (Figure 4.2).

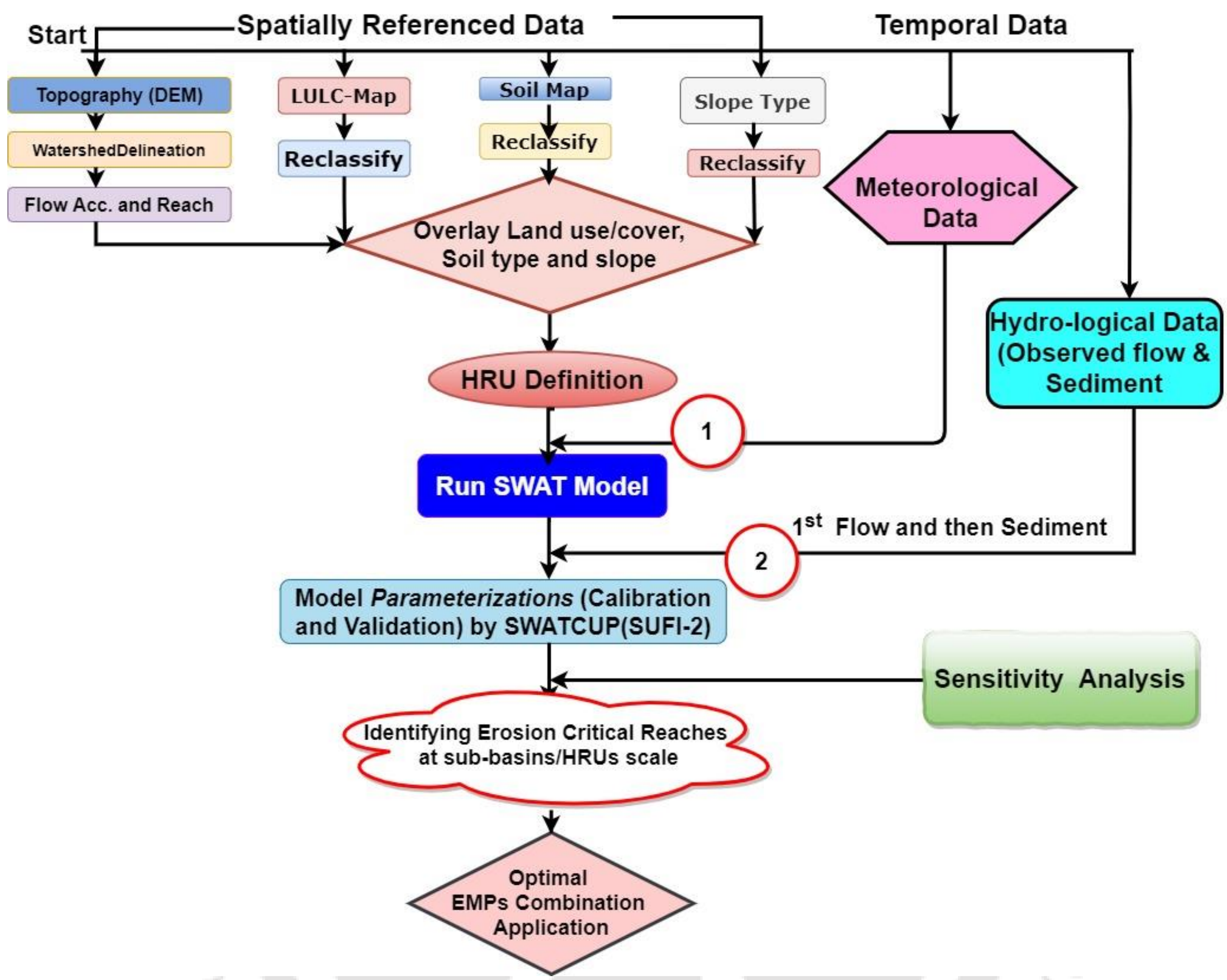

Figure 4. 2 Work flow chart of the study methodology (steps required to flourish the activities of SWAT model

The current SWAT model evaluates surface erosion and sediment yield due to runoff for each HRUs using equation 1 (MUSLE) (Williams 1975).

$$Q_{SED} = 11.8*(Q_{peak}*Q_{Surface}*A_{hru})^{0.56} * K_{USLE} * C_{USLE} * P_{USLE} * LS_{USLE} *CFRG \qquad (4.1)$$

Where; Q_{SED} = sediment yield (ton/ha/day) from specific HRU, $Q_{Surface}$ = surface runoff (mmH2O/ha/day), A_{hru} = area of HRUs in (ha), Q_{Peak} = peak discharge (m^3/s), K_{USLE} = soil erodibility factor, C_{USLE} = cover and management practice factor, P_{USLE} = conservation support practice factors, LS_{USLE} = topographic factor, CFRG = coarse fragment factor.

Soil Erodibility Factor (K) (Mg h MJ^{-1} mm^{-1}) is the soil resistance to erosion and susceptible to different soil properties, transportability of sediment yield, and runoff rate for specific rainfall input. The K-factor can be estimated based on the values of soil parameters (texture, organic matter (OM), structural and permeability class) (Wischmeier et al. 1978).

K (factor) = 27.661* $m^{1.14}$ *(12−OM) +0.0043* (s−2) +0.0033* (p−3) (4.2)

$$m = [(100 - C)(h + a)] \quad (4.3)$$

'C' is % of clay (< 0.002 mm), 'h' is % of silt (0.002 - 0.05 mm), 'a' is % of very fine sand (0.05 - 0.1 mm), OM is the organic matter content (3-6%), s = structure size code, which is (1) very structured or particulate; (2) is fairly structured; (3) is slightly structured; (4) is solid: The soil in the study basin is found to be in the category of slightly structured. Therefore, s = 3, p = class of permeability code (Pérez et al., 2007), in which (1) is rapid; (2) is moderate to rapid; (3) is moderate; (4) is moderate to slow; (5) is slow; (6) is very slow. Hence, p = 4.

Table 4. 1 Properties of the Genale watershed for soil erodibility factor (K)

Serial number	Soil properties	Value ranges
1	Silt (%)	15
2	Sand (%)	24
3	Clay (%)	61
4	Class Texture	Clayey Loam
5	Drainage	Well-drained
6	Organic matter (%)	4.6
7	Density	2.5

Therefore, the K-factor for the Genale watershed was found based on the FAO digital soil database (http://www.fao.org/land-water/land/land-governance/land-resources-planning-toolbox/category/details /en/c/1026564/). Hence, the soil structure is slightly structured and has moderate to slow drain.

$$K = 27.661 \times \left((18 + 26) * (100 - 56)\right)^{1.14} \times 10^{-6} \times (12 - 4.6) + 0.0043 \times (3 - 2) + 0.0033 \times (4 - 3)$$

K=0.147 Mg h MJ−1 mm−1

Topographic Factor (LS): The combined effects of slope-length and slope-gradient represent the ratio of soil loss per unit area on a field to the corresponding loss from 22.13 m length on the same soil type of a uniform with 9% slope (Wischmeier et al. 1978). It can be determined using remote sensing and GIS techniques. The SRTM DEM grid size used in the Genale study area was 90 m*90 m; the evaluated value of LS used 90 m (i.e., Z = 90 m).

$$LS = \left(\frac{z}{22.13}\right)^{y}(0.0654 + 0.0456b + 0.00654b^{2}) \qquad (4.4)$$

Where; LS=slope steepness length factor, Z is the slope length (m), b is slope/gradient steepness (%), y is the dimensionless exponential (ranges from 0.2 for slope ≤ 1% to 0.5 for slope ≥ 10%)

Cover and Management Factor (C); the erosion capacity of surface runoff can be affected by vegetation cover by changing the hydrodynamic characteristics of surface runoff (Gelagay and Minale 2016, Singh et al. 2020). The cover management factor for an area classified as water body was taken as '0', agricultural (AGRL) (0.25), range brushland (RNGB) (0.014) represents cover, and management factors used in the erosion critical study area (Duraes et al. 2016).

Conservation Support Practice (P) Factor: The ratio of soil loss with a particular support practice to the corresponding loss from an agricultural area up and down the slope. It has to be taken as '1', assuming no support practices within the watershed.

Course Fragment Factor (CFRG): This can be estimated using equation (5):

$$CFRG = \exp(-0.053 * Rock) \qquad (4.5)$$

Whereas; Rock is the percentage of the soil layer in the uppermost, and it is evaluated by applying the empirical formula (Poesen et al. 1998), which computes rock fractions based on the sub-basins slope. In this study, 20% of the uppermost soil layer is assumed to be a rock. Therefore, CFRG = exp (−0.053 × Rock) = exp (-0.053*0.2) = 0.98

4.1.1 Estimation of Surface runoff ($Q_{Surface}$)

Surface runoff is computed by the daily runoff model using the Soil Conservation Service (SCS) Curve Number (CN) method. This technique is extensively used to predict watershed discharge from a given rainfall event mainly based on soil properties, slopes, land use, and hydrologic moisture condition (Arnold 1998, Momm et al. 2017).

$$Q_{Surface} = \frac{(P-0.2S)^2}{(P+0.8S)}\text{ ; for } P > 0.2S \tag{4.6}$$

The retention parameter(S) and prediction of lateral flow by the SWAT model is expressed as;

$$S = 254\left(\frac{100}{CN} - 1\right) \tag{4.7}$$

$$CN = \frac{25400}{S+254}\text{ ; has a range in between } 0 < CN < 100$$

CN = 100; represents zero potential retention (i.e. impervious catchment), CN = 0, represents an infinitely abstracting catchment with S = ∞, Where; P = daily rainfall, S = Potential retention (mm/day), CN = curve number.

4.1.2 Determination of maximum and minimum peak discharge of watershed

For aquatic ecological functions and maintenance, a sustainable water flow in the channel is very important. The peak discharge generated by a watershed at its outlet for a natural condition before human intervention, i.e., with a natural vegetative cover, can be used as an index of a healthy watershed. In such situations, the watershed does not suffer accelerated erosion due to anthropogenic activities. This condition will provide all required elements for aquatic ecological functions, and hence it is not desired to reduce the flow beyond this discharge and therefore considered the minimum peak flow limit. From the perspective of sediment management, the minimum and maximum limit of allowable peak discharge do not create a sheet, rill, floodplain erosion, and the watershed's natural drainage activity is not affected (Jia et al., 2011). Based on the above, to keep the ecosystem healthy with the natural flow condition, the peak discharge value obtained with the undisturbed natural cover condition using rational formula was considered the lower limit of peak discharge (Q_{min}). If the watershed area (A) is in km^2, the intensity of rainfall (i) is in mm/hr, and RC is the runoff coefficient, then the runoff rate is given by (Chin 2019).

$$Q_{peak} = \frac{RCiA}{3.6} \tag{4.8}$$

The intensity of rainfall used in the equation above should be corresponding to a duration equal to the time of concentration and desired return period. This requires an estimate of concentration time, which can be computed by using different empirical formulas. We have used the widely used empirical equation given by Kirpich (1940) to calculate concentration-time and peak discharge for baseline conditions and different EMP combinations. Although it may vary using different formulas, the absolute value of peak discharge will not significantly influence the result of the optimal EMP combination, as the optimal combination is decided based on its comparison with baseline condition and thus is a comparative study.

$$t_c = 0.01947 L^{0.77} \Delta S^{-0.385} \tag{4.9}$$

where t_c is a time of concentration in min, L is the maximum length of water travel along the watercourse in m, and ΔS is the slope expressed as the ratio of elevation difference between the outlet and remotest point in the catchment/sub-basin to the length. Once the concentration time has been determined, the rainfall intensity can be determined using the intensity-duration-frequency relation applicable to the catchment area. A generalized form is given in equation (4.10) (Al Islam and Hasan 2020).

$$i = \frac{KT^x}{(t_c + a)^n} \tag{4.10}$$

T is the return period in years, and K, x, a, and n are regression constants for a given geographical location, i- average rainfall intensity (cm/hr) and t_c- duration of rainfall (hr.) corresponding to the time of concentration. The soil conservation return period is generally considered ten years (Otim et al. 2019, Mati 2012), for culverts 25 years, and bridges 50 -100 years (Al Islam and Hasan 2020).

The range of runoff coefficients (RC) for different types of the land surface was obtained as; forest (0.05 - 0.25), agriculture (0.1 - 0.4), scrub/brushlands (0.02 - 0.45), and terracing (0.1 - 0.2) (Table 4.2).

Table 4. 2 Summary of model discharge for each prioritized sub-basin

Sub basins under sed. critical	Maximum Sub-basin Path/Length (Km)	Sub-basin Area (Km^2)	Sub-basin gradient, $S=\frac{\Delta h}{L}$	t_c (hr)	Rainfall Station Name	$i = \frac{KT^x}{(t_c + a)^n}$ The constants are specific to the given catchment; T	K	x	a	n	i	RC= R/P	$Q_{P(m^3/sec)} = \frac{RCiA}{3.6}$
Sub-6	119.08	2,315.3	0.0195	11.97	Worka	10	6.75	0.17	0.56	1.03	7.4	0.3	1,427.8
Sub-7	166.32	4,265.4	0.0137	17.73	K/Mengist	10	8.65	0.19	0.75	1.05	6.3	0.21	1,567.5
Sub-8	73.9	1,191.1	0.0191	8.35	Angetu	10	4.85	0.18	0.46	0.89	10.6	0.22	771.6
Sub-10	110.2	1,456.3	0.0197	11.23	GMS7	10	7.66	0.16	0.65	0.95	10.6	0.32	1,372.2
Sub-12	189.2	3,119.5	0.0153	18.77	M/Wolabu	10	5.25	0.15	0.55	1.02	3.6	0.27	842.3

Maximum allowable peak discharge (Q_{min}) is decided based on the carrying capacity of the downstream channel, as presented in equation 4.11.

4.1.2.1 Estimation of carrying capacity of the channel/reach

The maximum permissible peak discharge (Qmax) was evaluated based on the principle that the peak flow generated from a well-managed sub-basin for a design rainfall intensity should not cause flooding at immediate downstream (Sarma et al. 2015). Qmax was calculated by computing the flow carrying capacity of a most efficient channel section that can be conveniently installed at the outlet of each prioritized sub-basins (Figure 4.3) and (Figure 4.4) to carry away the flow safely. It follows the regime approaches for natural alluvial channels since it is a mobile boundary (unlined channel). For the unlined channel in the alluvium channel, the allowable velocity and the discharge should be checked for the stability of the channel to avoid scouring or silting. We may estimate the corresponding Manning's roughness coefficient 'n' for the given sediment particle size using Stricker's formula given by equation 4.12 (Li et al. 1976). Channel carrying capacity is the maximum rate of discharge that the channel/reach can carry without overflowing. We can estimate the carrying capacity for the unlined channel using Manning's equation when sediment particle size in the channel is specified.

$$Q = \frac{1}{n} A\, R^{2/3} \alpha^{1/2} \tag{4.11}$$

$$n = \frac{d_s^{1/6}}{25.6} \tag{4.12}$$

Where; n Manning's roughness coefficient, d_s grain size in (mm), α channel bed slope, Q- streamflow of the channel (m3/sec), R-hydraulic radius (m), A- cross-sectional area flow (m^2).

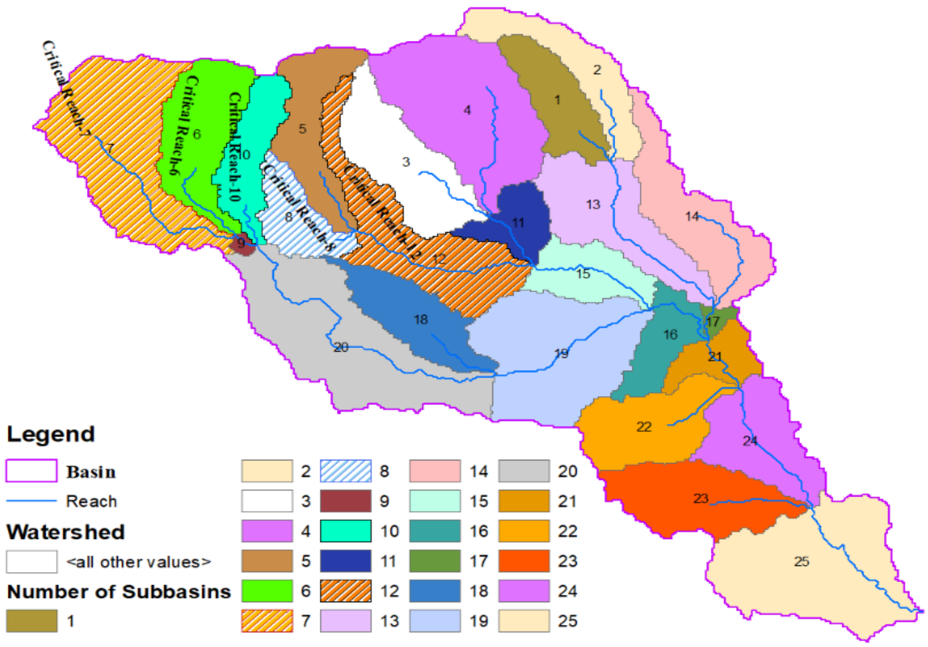

Figure 4. 3 Identified critical reaches for EMPs implementation within the Genale watershed

The safe carrying capacity of a trapezoidal unlined natural channel carrying sediment particles was estimated using Manning's equation, which was used as the upper bound of maximum allowable discharge. EMPs were planned so that the peak discharge generated by the design storm remained within this limiting value.

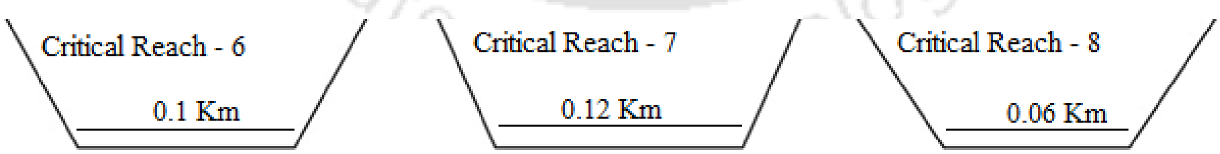

Figure 4. 4 Cross-section detail for the selected critical reach at sub-basin outlet to estimate channel carrying capacity

The prismatic channel section was considered to calculate the carrying capacity of the channel at the outlet of the basin/sub-basin, where peak discharge is calculated. The dimension of the short prismatic reach at the outlet was determined approximately based on the available width of the natural channel, as observed in satellite data, and then considering the channel to be of hydraulically efficient section (Figure 4.4). Figure 4.4 is helpful in calculating each critical reach's carrying capacity to provide a safe and non-flooding channel. For the available longitudinal slope of different ranges based on the sub-basins number & widths, a trapezoidal natural channel's safe carrying capacity was estimated and used as the upper bound of allowable peak discharge.

4.1.3 Selection of Potential Ecological Management Practices (EMPs)

The potential EMPs were selected based on existing agricultural practices, socio-economic aspects, locally available environmentally sustainable materials/native species, space availability, and geography of the study area. To suggest the relevant EMPs for the study area, the effects of these EMPs on sediment yield at the sub-basins level were evaluated for the watershed. After checking the percentage of vulnerable land-use regions present in the basin, locations for EMP application were decided, as economically, it may not be possible to cover all areas by EMPs within the watershed at a time. Accordingly, the selected potential EMPs applied to the site based on the unique soil types, land use cover and slope types of lumped HRUs created within the critical sub-basins are different from sub-basin to sub-basin. After checking the HRUs report analysis, the percentage of area covered by different EMPs is as follows; for critical sub-6, 7% contour forming, 9% grassed waterway, 6% terracing, 4% streambank stabilization, and 8% filter strips. Likely, for sub-7, 9% contour forming, 11% grassed waterway, 5% terracing, 3% streambank stabilization, 10% filter strips, etc. These five EMPs were considered based on land suitability and ease of implementation. The effectiveness of EMPs scenarios was estimated by comparing each one with the baseline scenario to obtain a percentage of sediment reduction using equation (4.13) (Uniyal et al. 2020).

$$\text{Effectiveness}(\%) = \frac{\text{Sed}_{\text{yld}}@\text{ baseline} - \text{Sed}_{\text{yld}}@\text{ EMPs}}{\text{Sed}_{\text{yld}}@\text{Baseline}} * 100 \tag{4.13}$$

4.1.4 Simulation of EMPs

The simulated EMPs included terracing, grassed waterway, filter strips, streambank stabilization, and contour farming for the selected critical sub-basins. A brief description of each EMP representation in the Arc SWAT before (pre-EMP) and after (post-EMP) condition is shown in Table 4.3 The model parameters and their values updated/modified the calibrated values and represent them in post-EMP conditions given in Table 4.3.

Table 4. 3 Model parameters' value used to represent EMPs/BMPs in the SWAT model

Types of EMPs used	Purpose of EMPs	SWAT parameters' input file extension	Value of EMPs in good condition for the implementation	References
Terracing	Reduce overland runoff to a safe outlet and reduce sheet & rill erosion and reduce slope length	CN_2 (.mgt) USLE_P(.mgt) SLSUBBSN (.hru)	Calibrated CN_2.mgt reduced by 5 0.10, if slope = 1 to 2% 0.12, if slope = 3 to 8% (0.1*SLOPE+0.9) *100/SLOPE	Tuppad et al. (2010), Uniyal et al. (2020). Arabi et al. (2006)
Filter Strips	Reducing overland flow velocity and reducing runoff volume & contaminants	FILTER-W (.mgt)	10m width of filter strips (Directly placing into the Arc SWAT).	Arabi et al. (2008), Tuppad et al. (2010).
Grassed waterway	will increase sediment trapping in a channel segment by reducing flow velocity, increase channel cover & roughness but reduce channel erodibility	CH_COV (.rte) CH_N_2 (.rte) CH_EROD (.rte)	[0-1], 0 (fully protected) 0.25 0.0 (non-erosive)	Neitsch et al. 2005, Arabi et al. (2008) Arabi et al. (2006)
Contour farming	Reduction of surface runoff by impounding water in small depressions & reduction of sheet and rill erosion	CN_2 (.mgt) USLE_P(.mgt)	Calibrated values of CN2 reduced by 3 0.5, for slope 1 to 2%,	Arabi et al. (2008), Uniyal et al. (2020) Arabi et al. (2006)

Streambank stabilization	To reduce sediment load in stream & maintain channel, reduce gully erosion and slope steepness	CH_COV (.rte) CH_N_2 (.rte) CH_EROD (.rte)	0.25 0.03 0.0 (non-erosive)	Tuppad et al. (2010), Uniyal et al. (2020) Arabi et al. (2006)

Note: CH_COV (.rte) -(Channel cover), CH_N2 (.rte) -(Manning's roughness), CH_EROD (.rte) -(Channel erodibility), CN2 (.mgt)- curve number, FILTERW (.mgt)-width of edge-of-field filter strip (m), USLE_P(.mgt)- support practice factor, SLSUBBSN (.hru)-slope length.

In the SWAT Model simulation, the representation of EMPs combination is also considered and applied to the selected critical sub-basins to explore sediment yield reduction.

4.1.5 Optimization and Cost analysis for different EMPs scenarios

For optimum allocation of EMPs in agricultural and brushland sub-basin areas, hydrological models SCS Curve Number (CN), Rational method, and MUSLE method estimated runoff, peak discharge, and sediment yield, respectively, and their limiting values were put as constraints. Affordability in terms of cost is a significant issue in implementing suitable EMPs for controlling soil erosion. Under resources constraint conditions, farmers use management practices like conservation tillage, terracing, filter strip, forest, buffer strip, and bio-retention at minimal construction and maintenance costs, without explicitly considering their impacts on the natural flow sediment regime. We assessed the effectiveness of combining different management practices following the concept of EMPs and depending on the slope angle and baseline land use/cover of the target area.

Objective function: The objective function (Equation- 4.14) was designed to minimize the total cost of EMPs (construction cost + annual cost of operation and maintenance) in the study area to control the yearly sediment yield and peak discharge within the permissible limits.

Minimize $$Z = \sum_{i=1}^{m}(Cc_i + Cm_i)A_i \quad (4.14)$$

Where: i = 1,2,3….m are the number of EMPs considered for application to the case study area, Cc_i and Cm_i are the construction cost and the maintenance cost of i^{th} EMPs respectively (USD/ha), A_i is the area under the i^{th} EMP and variable need to be optimized in the equation (ha).

The unit costs related to filter strips, grassed waterway, streambank stabilization, contour farming, and terracing used in this study were obtained from works of literature (Cuttle et al. 2007, Arabi et al. 2006, Wang et al. 2019, López-Ballesteros et al. 2019). Costs per unit area (USD/ha) of the EMPs are evaluated based on the study area's current market rate. The costs of EMPs included the actual construction costs and maintenance costs paid jointly by the government, stakeholders, and community residents. It is worth mentioning that although the actual cost of EMPs may differ from one region to another, the optimal combination of EMPs will not vary as long as the ratio of the unit cost of different EMPs remains the same in the other areas.

Constraints:

Sediment yield constraints: The annual average sediment yield from the catchment after installing EMPs should be greater or equal to the desired minimum sediment yield and less than or equal to the upper allowable sediment yield limit. In this study, the restriction of sediment yield is addressed using the Modified Universal Soil Loss Equation (MUSLE) in SWAT.

$$S_{\min} \leq \{11.8\, K\, (LS)\, P * CFRG\, [\sum_{i=1}^{n} C_i (Q_{Pi} Q_{Si} A_i)^{0.56} + C_j (\sum_{j=1}^{m} (A_j - \sum_{i=1}^{n} A_i) Q_{Pj} Q_{Sj})^{0.56} + C_r (Q_{Pr} Q_{Sr} A_r)^{0.56}]\} \leq S_{\max} \quad (4.15)$$

Where S_{min} is the minimum annual mean sediment yield expected from each Sub-basin, S_{max} is the maximum yearly mean sediment yield allowed from the sub-basins, A_i is the area of the i^{th} EMP in sub-basin (ha), A_j is the area of the j^{th} land cover with no EMP (ha), C_i cover management factor for the i^{th} EMP in the sub-basin, C_j cover management factor for the j^{th} land cover with no EMP in the sub-basin, C_r cover management factor for residential in the sub-basin, Q_{Pr} discharge for residential, Q_{Sr} surface runoff for residential and A_r area of residential in sub-basins (ha).

The lower limit of annual sediment yield has been set to some considerable requirements downstream from the environmental viewpoint. In contrast, the upper limit of the annual average sediment yield was obtained from MUSLE based on the soil erosion class using a hypothetical land cover condition, i.e., in a perfectly natural condition before any human intervention (pre-agricultural, pre-urbanized). Sediment in the watershed has some vital roles, like releasing minerals, nutrients and adsorbing pollutants from surface water, which help maintain and continue the watershed ecosystem. A certain minimum amount of sediment yield from the watershed is required to functioning the services. Contrarily, too much sediment yield causes different problems, such as clogging drains, removing fertile soil, and reducing the river/dam's carrying capacity. To avoid such troubles, allowable sediment yield must be kept within a natural permissible limit. The minimum restriction of annual sediment yield should be chosen in the watershed not to be affected by water chemistry at the downstream water body. There should always be some need for dissolved ions for the growth and survival of the aquatic ecosystems in a water body. The reason is Jain, and Ram (1997) rainwater has a relatively low ionic concentration, while soil and sediment yield generally contribute to the required additional ionic load through the process of leaching. There are no guidelines recommended from the literature about the required minimum sediment yield downstream, but it is important for maintaining and dissolving ions in water for the downstream aquatic ecosystems. Accordingly, 5% of the allowable maximum sediment yield was considered the required minimum sediment limits (S_{min}) in water to sustainably continue the aquatic ecosystems (Sarma et al. 2015). Hence, S_{min} = 5% of S_{max} and $S_{max} = S_{natural}$ (Table 4.4).

Table 4. 4 Summary of maximum and minimum sediment yields over the critical sub-basins & EMPs

Prioritized Critical Sub-basins	Existing Land Use/Cover	Existing Land Use/Cover Area (ha)	Sediment_Rate (t/ha/year)	S_{max} (ton/yr) x10^6	S_{min} = 5% of S_{max} x10^6
Sub-6	Agricultural	231,530	31.131	7.208	0.36
Sub-7	Range brush	426,540	12.35	5.268	0.263
Sub-8	Agricultural	119,110	23.961	2.854	0.143
Sub-10	Range brush	145,630	16.80	2.447	0.122
Sub-12	Range brush	311,950	21.10	6.582	0.329

Peak discharge constraint: The watershed peak discharge should remain within the maximum and minimum acceptable limits after applying EMPs. If there are no other acceptable criteria, the minimum limit amount of peak discharge was set as the peak discharge value from the watershed area with the natural land cover condition by using the rational formula. However, the upper bound was developed by considering the maximum flow carrying capacity of the downstream stream reach conveniently installed at the outlet of each critical sub-basins to remove the discharge safely.

$$Q_{min} \leq \{0.2778\ [\sum_{i=1}^{n} RC_i I_i\, A_i + \sum_{j=1}^{m}(A_j - \sum_{i=1}^{n} A_i) RC_j I_j + RC_r A_r]\} \leq Q_{max} \quad (4.16)$$

Where; Q_{min} is the lower limit of peak runoff expected from the watershed (m^3/s) for environmental requirements point of view, Q_{max} is the maximum allowable peak discharge from the watershed (m3/s), A_i area of the i^th EMP in sub-basin (ha), A_j area of the j^th land cover with no EMP (ha), RC_i runoff coefficient for the i^th EMP in the sub-basin, RC_j runoff coefficient for the j^th land cover with no EMP in the sub-basin, RC_r runoff coefficient for residential, A_r area of residential in sub-basin (ha).

EMPs area suitability constraint: The application area of an EMP in the watershed should not exceed the available suitable size in that watershed for that EMP. That means an EMP is allowed only when an appropriate area available for the EMP in that watershed is greater than or equal to a minimum feasible area required to implement that particular EMP.

$$0 \leq A_i \leq A_{i-max} \quad (4.17)$$

$$A_i + A_j = A_{tot} \quad (4.18)$$

where A_i is the area under the i^{th} EMP, A_{i_max} is the area available for i^{th} EMP, A_j is the area under j^{th} land-use cover after applying EMP, and A_{tot} is the total area after EMP application.

4.2 Results and discussions

The important streamflow and sediment concentration data range for uncertainty analysis, parameterization, calibration/validation used in this study were from 1990 - 2013. The model was created with DEM, land use, soil type, and slope for the Genale catchment, which formed 25 sub-basins, 464 HRUs with a watershed area of 54,942 Km2.

4.1 Uncertainty analysis for streamflow and sediment

Analysis of sensitivity helps determine the relative ranking of parameters depending on how it affects the output variance due to input variability. This is reducing uncertainty and provides parameter estimation guidance for the calibration step of the model. Sensitivity analyses were conducted based on the global sensitivity produced by the Sequential Uncertainty Fitting version - 2 (SUFI - 2) algorithm in SWAT - CUP. After so many iterations based on the p-value and t-stat values, ten parameters were revealed to be sensitive to streamflow, and eight parameters are sensitive to sediment load. Therefore, a sensitivity was conducted to optimize the unknown variables, and the most sensitive parameters which were found to have the most considerable effect on the streamflow and sediment load in the model result were identified. Analysis of sediment load and streamflow sensitivity was carried out for calibration period 1990 to 2005 and validation period 2006 to 2013. Based on the p-value and t-stat results obtained from sensitivity analysis, the ranks of parameters were assigned. The predicted streamflow was the most sensitive for the initial SCS Curve Number II (CN2) and the soil layer's available water capacity (SOL_AWC.sol). On the other hand, the simulated sediment was sensitive to the linear re-entrainment parameter for channel sediment routing (SPCON.bsn), soil layer's available water capacity, curve number (Table 4.5).

Table 4. 5 Fitted values and rank of parameters used in the SWAT model calibration/validation (1990-2013)

Process	Parameter Name	Description of the parameter	Range value	Fitted value	p-value	t-stat	Rank
Streamflow	CN2.mgt	SCS runoff curve number	35-98	-0.17	0.0	-42	1
	SOL_AWC.sol	Available water capacity of the soil layer	0-1	1.0	0.004	2.9	2
	SOL_K.sol	Saturated hydraulic conductivity	0-2000	0.566	0.12	-1.5	3
	SOL_BD.sol	Moist bulk density	0.9-2.5	0.984	0.20	1.2	4
	ALPHA_BF.gw	Baseflow alpha-factor (days).	0-1	0.570	0.21	-1.2	5
	REVAPMN.gw	Threshold depth of water in a shallow aquifer for "revap" to occur (mm)	0-500	408.6	0.308	-1.0	6

	GW_REVAP.gw	USLE support practice factor	0-1	1.2	0.49	-0.6	7
	ESCO.hru	Soil evaporation compensation factor	0-1	0.27	0.65	-0.4	8
	HRU_SLP.hru	Average slope steepness	0-1	0.578	0.72	0.34	9
	SURLAG.bsn	Surface runoff lag time	0.05-24	0.072	0.96	-0.05	10
Sediment	SPCON.bsn	The max amount of sediment that can be retrained during channel routing.	0.0001-0.01	0.0002	0.0	-29.5	1
	SOL_AWC(.)sol	Available water capacity of the soil layer	0-1	0.639	0.0	14.2	2
	CN2.mgt	SCS runoff curve number	35-98	-0.24	0.0	-10	3
	SOL_K(..).sol	Saturated hydraulic conductivity	0-2000	0.845	0.0	7.18	4
	SPEXP.bsn	Exponent parameter for calculating sediment retrained in channel sediment routing.	1-1.5	1.156	0.0	-5.63	5
	CH_COV1.rte	Channel erodibility factor.	-0.05-0.6	0.78	0.145	-1.44	6
	USLE_K(..)sol	USLE equation soil erodibility (K) factor.	0-0.65	0.012	0.57	-0.6	7
	USLE_P.mgt	USLE equation support parameter	0-1	0.029	0.73	0.35	8

4.2.1 Model calibration and validation

Calibrated/validated parameters and the fitted values are the modeler's critical annotation from the calibration action used for the required objectives. Calibration of streamflow and sediment load was executed with several iterations of 500 simulations number; each was carried out for the monthly calibration period of 1990 - 2005. Model validation is needed to prove whether the calibrated parameters also work for other data of different years within the catchment. Validation period (2006 - 2013) results showed satisfactory performance for streamflow and sediment load (Figure 2.5 and 3.5). Table 4.6 shows the actual ranges of performance criteria for the model.

Table 4. 6 Actual ranges of performance criteria for SWAT output during calibration and validation action

Types of assessment		P-factor	R-factor	R^2	NSE	PBIAS	RSR	Rating
Flow	Calibration	0.51	0.78	0.87	0.81	-2.1%	0.50	good
	Validation	0.54	0.86	0.85	0.78	-0.5%	0.52	good

Sediment	Calibration	0.48	0.37	0.84	0.79	3.8%	0.61	satisfactory
	Validation	0.43	0.39	0.82	0.75	3.9%	0.67	satisfactory

Uncertainty measure of SWAT- CUP (SUFI-2) indicated that P-factor of 0.51 and R-factor of 0.78 for calibration and P-factor of 0.50 and R-factor of 0.86 for validation (Table 4.6). P-factor and R-factor are the two indices calculated to evaluate the model uncertainty. Thus, the P-factor of 1 and R-factor of zero indicates that the simulation precisely conforms to the observed data without sources of uncertainty, which is impossible in the reality of hydrological modeling. In this study, P-factor for calibration and validation is 0.51 and 0.50, respectively, which means about 51% of calibration and 50% of validation of the observed flow were bracket by 95PPU band.

Refer Figure 2.5 Monthly observed and simulated streamflow for the calibration period (1990-2005) and validation (2006-2013).

Refer Figure 3.5 Monthly observed and simulated sediment load plot for the calibration (1990-2005) and validation (2006-2013).

As indicated, the model's simulated and observed streamflow and sediment load agreed/ showed a satisfactory performance during the calibration and validation action (Figure 2.5 and 3.5).

4.2.2 Identification of critical sub-basins in the study area

The average annual sediment yields of 24 years (1990 to 2013) from the MUSLE simulation for each sub-basin in the study area are used to identify the critical erosion reach based on erosion hazards along with soil erosion class change (Figure 4.5). It is possible from Figure 4.5 that out of 25 sub-basins, five sub-basins (sub-6, 7, 8, 10, and 12) covering 22.47% area of the watershed placed under critical sub-catchments, which requires urgent action by stakeholders and watershed decision-makers. It is worth noting that the sediment yields from five critical sub-basins encompassing 22.47% of the study area exceeded the recommended upper tolerance limit of the soil loss class of 12.35 ton/ha/yr.

The effect of each EMP scenario on changing in a soil-erosion class of sub-basins is illustrated (Figure 4.5). Moreover, streambank stabilization and grassed waterway show the same improvement in soil erosion classes except in sub-8 and 19. Hence, sub-6 changed from very high to high; sub-12 changed from very high to moderate; sub-10 from high to moderate, and sub-7 from moderate to low under two scenarios (streambank stabilization and grassed waterway). In contour farming, sub-basins 6, 8, and 12 changed from very high to moderate, sub-10 from high to low, and sub-7 from moderate to low. In the case of filter strips & terracing scenarios, sub-basin 6 was improved from very high to moderate; sub-8 and sub-12 from very high to low; sub-7 from moderate to low and sub-10 from high to low. Finally, in the case of EMPs combinations, sub-6 and 8 changed from very high to low, sub-12 from very high to very low, sub-10 from high to very low, and sub-7 changed from moderate to very low class. The MUSLE model analysis revealed that terracing was the best solution for steep slope areas because it prevents soil particle detachment and lowered loss of soil.

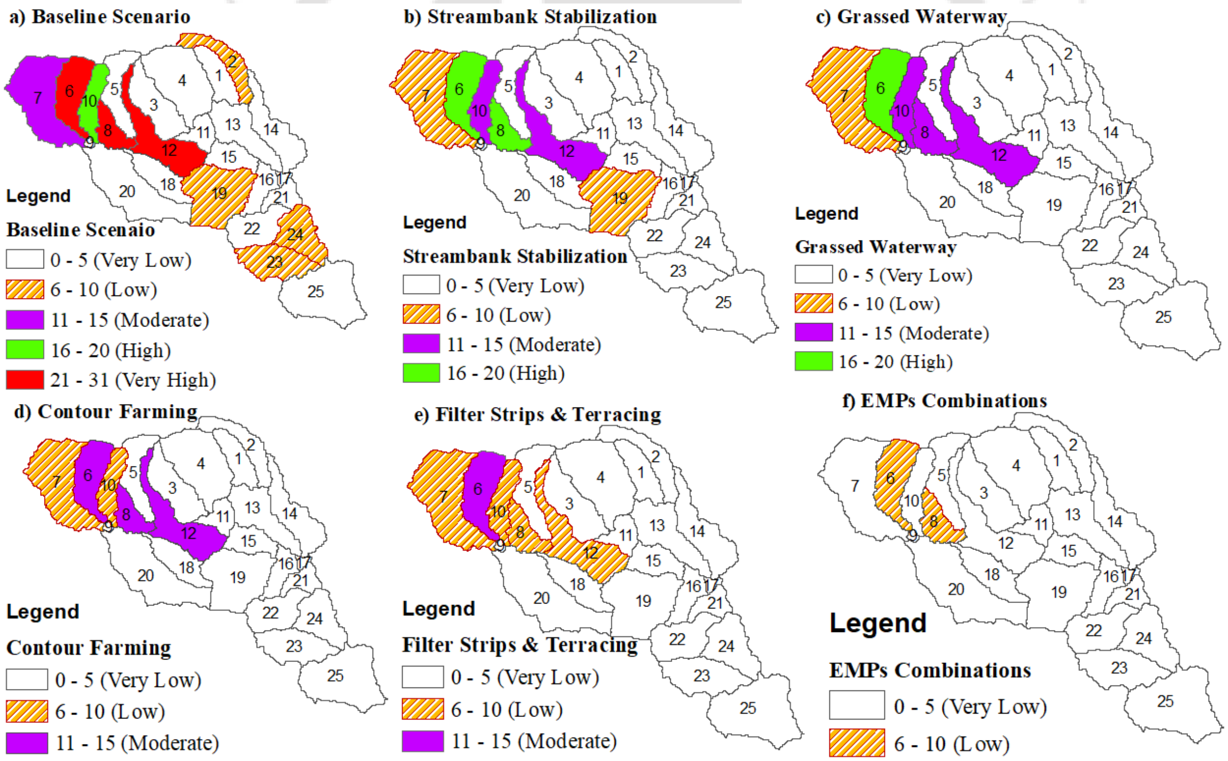

Figure 4. 5 Impacts of EMPs scenarios on changing soil erosion class in the study area over 1990-2013

4.2.3 Impacts of EMPs on sediment yield reduction at sub-basins scale

The results from the simulation of 5 individual EMPs (Table 4.7) indicate that all the individual EMPs are proceeded to reduce average annual sediment yields of 1990 – 2013 at the sub-basins scale. At the sub-catchment level, the maximum reduction in the sediment yield was attained by EMPs combinations (78.5%) followed by terracing (61.8%) and filter strips (54.3%) ((Table 4.7). The increase in channel roughness and channel cover causes a reduction in the surface runoff and channel erodibility, which reduces sediment transport in the reach and sub-basins degradation. From the results, it can be wind up that a reduction in sediment yield at the sub-basin level is due to the well-established and effectiveness of EMPs.

Table 4. 7 Effectiveness of five EMPs on sediment reduction for selected critical sub-basins over 1990-2013

Selected Critical sub-basins	Baseline condition	Simulated average annual sediment yield (ton/ha/yr.)					
		Streambank Stabilization	Grassed Waterway	Contour Farming	Filter strips	Terracing	EMPs Combinations
Sub-6	31.13	18.01	16.45	15.01	13.70	10.54	6.22
Sub-7	12.35	7.80	7.69	6.22	6.73	5.83	2.86
Sub-8	23.96	15.36	13.72	11.46	8.93	7.35	5.40
Sub-10	16.81	10.86	10.47	9.14	7.75	6.29	3.58
Sub-12	21.12	13.52	12.46	11.70	9.86	8.81	4.32
% of reduction	-	37.3%	41.3%	48.8%	54.3%	61.8%	78.5%

As shown in Table 4.7, the simulated average annual sediment yields from each sub-basin under different scenarios range: 0 to 31.13 ton/ha/yr for the Baseline scenario, 0 to 18.01 ton/ha/yr under streambank stabilization, 0 to 16.45 ton/ha/yr under grassed waterway, 0 to 15.01 ton/ha/yr under contour farming use, 0 to 13.70 ton/ha/yr under filter strip use, 0 to 10.54 ton/ha/yr in terracing, and 0 to 6.22 ton/ha/yr under EMPs combinations. It is also clear that in terracing, it is possible to curb the soil loss from each sub-basin within its permissible upper limit of soil loss (i.e., 14.94 ton/ha/yr). The implementation of different EMPs could result in up to 78.5% reduction in the average annual sediment yields for EMPs combinations, 61.8% for terracing, 54.3% for filter strips, 48.8% for the contour farming, 41.3% for grassed waterway, and 37.3% for streambank stabilization at the sub-basins level (Table 4.7). In this finding, it is vital to implement appropriate EMPs combinations and an adequate number of nature-based EMPs to minimize soil erosion to a reasonable extent.

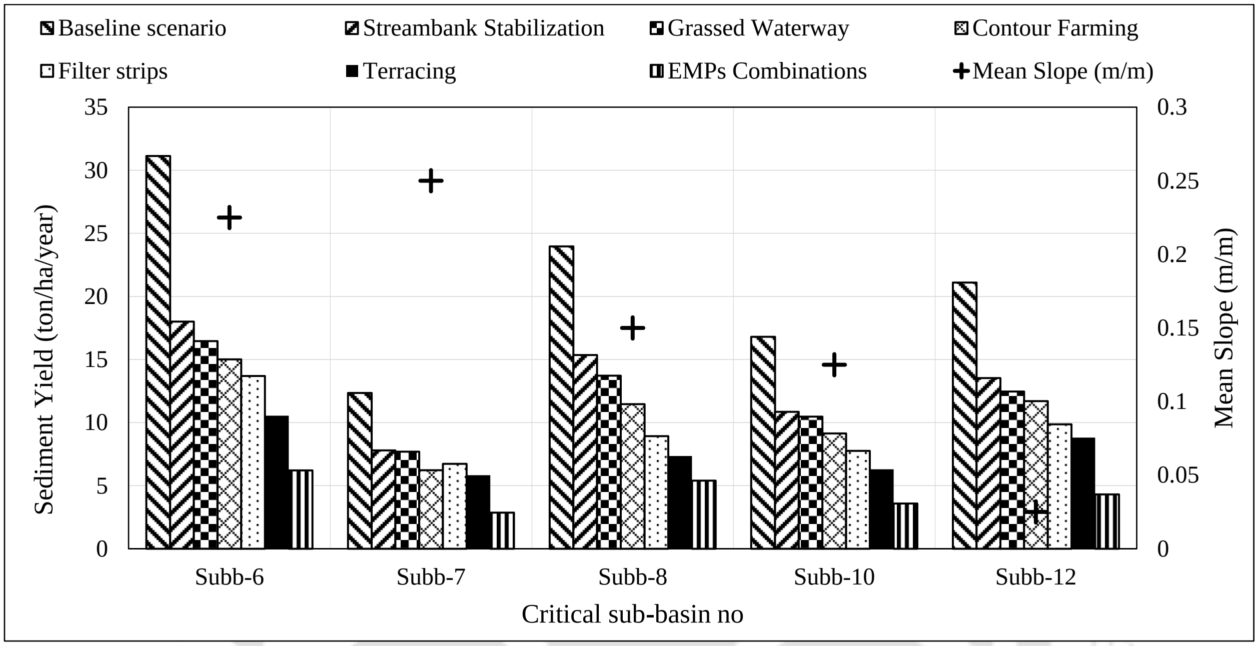

Figure 4. 6 Sediment yield reduction at treated sub-basins under five scenarios and mean slope over 1990-2013

Based on the results in Figure 4.6, it can be understood that the implementation of nature-based EMPs under terracing is most desirable for the study area to sustainably and efficiently manage the critical sub-basins at the individual level. The suggested EMPs could be implemented phase-wise according to the socio-economic, human resources, and site-specific conditions to provide sustainable watershed management practically. EMPs combination offers an economical solution in selecting nature-based management practices to tackle soil erosion problems and high runoff generation from agricultural, brushland, and sloppy watersheds containing considerable plots.

4.2.4 Optimal Combination of EMPs areas and Cost-effectiveness analysis

Cost is a critical factor in applying EMPs, and we need to optimize the cost of EMPs for implementation in the study area. The optimal cost of different EMPs for achieving these desirable limits of sediment yield was based on the optimal available space, and it was obtained using MATLAB programming. The total cost for the five critical sub-basins is found to be 1.844 billion Ethiopian birrs (US$46.101 million) (Table 4.8), which was composed of terracing, contour farming, filter strips, grassed waterway, and streambank stabilization sub-basin wise. The combination of optimal EMP satisfies the constraints of suitable topography and available EMP areas while minimizing cost. After applying EMP technology, the annual sediment yield from each sub-basin became almost in a natural condition. The total critical sub-basins cost for EMPs implementation is depicted in (Table 4.8). The current study was anticipated to develop a scientific approach to choose the most effective EMPs combinations for reducing sediment yield, emphasizing economic feasibility.

Table 4. 8 Optimal area available and total Cost analysis of EMPs for the critical sub-basins (5-Sub-basins)

Critical sub-basins	Existing LULC	Existing LULC Area (ha)	Optimal EMPs Area Combinations (ha) and land use after EMPs applications					
			Terracing	Contour Farming	Filter strips	Grassed waterway	Streambank Stabilization	Total EMPs Cost (USD*10^6)
Sub-6	Agricultural	231,530	5715	2078	13683	20838	11310	16.163
Sub-7	Range brush	426,540	16771	12621	1312	5254	0	10.518
Sub-8	Agricultural	119,110	1822.8	547.1	1014.3	771.5	311.1	1.362
Sub-10	Range brush	145,630	8856.3	3135.7	1470.2	4311.8	0	5.301
Sub-12	Range brush	311,950	12413	14058	4372	9315	3674	12.757
Total								46.101

The application of EMPs is limited due to area availability and budget constraints but provides nature-based solutions in a sustainable and economically viable manner for reducing soil erosion and peak discharge. A cost analysis was used to evaluate the cost-effectiveness of EMPs combinations. However, the economic cost has been a significant element for screening the application of EMPs. Despite its high implementation cost, terracing technology (high space availability) effectively reduces sediment yield in sub-basins. The space availability and the cost for EMPs application are directly proportional to each other in critical sub-basins (Figure 4.7). The space availability for terracing is very high except in sub-6, and the implementation cost is also high. Nevertheless, for sub-8, the optimal cost is minimal as the respective area availability is small (Figure 4.7). This shows that the optimal cost is dependent on the availability of space.

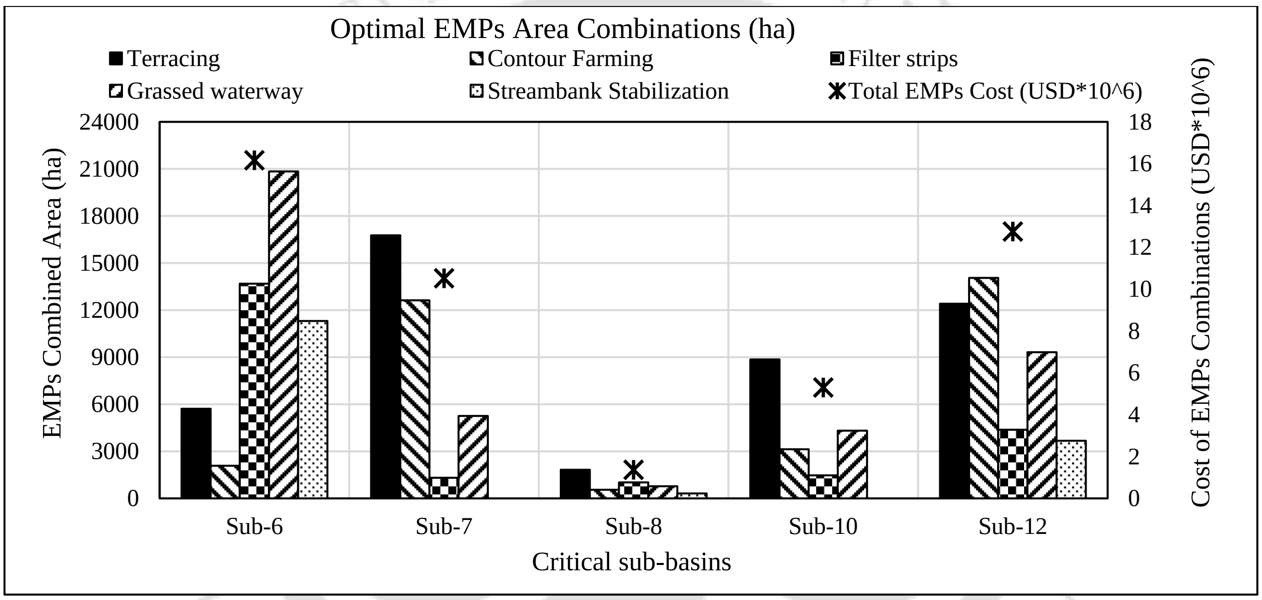

Figure 4. 7 The relationship/variation between the cost of EMPs combinations and area availability over critical sub-basins

From Figure 4.7, as the optimal cost of sediment yield reduction depends on area availability constraint, it did not directly reflect sediment yield change in the basins. Moreover, sub-6 with high sediment yield manifests high demand of cost while sub-8 still with high sediment yield reflects the small value of EMPs cost, and it is because implementation cost is highly dependent on the optimal area available within the critical sub-basins (Figure 4.7).

The non-linear optimization program is computationally more intensive; it gives a more realistic scenario of the total cost-effectiveness of a watershed management practice through EMPs combinations for the agricultural and brushland area of the sub-basin. Actions are needed to raise awareness of the watershed soil degradation problem and remove the barriers limiting the adoption of EMPs combinations.

Sediment and water conservation efficiency and relative cost of these EMPs play a crucial role in identifying the optimal EMP combination. This study is unique in analyzing the comparative cost-effectiveness of terracing, filter strips, grassed waterway, streambank stabilization, and contour farming combination, and space availability for each option in the context of study areas. The cost estimate is thus appropriate. Inclusion of cost estimation by considering HRUs level provides new and important insights and can prove helpful for future decision-making within affordable cost.

4.3 Conclusions

Land-use changes due to agricultural and built-up activities are a dynamic process and inescapable. The development of farmland that removes natural vegetative covers/forests amplifies soil susceptibility to erosion and other processes, transforming the watershed into a risk-scape. This article deals with the appraisal of the space availability and cost-effectiveness of five potential EMPs, namely; contour farming, grassed waterway, terracing, streambank stabilization, and filter strips combination in reducing the sediment yields at sub-basin scales in the Genale River using the hydrological model (MUSLE) in SWAT, and an optimization programming using MATLAB. The study provides a new methodology to identify the optimal combination of EMPs and their spatial distribution and thus provides important insights to help future decision-making within affordable cost.

Identifying critical sub-basins based on the upper tolerance limit of sediment rate/loss (12.35 ton/ha/yr) revealed that 5 sub-basins (sub-6, 7, 8, 10 and 12) were covered 22.47% of the study area are under erosion critical condition. The study area's critical sub-basins deserve immediate attention for implementing suitable preventive measures to control soil erosion, minimize sedimentation and water quality problems in the downstream riparian. From the scenarios' analysis, the implementation of EMP under the terracing scenario as an individual and EMPs combination is the most effective in the study area to control sub-basin degradation under financial constraints.

The resulted optimization model minimizes the overall implementation and maintenance cost of EMPs for five prioritized critical sub-basins satisfying the constraints like allowable sediment yield, allowable peak discharge, and maximum EMP area availability. Accordingly, the model can suggest a modification of landscape conservation in an ecologically and economically sustainable manner.

From the results, some sub-basins with high sediment yield manifest high demand of cost while others with high sediment yield reflect the relatively small value of EMPs cost, and it is because the implementation cost is highly dependent on the optimal area available within the critical sub-basins. The total optimal cost for the selected five critical sub-basins is found to be 1.844 billion Ethiopian birrs (US$46.101 million), which was composed of terracing, contour farming, filter strips, grassed waterway, and streambank stabilization area combinations.

Limiting the maximum sediment yields close to the natural value and restricting water yield within the downstream channel's maximum carrying capacity eliminates hazards like sedimentation, flooding, and water quality deterioration.

It is worth highlighting that EMPs approaches are nature-based solutions for improving watershed health and productivity in the environment. Analysis till HRUs scale brings more clarity in the erosion aspects and helps to narrow down to the critical areas, and it becomes easier to address the challenges with low human resources, low cost, and within a short time where impacts were significant.

EMPs serve as a powerful tool for the policy and decision-makers to formulate effective management measures for safeguarding vulnerable sub-basins against the impacts of degradation/soil erosion. We suggest that local authorities adopt terracing practice as a control measure if a single EMP is applied individually. However, if the combination of EMPs is applied, it performs much better than any single EMP. Choosing economically attractive and socially acceptable EMPs through community participation is also an important key to successfully implementing EMPs in the affected areas.

Chapter 5

Anthropogenic Land Use/Cover Change Detection and Its Impacts on Hydrological Responses of Genale Catchment, Ethiopia

5.0 Introduction

The land is one of the non-renewable/dynamic resources, and mapping of land use land-cover (LULC) is fundamental for designing and developing land and water resources with appropriate tools (Manjunatha and Basavarajappa, 2020).

Image accuracy assessment is an essential step in the LULC map classification process. The target is to quantitatively evaluate how effectively pixels were grouped into the correct feature classes in the area under investigation (Bharatkar and Patel, 2013; Kaya and Görgün, 2020). The accuracy assessment determines how well a classification worked between the ground truth data and classified image by pixels to interpret the use of someone else's classification. Through image analysis, all pixels in an image/map are assigned to a particular classes/themes, which results in a classified image that is a thematic map of the original image (Hussain et al., 2019; Abdelkareem et al., 2017). Supervised classification is the approach most often used for the quantitative investigation of remote sensing image data. The concept of separating the spectral domain into different regions associated with the ground truth covers classes of interest to a particular classification by features/pixels present in a scene (Elimy et al., 2020). Most investigator prefers it because it generally gives more class definitions and higher accuracy than unsupervised techniques (Adam 2011). Supervised classification uses a maximum likelihood classifier principle on statistical decision making, and then classification is done by overlapping signatures and pixels input bands to the class of highest probability (Bharatkar and Patel, 2013). The Maximum Likelihood decision rule is still one of the most widely used supervised classification algorithms, and its accuracy is well documented (Rwanga and Ndambuki, 2017).

The major elements of a sampling technique include sampling units (pixels/features or polygons), sampling design, and sample size in image processing. Bharatkar and Patel (2013) suggest that at least 50 coaching pixels per class are meaningful during image classification. If the area of interest exceeds 500 km^2 or the number of LULC categories exceeds 12, then a minimum of 75 - 100 training feature classes should be taken per class. The idea of quantitative accuracy assessment is to identify the sources of errors. Apart from classification errors, other sources of errors, such as interpretation errors, position errors resulting from the registration, and low quality of training samples, all affect classification accuracy. The most common means of asserting classification accuracy is to compare a class by class basis the relation between known reference data (ground truth) from google earth and the corresponding results of an evaluated classification (Adam 2011; Abdelkareem et al., 2017; Erasu 2017). In the LULC map, classification error occurs when a pixel (or feature class) associated with one category is assigned to another category. The name of accuracy classification error arranged in a square matrix establishes a standard category represent the end product of a created map which helps to find a site-specific error in the process is known as an error/confusion matrix. The most common/suited accuracy classification error estimator, the confusion matrices/overall accuracy, and Kappa coefficient (K_{hat}) measure statistical analysis for accuracy agreement between ground truth data and evaluated classification. Kappa coefficient analysis is accepted as a powerful technique for monitoring a single confusion matrix and for comparing the differences between individual error matrices (Rwanga and Ndambuki, 2017).

The use of remote sensing and GIS techniques is nowadays delightful to meet the mapping and monitoring changes over time to point out the impact of built-up and agriculture on the forest and natural heritage of the waterbody (Tomar 2017; Erasu 2017). LULC is a dynamic aspect that modifies through time and space due to human-made burden (anthropogenic) and development. Evaluating the present LULC and its unscientific change is good to know for urban planners, policymakers, natural resources managers, and remote sensing action is an effective mechanism for detecting and analyzing temporal changes and should be monitored regularly as it causes irreversible impacts on the environment (Navin and Agilandeeswari, 2019; Manjunatha and Basavarajappa, 2020). The detailed process of LULC change detection is essential in gathering the specific information about the quantitative change of land cover area (percentage of area) for different years' maps. There is a rapid and large-scale alteration of LULC significantly across the globe due to an increase in a high rate of climatic changes, industrialization, urbanization, rapid population growth, and overdemand of the growing socio-economic resources (Sansare and Mhaske, 2020). The current target is to detect LULC pattern changes and their aerial extent due to different socio-economic factors in the study area. LULC changes on the earth's surface are generally divided into land use and land cover, which are two concepts and are usually used interchangeably. LULC dynamic change affects the hydrological process (runoff generation, water yield, sediment yield, streamflow, etc.) with the increasing urbanization & agriculture.

Knowing the consequences of different LULC is required to review sustainable water resources management, land use planning, and development (Sansare and Mhaske, 2020). Generally, most of the registered LULC changes were the results of the anthropogenic activities achieved to satisfy the immediate needs of human beings. These spontaneously rapid LULC changes bring adverse impacts on the environment and water resources potential of a nation.

In the Horn of African countries, primary in Ethiopia, water resources management and planning challenges are the extreme hydrological variability and seasonality nature of its most fascinating surface and groundwater resources. However, the primary water resources contributor for the Genale watershed is mainly groundwater. Erosion of soil by water action is also one of the major restraints of agricultural production in Ethiopian highlands that affects productivity and the primary sources of reservoir sedimentation. Although the country is blessed with sufficient water resources, recent 21^{st-}century natural forest cover has been dismissed and causes land degradation and water flow extremes (Choto and Fetene, 2019). In this view, LULC plays a significant role in water transport in the hydrologic system and chiefly aids in reducing overland flows. As a result of its effect on evaporation, transpiration, and solar radiation interception, LULC is a propulsive factor in the energy balance equation in the hydrological process (Tadesse et al., 2015). Genale watershed is one of Ethiopia's Genale Dawa River Basin system sub-basins, with different tributaries, different distributaries, and dendritic drainage patterns.

The watershed is a degraded field with anthropogenic land use activities with agricultural on steep slopes and built-up areas. In the Genale watershed, no research has been done to investigate the impacts of LULC change on the hydrological response of the watershed. Therefore, the dynamics of LULC change in this catchment require hydrologic modeling that provides a helpful tool in water resources management & plan for many years and is usually used to predict land-use impacts on streamflow and sediment yield. For water resources, stakeholders, and decision-makers, knowing how and how much LULC changes will influence water availability at the sub-basin/HRUs scale is more important for planning appropriate soil and water mitigation measures (Aragaw et al. 2021). Therefore, research is required at the sub-basin/HRUs scale better to recognize the hydrological responses conditions to LULC changes. Notably, water resources for energy generation may face severe problems due to changes in hydrological regimes, particularly increases in sediment yield of the watershed due to LULC change. The SWAT model has been used to predict land use/cover change impacts on soil and water losses. The results illustrate that even nearly limited land-use change, from forest to arable/cultivable land or vice versa, significantly affects regional and local soil erosion rates and sediment supply to rivers (Huang and Lo, 2015; VanRompaey et al., 2002). The quantitative hydrological investigation due to land use/cover change by the SWAT model is a good approach for identifying the LULC change detection and impact of land-use change on the hydrological process of the Genale watershed. This suggests quantitative knowledge that would allow stakeholders and decision-makers to make better land, soil, and water resource management and plan choices. Besides quantifying the gross impacts of LULC changes on hydrological responses by applying a hydrological model, it is also informative to analyze the effect and contribution of individual LULC change on different hydrological components of a catchment (Gashaw et al. 2018). The multivariate statistical design is helpful to explore the interaction of each LULC type (independent variable) with different hydrological responses (dependent variables) and confirm whether the observed LULC change is significant enough to induce the change in hydrological processes. It can be applied to address the LULC class responsible for changing hydrological components (Shawul et al., 2019). Moreover, this approach is applicable for solving multicollinearity problems, which occur when at least two predictors (independent variables) in the model are correlated. The study is interacting with the individual LULC changes to hydrological elements using multivariate statistical correlation to quantify the contribution of changes in hydrological responses.

The main spotlight of this study is (1) Appraisal of image processing/assessment of image classification accuracy, (2) to examine the LULC change detection of different periods, (3) to evaluate the impacts of different LULC changes on hydrological responses in Genale watershed, Ethiopia.

5.1 Materials and methodology

The study aims analysis of land use/cover change by classifying satellite imageries of the Genale watershed. The data set used to monitor LULC change detection was the 24-year data collected for the period from 1990 to 2013. The mechanism contains four stages: 1) pre-processing (image rectification and restoration), 2) image classification, 3) post-processing (information extraction), and 4) land-use change detection. Remote sensing and GIS are essential for producing land use/cover maps through a method called image classification.

In this finding, the Soil and Water Assessment Tool (SWAT) model interfaced with GIS was used to evaluate the impacts of LULC change on hydrological responses of the catchment (Figure 5.1).

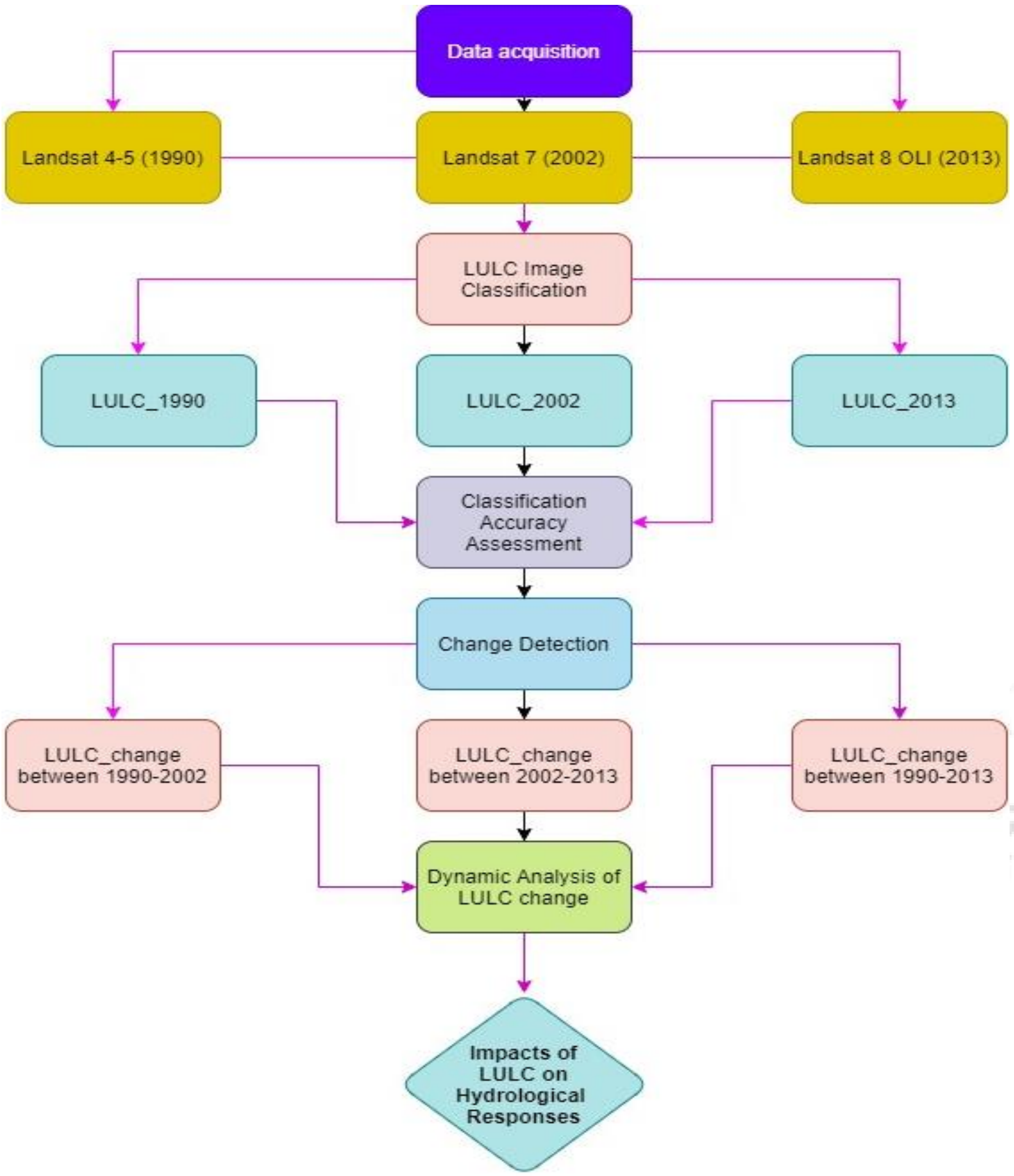

Figure 5. 1 Flow chart and methodology of the study area

5.1.1 Data sources, preparation, and image processing

For the present study, Landsat 4-5, Landsat-7, and Landsat 8 OLI (operational land imager) spatial resolution of 90 m are used.

The USGS (united states geological survey) earth explorer database system was used for generating LULC maps. Processing of satellite imageries before detection changes is imperative and has a unique aspiration to build a more direct association between the biophysical phenomena on the ground and the data acquisition (Coopin et al., 2004). The main aim of image processing and classification is to automatically categorize all pixels in an image into LULC categories to draw out helpful, confined information. Image classification was done to designate multi-spectral signatures from the landsat datasets to different years of LULC. LULC types are frequently mapped from digital, remotely sensed data through supervised digital image classification (Campbell and Wynne, 2011).

Table 5. 1 Detail sources of satellite imageries used in this study with the output file are in GeoTIFF format

Landsat satellites Type	Sensor onboard	Availability	Path/Row (Mosaiced is done respectively)	Pixel size (m)	No of spectral bands	Date of acquisition
Landsat 8	OLI and TIRS (Thermal Infrared Sensor) Level-1	February of 2013 to present	(166), (167) & (168)/ (56&57), (55, 56 & 57) & (55 & 56)	90	11	December 10, 2013
Landsat 7	Enhanced Thematic Mapper Plus (ETM+) Level-1	July, 1999 to present)	(166), (167) & (168)/ (56&57), (55, 56 & 57) & (55 & 56)	90	8	January 27, 2002
Landsat 4-5	Thematic Mapper (TM) Level-1	July 1982 to May 2012	(166), (167) & (168)/ (56 & 57), (55, 56 & 57) & (55 & 56)	90	7	December 18, 1990

5.1.2 Land-Use/Land-Cover Supervised Classification System

Supervised (known spectral signatures) is the process commonly used for quantitative analyses of remote sensing image data and assigns each pixel in the image to which its signature is most comparable categories. Finally, eight types of LULC classes were generated in the study area (Table 5.2).

Table 5. 2 Description of the different LULC classification systems of the Genale watershed

S. No	LULC Categories	General description of different sub-class included	SWAT Code
1	Shrub/bush land	Scrubland, brush/bushland, herbs, vegetation types, sparse woodland, rangelands, orchard stemmed woody plant, and other grasslands	RNGB
2	Agricultural land	Farm plantations, croplands, palms, bamboo plantation, terraced land, vegetable/fruit land, irrigated arid land, wooded/cultivated areas	AGRL
3	Forest	Reserved and protected forest, mixed forest, deciduous forest, Arboreal forest, shrubbery area, and economic forest, scrub forest	FRST
4	Built up land	Towns, villages, buildings, huts, churches, mosques, tombs, graves, post-office, power lines, transportation roads, bridges	URBN
5	Pasture land	Grassland, savanna, heathland, moorland, machair, rangeland, legumes	PAST
6	Barren land	Vacant land, barren rocky, land with/without scrub, Mining/ industrial wastelands, exposed soil, salt-affected area, and land that cannot be utilized	BARR
7	Water bodies	Lakes, rivers/streams, reservoirs, swamps, springs, canals, ponds, bays, etc.	WATR
8	Wetlands	Swamps, flora, fauna, coastal lagoons, Inland and maritime wetland	WET

5.1.2.1 Assessment of Classification Accuracy

Accuracy assessment is the most important final step in the image classification process, and the objective is to assess both qualitative and quantitative sampling of different pixels effectively into the correct land cover classes. Errors arise when a pixel (or feature) belonging to one class is assigned to another category. In order to execute accuracy assessment precisely, we need to compare two sources of information which include: interpreted land use/cover map image derived from the remote sensing data and reference land use map of high-resolution images or ground truth data (google earth pro) (Treitz and Rogan, 2004). Accuracy in image classification is influenced by inclusion errors (commission error) and exclusion errors (omission error). The landsat classified imagery needs to be assessed for accuracy before the same could input any hydrological applications.

Error/confusion matrix

A confusion matrix is a square cluster of columns and rows (n×n array where n represents the number of classes) in which each row and column represents one class in the defined map. Error matrix match on a class by class basis, the relationship between land-use map of ground truth data, and the corresponding results of an automated classification on Arc GIS.

Reliability or User's Accuracy corresponds to an error of commission (inclusion); it refers to the probability that a category on the classification image will be correct when used on the ground and a pixel/features designated as a specific class in the land use map is this category. Commission error is the number of spectral signatures mistakenly included in an information class.

$$\text{User's accuracy} = \frac{\text{Total number of correctly classified pixels in each category}}{\text{Total number of classified pixels of reference category (User's Total)}} * 100\% \quad (5.1)$$

Producer's accuracy corresponds to an error of omission (exclusion): it is the amount of a land category correctly

classified on the classification image or the probability that any feature/pixel of an area on the ground in that class has been correctly classified as such, which indicates how well the training sample sets pixels of a given cover type are classified. Omission error is the number of spectral signatures mistakenly excluded from an information class.

$$\text{Producer's accuracy} = \frac{\text{Total number of correctly classified pixels in each category}}{\text{Total number of classified pixels of reference category (Producer's Total)}} * 100\% \quad (5.2)$$

Where: a_{ii} number of samples correctly classified, a_{i+} column total for class i, a_{+i} row total for class i.

Overall accuracy: is a measure of accuracy assessment for the entire land use map image across all classes present in the categorized image and is the percentage of correctly categorized samples of a confusion matrix.

$$\text{Overall accuracy} = \frac{\text{Total number of correctly classified pixel (sum of diagonal elements)}}{\text{Total number of reference pixels (accuracy sites)}} * 100\% \quad (5.3)$$

Kappa coefficient analysis (K_{hat}) is a distinct multivariate technique for accuracy assessment between two maps considering all elements of the confusion matrix and having several advantages over other techniques. Its value ranges from 0 to 1. If the kappa coefficient is equivalent to 0, there is no compromise between the classified image and the reference ground truth image, and if it equals 1, then the categorized image and the reference image are precisely the same.

$$\mathrm{Khat} = \frac{N\sum_{i=1}^{r} X_{ii} - (\sum_{i=1}^{r} X_{i+} * X_{+i})}{N^2 - (\sum_{i=1}^{r} X_{i+} * X_{+i})} = \frac{\mathrm{Observed} - \mathrm{Expected}}{1 - \mathrm{Expected}} \tag{5.4}$$

Where r = number of columns/rows in the confusion matrix, X_{ii} is the number of the observations in row i and column i (on the major diagonal), and X_{i+} and X_{+i} are the marginal totals for row i and column i, respectively, and N is the total number of observations included in the matrix.

Table 5. 3 Rating criteria of kappa statistics efficiency (Rwanga and Ndambuki, 2017)

ID	Kappa statistics analysis	Strength of the agreement
1	< 0	Poor
2	0.00 - 0.20	Slight
3	0.21 – 0.40	Fair
4	0.41 -0.60	Moderate
5	0.61 – 0.80	Substantial
6	0.81 – 1.00	Almost perfect

5.1.2.2 Change detection

This paper aimed to detect and estimate the amount of change from different classified land use maps during the period from 1990 to 2013 analysis the change in the agricultural, built-up areas, and forest by subtracting the classified image over (1990-2002, 2002-2013, and 1990-2013) from each other using RS jointly with GIS technique (Esam et al., 2012). LULC change detection was used to identify, characterize, and quantify differences between imageries of the same study area and different periods, while changes of percentage were evaluated by dividing it with the total area and multiplying by hundred. The dynamic indicator of land use/cover is used to quantitatively investigate/monitor the change in intensity of one land use type (Yuhai 1999). The value of dynamic index K is computed as;

$$K = \frac{U_b - U_a}{U_a} * \frac{1}{T} * 100\% \quad (5.5)$$

where U_a and U_b are the area of a particular land-use/cover type at the beginning (previous) and end (recent) of the study period, respectively, T is the interval length of period/ the duration of the study (in years), K is the rate change of area per year of a specific land-use/land-cover categories. Refer chapter two of the thesis for the detail description of Soil and Water Assessment Tool (SWAT) model.

5.2 Results and Discussions

The model was built with DEM, land use/cover, soil properties, and slope types for the Genale watershed, which formed 25 sub-basins, 464 HRUs with a drainage area of 54,942 Km^2. A SWAT hydrological model adequately simulates streamflow, and sediment load typically accounts for the precise calibration/validation of parameters under different year land cover.

5.2.1 Land Use Land Cover Change Analysis

The LULC change detection map shows eight (shrub/bushland, built up, forest, agriculture, bare land, pastureland, water bodies, and wetlands) categories of LULC through image processing and classification through image processing and classification processing and classification created unifying these classes for 1990, 2002 and 2013. The spatial analysis of LULC has been executed to describe the overall land use cover patterns throughout the catchment. An image was checked with an accuracy matrix using 334 randomly selected control points. The accuracy assessment was achieved using LULC maps and ground truth data on Google Earth Pro (Figure 5.2). The supervised classification based on maximum likelihood was done with the help of signature files and resulted in 8 major LULC classes.

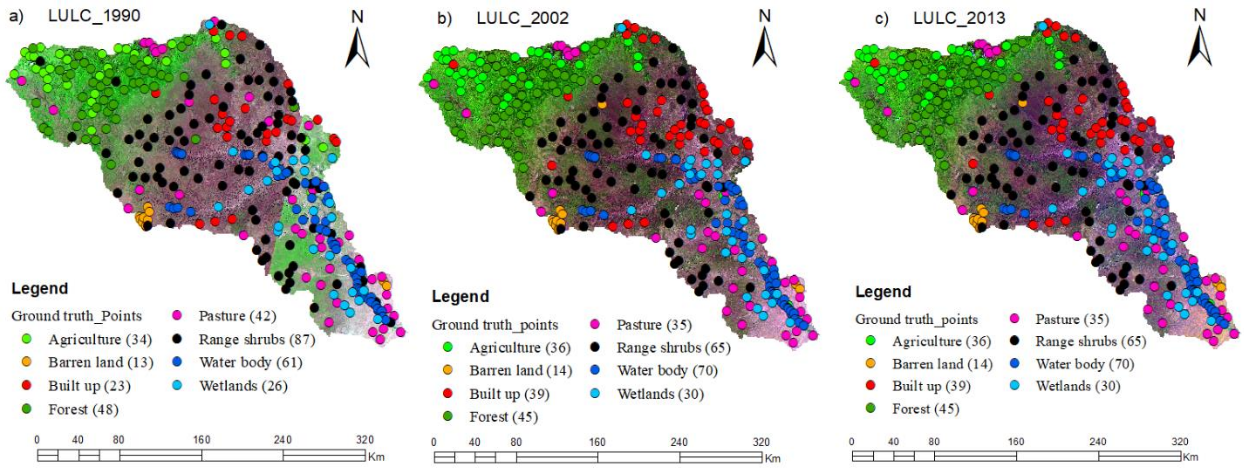

Figure 5. 2 Image accuracy assessment points (ground truth points) over 1990, 2002, and 2013

Accuracy assessment, planning for future developments with the right decisions, and adequately managing resources requires insightful the location of those resources and their spatial interaction (Congalton and Green 2019). In designing the accuracy assessment sample, this finding utilized randomly selected points for each class of LULC and thus used 334 points for each image (Figure 5.2).

5.2.1.1 Overall classification accuracy and Kappa coefficient analysis

The classification accuracy assessment in terms of Kappa coefficient and error/confusion matrices are essential for classification results to be confident that to what extend the classification is accurate.

Table 5. 4 How to summarize and quantify accuracy assessment using confusion matrix for the LULC-2013

	Agriculture	Barren land	Built up	Forest	Pasture land	Range shrubs	Water body	Wetland	User (Total)	User's accuracy	Commission Error
Agriculture	30	0	0	4	0	2	0	0	36	83.33%	16.6%
Barren land	0	13	0	0	1	0	0	0	14	92.86%	7.1%
Built up	2	0	23	1	4	9	0	0	39	59%	41%
Forest	2	0	0	41	0	2	0	0	45	91.11%	8.9%

Pasture	0	0	0	0	32	3	0	0	35	91.4%	8.6%
Range shrubs	0	0	0	1	2	61	1	0	65	93.85%	6.15%
Water body	0	0	0	1	1	7	60	1	70	85.7%	14.28%
Wetlands	0	0	0	0	2	3	0	25	30	83.33%	16.67%
Producer (Total)	34	13	23	48	42	87	61	26	334		
Producer's accuracy	88.23%	100%	100%	85.4%	76.2%	70.1%	98.4%	96.2%			
Omission error	11.8%	0	0	14.6%	23.8%	29.8%	1.6%	3.85%			

The user and producer accuracy, the results revealed excellent for approximately all the classes in all years except in the built-up, pasture, and shrubs classes. In built-up land, the recorded user accuracy value is satisfactory and difficult (Table 5.4).

$$\text{Overall accuracy} = \frac{\text{Total number of correctly classified pixel (sum of diagonal elements)}}{\text{Total number of reference pixels (accuracy sites)}} * 100\%$$

$$= \frac{(30 + 13 + 23 + 41 + 32 + 61 + 60 + 25)}{334} * 100 = 85\%$$

$$\text{Kappa coefficient} = \frac{\mathrm{N} \sum_{i=1}^{r} \mathrm{X}_{ii} - (\sum_{i=1}^{r} \mathrm{X}_{i+} * \mathrm{X}_{+i})}{\mathrm{N}^2 - (\sum_{i=1}^{r} \mathrm{X}_{i+} * \mathrm{X}_{+i})}$$

$$\text{Kappa} = \frac{334 * \ (30 + 13 + 23 + 41 + 32 + 61 + 60 + 25) - (34 * 36 + 13 * 14 + 23 * 39 + 48 * 45 + 42 * 35 + 87 * 65 + 61 * 70 + 26 * 30)}{334^2 - (34 * 36 + 13 * 14 + 23 * 39 + 48 * 45 + 42 * 35 + 87 * 65 + 61 * 70 + 26 * 30)}$$

$$= 0.828$$

The value of kappa 0.828 means there is 82.8% better agreement than by chance only. These values illustrate that the Landsat and the methodologies used were accurate, and the classification is almost perfect since it is greater than 0.8. The advantage of kappa coefficient analysis in relation to overall accuracy is statistically compared products of two classifications. Unlike the overall accuracy, the kappa coefficient includes errors of commission and omission. The land use/cover classification has shown that user's Accuracy and producer's Accuracy are greater than 80%, except in pasture, shrubs, and built up and the overall accuracy of 85% (Table 5.4). The results revealed that the overall accuracy of the LULC classification was 77.6%, 81.5%, and 85% for 1990, 2002, and 2013 respectively, and coefficients of kappa for the same years were 74.8%, 78.5%, and 82.8%, respectively.

5.2.1.2 Change detection

LULC change detection process encompasses the application of multi-temporal data sets to differentiate areas of land cover change between two or more dates and conducts should comprise data acquired by the same sensor and be registered using the exact spatial resolution viewing spectral bands, geometry, radiometric resolution. Change detection can be characterized as the process of identifying differences in the state of a phenomenon by observing it at different periods 1990, 2002, & 2013 (Figure 5.3).

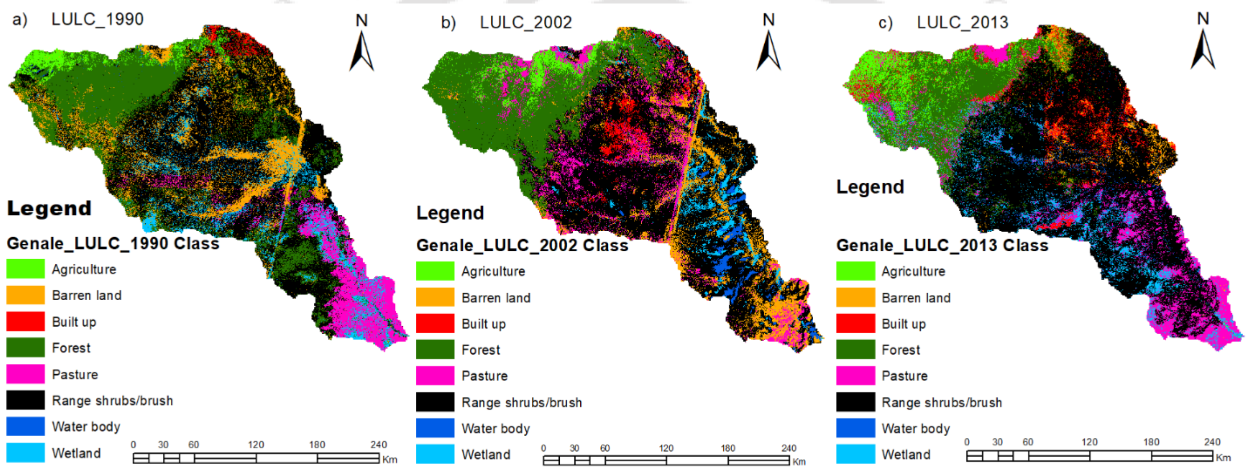

Figure 5. 3 Land use/cover classification of Genale watershed for the period 1990, 2002, and 2013

Table 5. 5 Summary of the area and relative changes statistics in LULC over 1990 to 2013

S. no	LULC-Type	1990		2002		2013		Change (1990-2002)		Change (2002-2013)		Change (1990-2013)	
		Area (Km^2)	Area (%)	Area (Km^2)	Area (%)	Area (Km^2)	Area (%)	Area (Km^2)	Area (%)	Area (Km^2)	Area (%)	Area (Km^2)	Area (%)
1	Agriculture	1322	2%	1593	3%	3288	6%	271	21%	1695	6%	1966	60%
2	Barren land	7361	13%	6442	12%	3014	5%	-919	-11%	-3428	-53%	-4347	-44%
3	Built up	874	2%	1339	2%	2730	5%	465	53%	1391	4%	1856	68%
4	Forest	13293	24%	12624	23%	9216	17%	-670	-5%	-3408	-27%	-4077	-44%
5	Pasture	3990	7%	5146	9%	6336	12%	1156	29%	1190	23%	2346	37%
6	Range shrubs	23902	44%	24717	45%	26208	48%	815	4%	1491	6%	2306	9%
7	Water body	365	1%	1040	2%	858	2%	675	84%	-182	-18%	493	57%

8	Wetland	3835	7%	2041	4%	3292	6%	-1794	-47%	1251	61%	-543	-17%

Table 5.5 shows all the major classes of LULC of the basin determined in the change analysis. The results revealed that there is a rapid decrease in the forest (5%, 27%, and 44%), barren land (11%, 53%, and 44%), wetland (47%, 61%, and 17%) from 1990-2002, 2002-2013, and 1990-2013 respectively which is due to the conversion of green forest & barren land into settlement area or fallow lands, and there is a significant increase in built-up (53%, 4%, and 68%), agriculture (21%, 6%, and 60%), and water body (84%, 18%, and 57%) from 1990-2002, 2002-2013, and 1990-2013 respectively. From the 1990 land use/cover classes, about 44 % was devoted to range shrubs, whereas agricultural land and plantation shared 2%. The LULC changes include forestation, an increase in wetlands, and changes in agricultural and built-up (Figure 5.4).

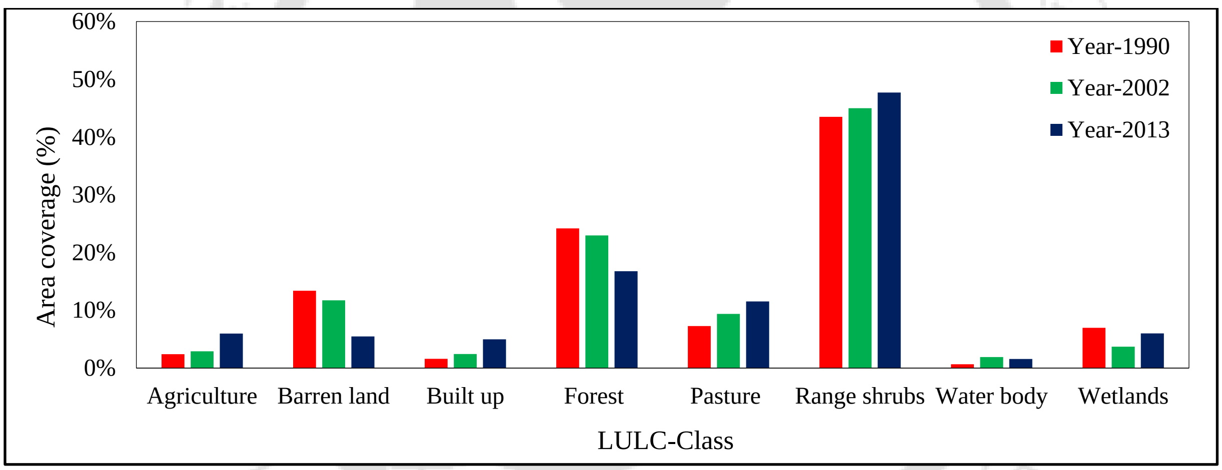

Figure 5. 4 The dynamics pattern of LULC changes for the years 1990, 2002, and 2013

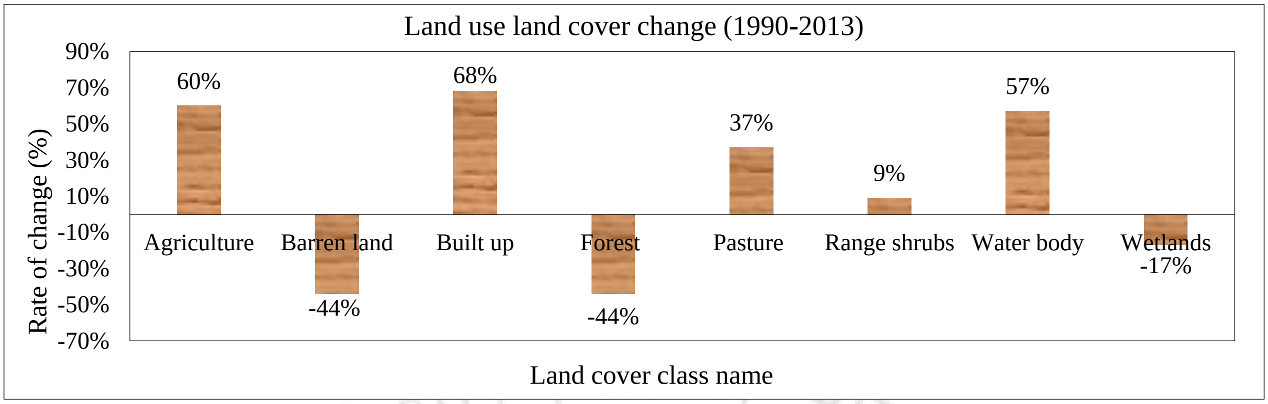

Figure 5. 5 Change in area of LULC between 1990 and 2013 for Genale Basin

Figure 5.5 is showing the LULC changes that have been taken place in the area through (bar graph) graphical representation. There is a fall/decreased in the percentage of the barren land (44%), forest (44%), and wetlands (17%), which deliberately shows replaced by other land cover changes like built up, agriculture, range shrubs, and pasture land. Nevertheless, the change in built-up, water body, pasture, and agriculture is significantly increased in the catchment by 68%, 57%, 37%, and 60%, respectively (Figure 5.5).

5.2.1.3 Impacts of LULC change induced on hydrological responses

Model parameter sensitivity analysis for streamflow and sediment

Sensitivity analysis was performed to navigate the calibration/validation process and point out the optimized parameters that significantly impact the streamflow and sediment load. Sensitivity analyses were conducted based on the global sensitivity produced by the sequential uncertainty fitting version-2 (SUFI-2) algorithm in SWAT CUP. Uncertainty was performed with several iterations of 500 simulations number. Based on the p-value and t-stat values, 10 and 8 parameters revealed a meaningful effect on streamflow and sediment load, respectively, to finalize the model parameters. The simulated flow was the most sensitive for the initial SCS curve number II (CN2) and available water capacity (SOL_AWC.sol). Likewise, the simulated sediment was sensitive to the amount of sediment that can be re-entrained during channel sediment routing (SPCON.bsn), (SOL_AWC.sol), CN2, etc.

Refer chapter four, Table 4.5 Fitted values and rank of parameters used in the SWAT model sensitivity analysis, calibration and validation (1990-2013) for streamflow and sediment flow.

Refer chapter three, Table 3.2 SWAT statistical performance index acceptable range (Abbaspour et al.,2011; Moriasi et al.,2007)

Refer from chapter three, Table 3.3 Actual index value for SWAT output during calibration/validation processSensitivity measure of SWAT- CUP (SUFI-2) reflected that P-factor of 0.51 and R-factor of 0.78 for calibration and P-factor of 0.50 and R-factor of 0.86 for validation considering flow (Table 3.3).

Refer from chapter two, Figure 2.5 Monthly observed and simulated streamflow for the calibration period (1990-2005) and validation (2006-2013).

Refer Figure 3.5 Monthly observed and simulated sediment load plot for the calibration (1990-2005) and validation (2006-2013). As indicated, the model's simulated and observed streamflow and sediment load agreed/ showed a satisfactory performance during the calibration and validation action (Figure 2.5 and 3.5).

The results exhibited that the SWAT model is an essential tool to simulate the spatiotemporal status of hydrological responses about a different period of LULC change due to anthropogenic and socio-economic change in the Genale watershed. The dynamics change in LULC classes between 1990 and 2013 continuously have shifted from the forest, range shrubs, and barren land into agricultural, built up, pasture, and wetlands have significantly contributed to increasing the groundwater flow and water yield while slight reduction of evapotranspiration and surface runoff occurred (Figure 5.6). As LULC changes in the study area (1990 to 2013), the generated annual average water balance components are also changed. The average annual evapotranspiration (ETmm) decreased from 413.85 to 385.2 mm, percolation (PERC) decreased from 408.81 to 383.29 mm, groundwater flow (GW_Qmm) decreased from 377.88 to 366.8 mm, and lateral flow (LAT_Qmm) decreased from 5.3 to 3.65 mm while surface runoff (SURQmm) increased from 41.85 to 75.8 mm, water yield (WYLDmm) increased from 421.15 to 447.12 mm (Figure 5.6).

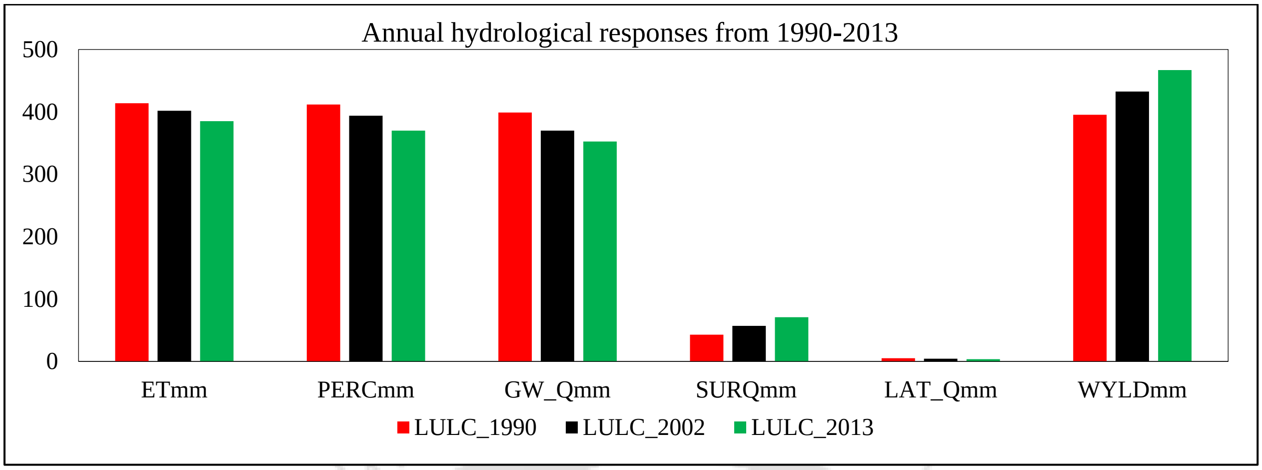

Figure 5. 6 Average annual hydrological response of for three years LULC map of Genale catchment

The results point out that the consequence of deforestation, agriculture, and settlement in the study area decreased ETmm, which again led to increased surface runoff, sediment yield, and water yield. The groundwater and lateral flow showed a declined trend in the study area (Figure 5.6) significantly from 1990 to 2013.

The SWAT has classified the catchment into 25 sub-basins. Five of them were selected as critical based on sediment yield (higher and lower) and forest coverage from these sub-basins.

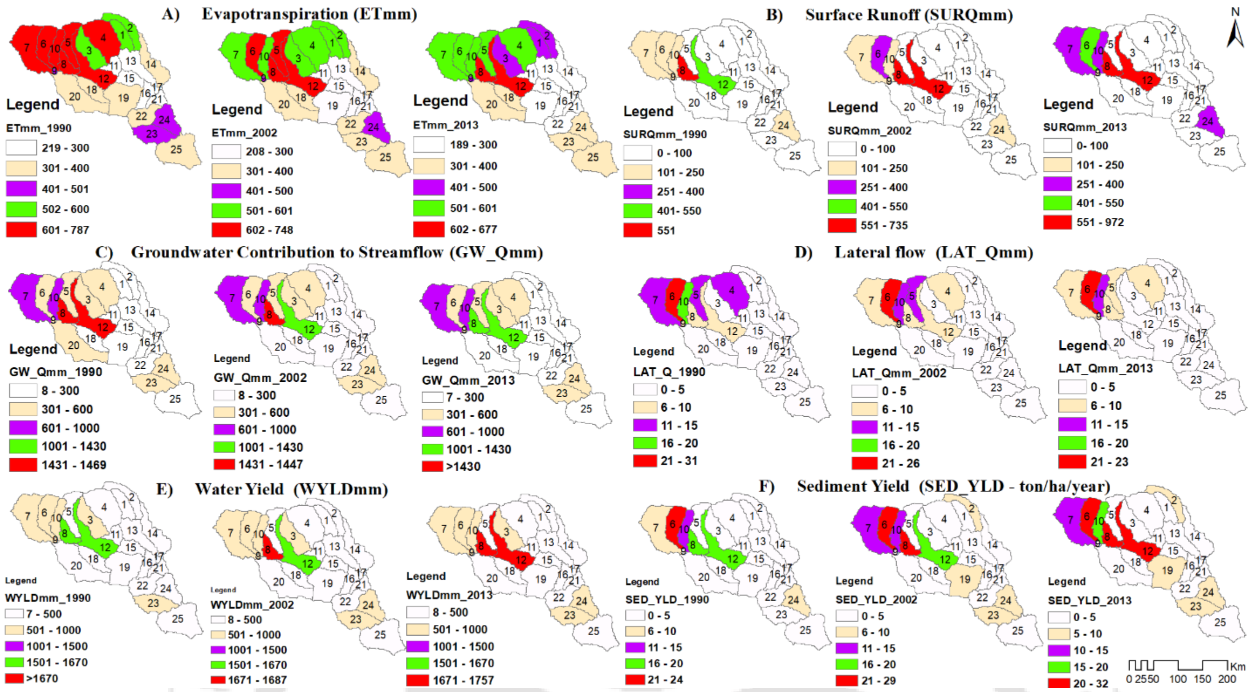

Figure 5. 7 Spatial variability of hydrological responses at the sub-basin level between LULC maps 1990, 2002, and 2013 in Genale watershed

The study results revealed an increase in generated surface runoff, water yield, and sediment yield in all indicated sub-basins from land use/cover map 1990 to 2013 while evapotranspiration, groundwater flow, and lateral flow are reduced the respective sub-basins. This was due to an increase in agricultural land, built-up area, pasture land, and decreased forest land and shrubs land (Figure 5.7). Those sub-catchments having the lowest hydrological responses have made a very small change in land use/cover. Sub-basins 6, 7, 10, 12, and 24 show an increasing surface runoff, and sub-basins 8, 12, and 24 show an increasing water yield in the watershed from 1990 to 2013 (Figure 5.7). Sub-basins 2, 7, 8, 10, 12, 19, and 23 indicate an increase in sediment yield over different land use maps from 1990 to 2013 (Figure 5.7). Evapotranspiration significantly impacted surface runoff in each sub-basin (i.e., higher evapotranspiration contributes to lower surface runoff and vice versa). Based on LULC change, the most significant change in hydrological components is an increase in surface runoff and sediment yield and a decrease in groundwater flow and evapotranspiration, which mainly occurred upstream of the watershed (Figure 5.7).

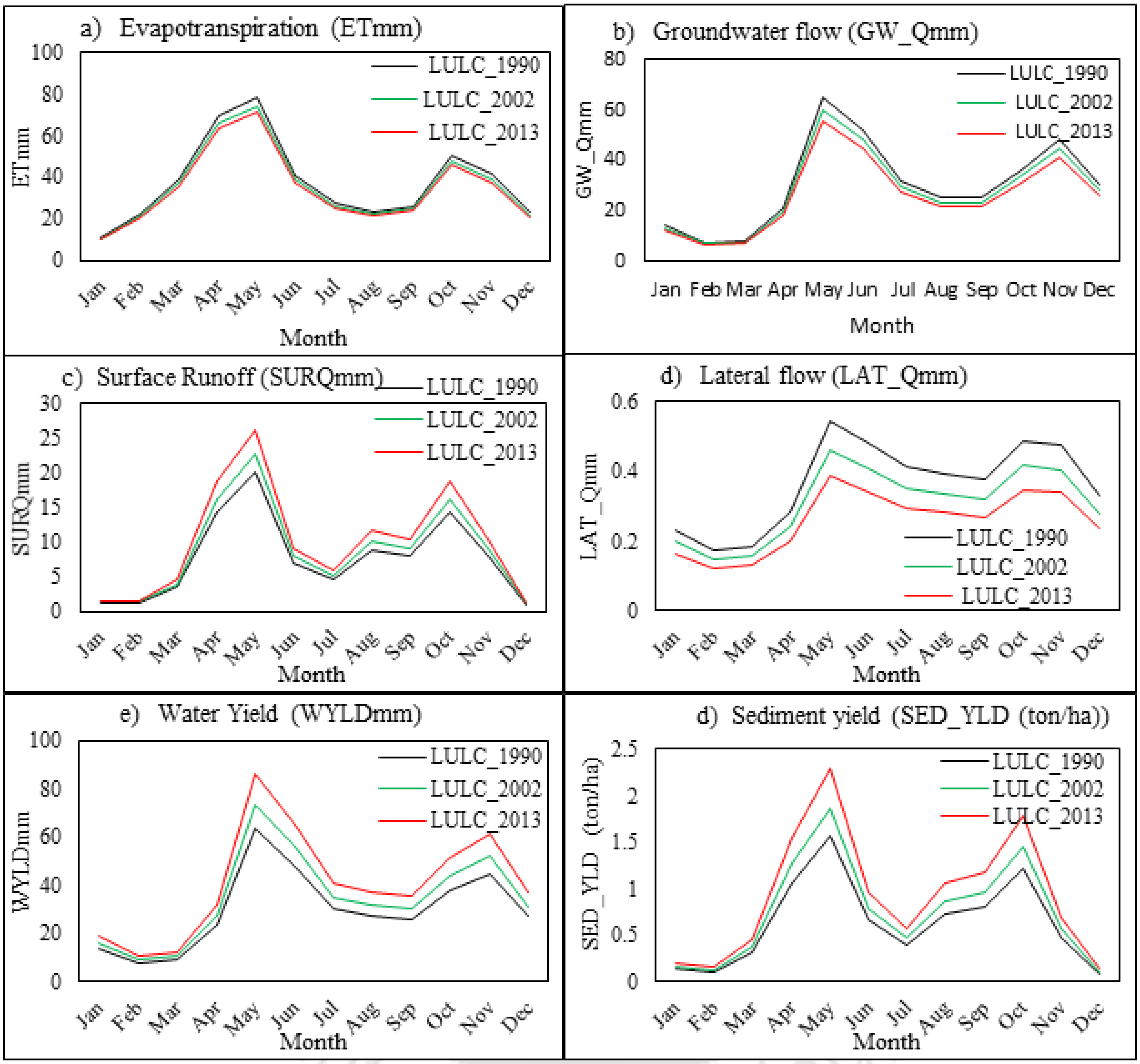

Figure 5. 8 Monthly average (1990–2013) hydrological components in the different LULC periods (1990, 2002, and 2013) of the Genale watershed

The monthly time extent of the model shows the ETmm losses, groundwater flow, & lateral flow are showing a decreasing trend while surface runoff, water yield, and sediment yields are increasing over LULC map 1990, 2002, and 2013 in the catchment (Figure 5.8). ETmm was a fundamental water availability determinant because it negatively impacts the generated surface runoff on the 1st and then led to water yield and sediment yield.

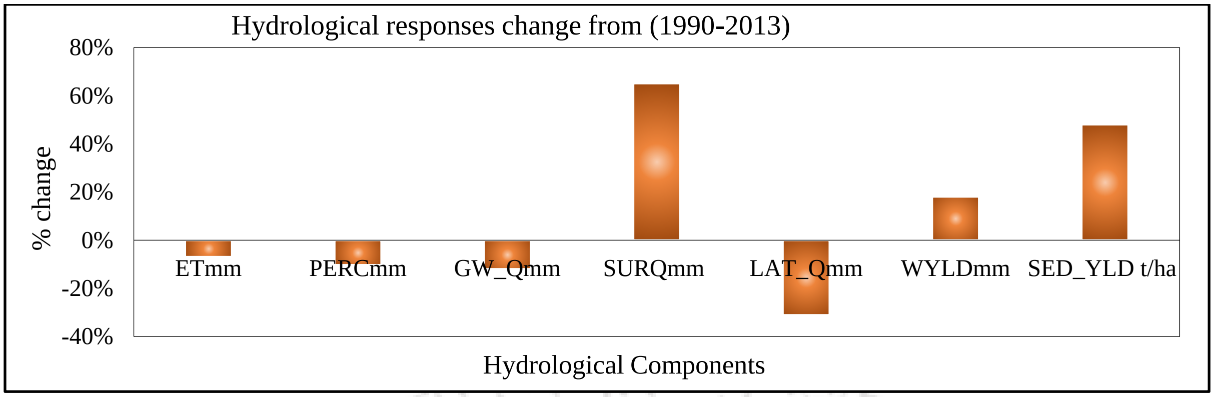

Figure 5. 9 Hydrological responses relative change under a different period of LULC map (1990 – 2013)

The annual mean catchment evaluates SURQ_mm, GW_mm, WYLDmm, LAT_Qmm, PERCmm, sediment yield, and ET with their relative changes at the watershed outlet under different LULC maps from 1990, 2002, and 2013. Therefore, it reduces infiltration rate due to the top layers of the soil being impervious, resulting in a consistent increase in surface runoff and sediment yield in the catchment (Figure 5.9). Comparing sub-basins scale (Figure 5.7) and at the watershed level as a whole (Figure 5.9), the impacts of LULC change induced on the responses of hydrological components greatly reflected at sub-basins scale because of the uneven spatial distribution of land cover modification. LULC change impacts were significant at a smaller scale whereas relatively small at the catchment scale due to compensating effects.

5.2.1.4 Impacts of individual LULC change induced on hydrological responses changes

Table 9 shows a correlation matrix of eight LULC classes and eight hydrological elements. The results exhibit that approximately all LULC classes have a fair correlation with various hydrological elements. Additionally, appropriate correlations among the hydrological components are also observed. For instance, agricultural land had a positive correlation with surface runoff (0.702), water yield (0.535), and sediment yield (0.348), while the correlation of agriculture with groundwater, lateral flow, percolation, and evapotranspiration is negative (Table 9). On the other hand, the correlation between surface runoff, water yield, and sediment yield is positive, but it is negative between surface runoff and groundwater, between surface runoff and lateral flow, water yield, and evapotranspiration (Table 9). Forest land shows a high correlation with surface runoff, lateral flow, water yield, evapotranspiration with correlation coefficients of -0.958, +0.759, -0.760, and +0.729 respectively. In contrast, Forest land shows a relatively low correlation with other hydrological elements (Table 5.6).

Table 5. 6 Correlation matrix for changes in LULC and hydrological responses between 1990 and 2013

Note: RNGB: range shrubs; AGRL: agriculture; FRST: forest; URBN: built up; PAST: pasture; BARR: barren land; WATR: water body; WET: wetlands; GW_Q: groundwater; SURQ: surface runoff; LAT_Q: lateral flow; PERC: percolation; WYLD: water yield; ET: evapotranspiration; SYLD: sediment yield.

Variables	RNGB	AGRL	FRST	URBN	PAST	BARR	WATR	WET	GW_Q	SURQ	LAT_Q	PERC	WYLD	ET	SYLD
RNGB	1.000	-0.764	0.847	-0.683	-0.781	0.705	-0.817	-0.633	0.533	-0.877	0.526	0.307	-0.797	0.876	-0.510
AGRL		1.000	-0.766	0.453	0.772	-0.968	0.761	0.814	-0.733	0.702	-0.620	-0.475	0.535	-0.499	0.348
FRST			1.000	-0.532	-0.601	0.785	-0.698	-0.624	0.497	-0.958	0.759	0.591	-0.760	0.729	-0.578
URBN				1.000	0.145	-0.259	0.199	0.723	-0.691	0.495	0.129	0.346	0.174	-0.867	-0.180
PAST					1.000	-0.804	0.950	0.383	-0.298	0.667	-0.697	-0.577	0.815	-0.425	0.688
BARR						1.000	-0.814	-0.704	0.614	-0.718	0.778	0.663	-0.608	0.374	-0.488
WATR							1.000	0.482	-0.407	0.697	-0.728	-0.571	0.808	-0.444	0.637
WET								1.000	-0.986	0.453	-0.193	0.004	0.130	-0.512	-0.171
GW_Q									1.000	-0.306	0.064	-0.126	0.007	0.416	0.312
SURQ										1.000	-0.766	-0.615	0.879	-0.793	0.726
LAT_Q											1.000	0.966	-0.807	0.223	-0.857
PERC												1.000	-0.697	0.015	-0.847
WYLD													1.000	-0.610	0.921
ET														1.000	-0.313
SYLD															1.000

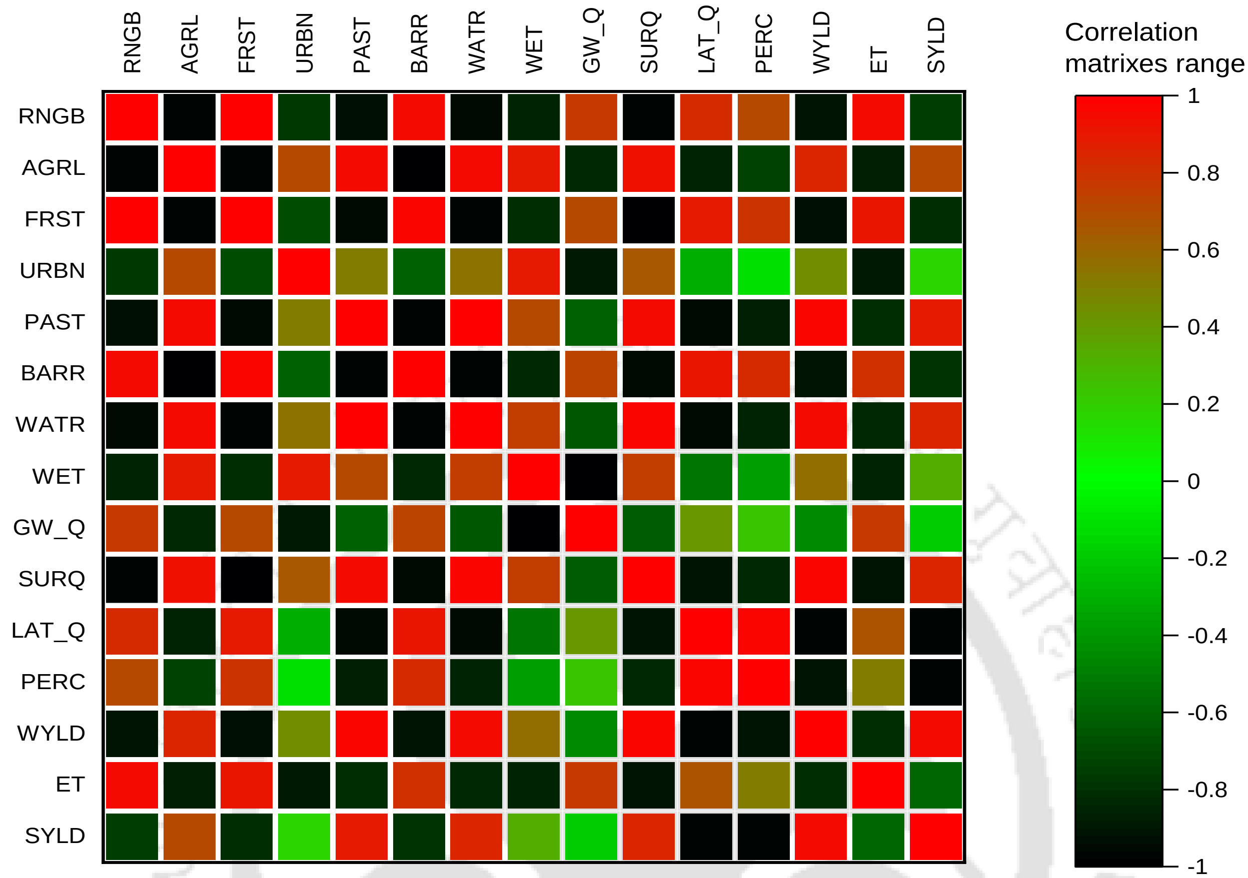

Figure 5. 10 Qualitative pictorial heat map showing correlation matrixes of LULC and hydrological components

Note: RNGB: range shrubs; AGRL: agriculture; FRST: forest; URBN: built up; PAST: pasture; BARR: barren land; WATR: water body; WET: wetlands; GW_Q: groundwater; SURQ: surface runoff; LAT_Q: lateral flow; PERC: percolation; WYLD: water yield; ET: evapotranspiration; SYLD: sediment yield.

The qualitative image of the correlation matrix (Figure 5.10) gives a descriptive/visual representation of the induced relationship between LULC types and hydrological elements. Heat map is qualitative way of data analysis by visualization to discuss which areas get the most attention, shows you in a visual way which can be easy to assimilate and make decisions from.

5.3 Conclusions

Remote sensing (RS) and Geographical information system (GIS) can be a powerful tool to convey good opportunities for integrated analysis of different year spatiotemporal data, image accuracy assessment, mapping, and evaluating LULC change detection process. The dynamic LULC change, notably settlement, forest, wetland, and agricultural areas, is further fancy for obtaining up-to-date information regarding newly constructed houses, cultivating, newly established industries, and commercial developments (human activities and modifications).

The utmost aim of this work was to determine the significant amount of LULC change that had been taking place in the given study area for different twelve years span of 1990 to 2002 and 2002 to 2013. This work simulates hydrological components change impacted in response to different year LULC change induced by anthropogenic activities. The LULC changed by increasing settlements, agriculture, water body by decreasing forest cover, and barren lands from 1990 to 2013. Based on an increase in agriculture, built-up, and pasture areas leads to a decline in a forest, barren land, and wet lands, the annual mean surface runoff demonstrated a continuously increasing trend, from 43.5 mm in 1990 to 57.85 mm in 2002, and to 75.5 mm in 2013. In contrast, groundwater, lateral flow, percolation, and ETmm showed declining trends. Notably, changes in hydrological elements were observed at the sub-basins scale, mainly associated with the uneven spatial distribution of LULC changes.

The statistical analysis is used for the correlation matrix of eight LULC classes and eight hydrological elements to evaluate impacts of individual LULC change induced on hydrological responses changes and shows good correlation.

This study has revealed that deforestation, agriculture, and settlement are the leading cause that should be controlled, and a system should be developed so that the government remains aware of every such human activity and can take necessary management measures accordingly. Therefore, continuous, site-specific, demand-driven, and integrated watershed conservation measures are required to arrest the catastrophic consequences of LULC change induced in the Genale watershed.

Chapter 6

Contribution, Findings and Novelty of the Research, Limitations, Conclusions and Recommendations

6.1 Contributions

The present research work endows the existing knowledge of the community service in relation to management of degraded sub-basins area.

The study has potential scientific merit in the context of evaluating spatiotemporal water availability for a better understanding of water resources status and supporting decision-makers in adopting a sustainable management strategy in the Genale Basin, Ethiopia. The research also has regional importance, as identification of sub-basins with high production of water and sediment yield is providing vital information to help water and sediment management under future climate change scenarios in the catchment and work towards this direction is not yet reported in the study area, i.e., Genale River Basin, Ethiopia. We believe the inclusion of projected prospective water yield under climate change scenarios will give a new dimension and will help the hydrologic community to identify the areas of water yield potential under different scenarios. Identification of critically degraded watershed area through HRU level study is providing a better opportunity to handle sediment management at optimal cost and with less effort with application of Ecological Managememt Practices(EMPs). Information about spatiotemporal variability of water and sediment yield at the sub-basin level will help judicious management of water and land resources through basin-level planning yet addressing the problem of the local community.

6.2 Findings and Novelty of the Research

Our effort was primarily towards identifying areas having high potential in water resources within the catchment and suggesting the local government authority for adequate water resources project investigation to solve the community problem related to water.

Understanding the effects of spatial heterogeneity on hydrologic parameters is essential to identify potential water yield in sub-basins and suggesting government and other agencies of water sectors to address community problems related to water and prioritize accordingly. Generally, the spatial distribution of water yields increases in areas of high precipitation.

The present study provides essential information to help decision-makers reduce sediment yield & peak discharge at an affordable cost and give feasible EMPs combinations for future soil and water conservation strategies in the Genale catchment, as the watershed is exposed to excessive degradadation/soil erosion due to high precipitation and runoff in the critical region.

Novelty of this study lies in applying HRUs level study in identifying most critical erosion prone area within a prioritized sub-basin to minimize the implementation cost of soil and water conservation practices. The study also has new insights in terms of providing a methodology to identify optimal combination of EMPs and evaluating their performances through SWAT model. These analyses serve as a powerful tool for the policy and decision-makers to formulate effective management measures for safeguarding vulnerable sub-basins/HRUs against the impacts of degradation/soil erosion at minimum cost.

Analysis at the sub-basins & HRUs scale response has given significant insight into the locations needing management practice within the catchment on a priority basis to take measures locally. Analysis till HRUs scale brings more clarity in the erosion aspects and helps narrowing down to the critical areas, and it becomes easier to address the challenges with low human resources, low cost, and within a short time where impacts were significant.

6.3 Limitations

Though a large basin size in a data survey provides reliable results, it is extremely time consuming, costly, less accurate, and difficult unless special support is given by the apprehensive sectors during data collection in the field. Therefore, limited sources and time constraints forced to limit the model output.

Data used in this study is up to 2013; therefore, data that are more recent can be used if actual field implementation is taken up. The present study can be further extended to include estimating other pollutants that may affect the water quality. With the increasing availability of satellite data of high spatiotemporal resolution, using up-to-date weather data range, more detailed study can be taken up to get an idea about delivery of other pollutants from the catchment to the stream system to address some emerging issues of environmental and ecological concerns.

These management practices could be applied to the basin, which has similar basin physiographic characteristics. One of the other limitations of this study is, difficulty in fixing constraints and space (area) availability) during cost optimization for EMPs implementation. There may be problem of access to private land. To take care of that aspect, the optimization model used in this study has the constraints of "land ownership" and thus this aspect can be addressed in the planning stage itself.

6.4 Conclusions and Recommendations

This research work was the first attempt to propose suitable watershed management in the area affected by progressively erosion. This study will help the regional governmental authority can prioritize projects to solve water-related problems of the community.

Based on the model results, sub-basins 6, 8, 12, 10, and 7 were identified as sediment-prone areas. Further investigation at the HRUs scale is taken up to understand critical erosion areas and minimize the cost of management practice, time & human resources. HRU analysis has revealed the immense scope of minimizing cost by concentrating management measures only in the critical HRUs. For example, Sub-basin-6 has 31 HRUs, of which only seven are assessed to have the high rates of sediment yield and thus prioritized as; HRU-159, HRU-160, HRU-161, HRU-168, HRU-170, and HRU-171, which are located on agricultural and arable lands of steep slopes. The impacts of individual LULC change on hydrological response show a good correlation matrix. The regional government needs to modify land development policies and sustainable plans for examining LULC change detection using satellite imagery to avoid illegal land expansion activities.

Considering the environmental and economic viewpoint, the total cost of EMPs (for five critical sub-basins), applied to reduce sediment yield, is 46.101 million USD or (1.844 billion Ethiopian birr). EMPs are environment friendly and cost-effective to reduce sediment yield.

If a landowner hesitate to go for terracing, this needs to be resolved beforehand by planning economically beneficial agricultural plan in the terraces and ensuring community participation in an organized way. Choosing economically attractive and socially acceptable EMPs through community participation is also an important key towards successful implementation of EMPs in the affected areas.

Our effort was primarily towards identifying areas having high potential in water resources within the catchment and suggesting the local government authority for adequate water resources project investigation to solve the community problem related to water. The quality of work could have been improved if the recent data had been available.

7. References

Abbaspour, K. C. (2011). User Manual for SWAT-CUP: SWAT Calibration and Uncertainty Analysis Programs. Eawag: Swiss Fed. Inst. of Aquat. Sci. and Technol., Duebendorf, Switzerland, 103.

Abbaspour, K. C., Vejdani, M., Haghighat, S., & Yang, J. (2007, December). SWAT-CUP calibration and uncertainty programs for SWAT. In MODSIM 2007, the international congress on modeling and simulation, modeling, and simulation society of Australia and New Zealand (pp. 1596-1602).

Abburu, S., & Golla, S. B. (2015). Satellite image classification methods and techniques: A review. International journal of computer applications, 119(8).

Abdelkareem, O. E. A., Elamin, H. M. A., Eltahir, M. E. S., Adam, H. E., Elhaja, M. E., Rahamtalla, A. M., ... & Elmar, C. (2017). Accuracy Assessment of Land Use Land Cover in Umabdalla Natural Reserved Forest, South Kordofan, Sudan. International Journal of Agricultural and Environmental Sciences, 3, 5-9.

Adam, P. H. E. (2011). Integration of remote sensing and GIS in studying vegetation trends and conditions in the gum Arabic belt in North Kordofan, Sudan.

Adeogun, A. G., Sule, B. F., & Salami, A. W. (2018). Cost-effectiveness of sediment management strategies for mitigation of sedimentation at Jebba Hydropower reservoir, Nigeria. Journal of King Saud University-Engineering Sciences, 30(2), 141-149.

Aish, A. M. (2014). Estimation of water balance components in the Gaza Strip with GIS-based WetSpass model. Civil Environ Res, 6(11), 77-85.

Al Islam, M., & Hasan, H. (2020). Generation of IDF Equation from Catchment Delineation Using GIS. Civil Engineering Journal, 6(3), 540-547.

Anaraki, M. V., Farzin, S., Mousavi, S. F., & Karami, H. (2021). Uncertainty analysis of climate change impacts on flood frequency by using hybrid machine learning methods. Water Resources Management, 35(1), 199-223.

Andualem, T. G., & Gebremariam, B. (2015). Impact of land use land cover change on streamflow and sediment yield: a case study of Gilgel Abay watershed, Lake Tana sub-basin, Ethiopia. Int. J. Technol. Enhanc. Merg. Eng. Res, 3, 28-42.

Arabi, M., Frankenberger, J. R., Engel, B. A., & Arnold, J. G. (2008). Representation of agricultural conservation practices with SWAT. Hydrological Processes: An International Journal, 22(16), 3042-3055.

Arabi, M., Govindaraju, R. S., & Hantush, M. M. (2006). Cost-effective allocation of watershed management practices using a genetic algorithm. Water Resources Research, 42(10).

Aragaw, H. M., Goel, M. K., & Mishra, S. K. (2021). Hydrological responses to human-induced land use/land cover changes in the Gidabo River basin, Ethiopia. Hydrological Sciences Journal, 66(4), 640-655.

Arai, F. K., Pereira, S. B., & Gonçalves, G. G. (2012). Characterization of water availability in a hydrographic basin. Engenharia Agrícola, 32(3), 591-601.

Arnold, J. G., Srinivasan, R., Muttiah, R. S., & Allen, P. M. (1999). Continental-scale simulation of the hydrologic balance 1. JAWRA Journal of the American Water Resources Association, 35(5), 1037-1051.

Arnold, J. G., Srinivasan, R., Muttiah, R. S., & Williams, J. R. (1998). Large area hydrologic modeling and assessment part I: model development 1. JAWRA Journal American Water Resources Association, 34(1), 73-89.

Ayele, M. A., & Gebremariam, B. (2020). Evaluation of Spatial and Temporal Variability of Sediment Yield on Bilate Watershed, Rift Valley Lake Basin, Ethiopia. Journal of Water Resources and Ocean Science, 9(1), 5-14.

Ayivi, F., & Jha, M. K. (2018). Estimation of water balance and water yield in the Reedy Fork-Buffalo Creek Watershed in North Carolina using SWAT. International Soil and Water Conservation Research, 6(3), 203-213.

Babaei, H., Nazari-Sharabian, M., Karakouzian, M., & Ahmad, S. (2019). Identification of critical source areas (CSAs) and evaluation of best management practices (BMPs) in controlling eutrophication in the Dez River Basin. Environments, 6(2), 20.

Bartholic, J. O. (2004). Predicting Sediment Delivery Ratio in Saginaw Bay watershed. Institute of Water Research, Michigan State University, East Lansing, MI.

Bharatkar, P. S., & Patel, R. (2013). Approach to accuracy assessment tor RS image classification techniques. International Journal of Scientific & Engineering Research, 4(12), 79-86.

Bhattarai, R., & Dutta, D. (2007). Estimation of soil erosion and sediment yield using GIS at the catchment scale. Water Resources Management, 21(10), 1635-1647.

Bieger, K., Hörmann, G., & Fohrer, N. (2015). Detailed spatial analysis of SWAT-simulated surface runoff and sediment yield in a mountainous watershed in China. Hydrological Sciences Journal, 60(5), 784-800.

Bonumá, N. B., Rossi, C. G., Arnold, J. G., Reichert, J. M., Minella, J. P., Allen, P. M., & Volk, M. (2014). Simulating landscape sediment transport capacity by using a modified SWAT model. Journal of Environmental Quality, 43(1), 55-66.

Boyce, R. C. (1975). Sediment routing with sediment delivery ratios. Present and prospective technology for predicting sediment yields and sources, 61-65.

Briak, H., Moussadek, R., Aboumaria, K., & Mrabet, R. (2016). Assessing sediment yield in Kalaya gauged watershed (Northern Morocco) using GIS and SWAT model. International Soil and Water Conservation Research, 4(3), 177-185.

Briak, H., Mrabet, R., Moussadek, R., & Aboumaria, K. (2019). Use of a calibrated SWAT model to evaluate the effects of agricultural BMPs on sediments of the Kalaya river basin (North of Morocco). International Soil and Water Conservation Research, 7(2), 176-183.

Campbell, J. B., & Wynne, R. H. (2011). Introduction to remote sensing. Guilford Press.

Chin, D. A. (2019). Estimating peak runoff rates using the rational method—Journal of Irrigation and Drainage Engineering, 145(6), 04019006.

Choto, M., & Fetene, A. (2019). Impacts of land use/land cover change on streamflow and sediment yield of Gojeb watershed, Omo-Gibe basin, Ethiopia. Remote Sensing Applications: Society and Environment, 14, 84-99.

Congalton, R. G., & Green, K. (2019). Assessing the accuracy of remotely sensed data: principles and practices. CRC press.

Coppin, P., Jonckheere, I., Nackaerts, K., Muys, B., & Lambin, E. (2004). Review article digital change detection methods in ecosystem monitoring: a review. International journal of remote sensing, 25(9), 1565-1596.

Cuttle, S. P., Macleod, C. J. A., Chadwick, D. R., Scholefield, D., Haygarth, P. M., Newell-Price, P., ... & Humphrey, R. (2007). An inventory of methods to control diffuse water pollution from agriculture (DWPA). User Manual (DEFRA Project ES0203), UK, 113p.

Daggupati, P., Douglas-Mankin, K. R., Sheshukov, A. Y., Barnes, P. L., & Devlin, D. L. (2011). Field-level targeting using SWAT: Mapping output from HRUs to fields and assessing limitations of GIS input data. Transactions of the ASABE, 54(2), 501-514.

Dibaba, W. T., Demissie, T. A., & Miegel, K. (2020). Watershed Hydrological Response to Combined Land Use/Land Cover and Climate Change in Highland Ethiopia: Finchaa Catchment. Water, 12(6), 1801.

Dolowitz, D. P., Bell, S., & Keeley, M. (2018). Retrofitting urban drainage infrastructure: green or grey? Urban Water Journal, 15(1), 83-91.

Dong, F., Liu, Y., Wu, Z., Chen, Y., & Guo, H. (2018). Identification of watershed priority management areas under water quality constraints: A simulation-optimization approach with ideal load reduction. Journal of Hydrology, 562, 577-588.

Duraes, M. F., de Mello, C. R., & Beskow, S. (2016). Sediment yield in Paraopeba River Basin–MG, Brazil. International Journal of River Basin Management, 14(4), 367-377.

Duru, U., Arabi, M., & Wohl, E. E. (2018). Modeling streamflow and sediment yield using the SWAT model: a case study of Ankara River basin, Turkey. Physical Geography, 39(3), 264-289.

Duru, U., Arabi, M., & Wohl, E. E. (2018). Modeling streamflow and sediment yield using the SWAT model: a case study of Ankara River basin, Turkey. Physical Geography, 39(3), 264-289.

El Harraki, W., Ouazar, D., Bouziane, A., El Harraki, I., & Hasnaoui, D. (2021). Streamflow Prediction Upstream of a Dam Using SWAT and Assessment of the Impact of Land Use Spatial Resolution on Model Performance. Environmental Processes, 1-22.

Elimy, E. A., Hassan, A. A., Omar, M. A., Nasser, G. A. E., & Riad, P. H. (2020). Land Use/Land Cover Change Detection Analysis for Eastern Nile Delta Fringes, Egypt.

Epelde, A. M., Cerro, I., Sánchez-Pérez, J. M., Sauvage, S., Srinivasan, R., & Antigüedad, I. (2015). Application of the SWAT model to assess the impact of changes in agricultural management practices on water quality. Hydrological Sciences Journal, 60(5), 825-843.

Erasu, D. (2017). Remote sensing-based urban land use/land cover change detection and monitoring. Journal of Remote Sensing & GIS, 6(2), 5.

Esam, I., Abdalla, F., & Erich, N. (2012). Land use and land cover changes of west tahta region, sohag governorate, Upper Egypt.

Farzin, S., & Valikhan Anaraki, M. (2021). Modeling and predicting suspended sediment load under climate change conditions: a new hybridization strategy. Journal of Water and Climate Change, 12(6), 2422-2443.

Frenken, K. (Ed.). (2005). Irrigation in Africa in figures: AQUASTAT Survey, 2005 (Vol. 29). Food & Agriculture Org…

Ganiyu, H. O., Adeogun, A. G., & Ahmed, I. A. (2019). Original Research Article Assessment of Water Resources Availability and Demand in Malete Watershed, North-Central Nigeria.

Gao, P., Li, P., Zhao, B., Xu, R., Zhao, G., Sun, W., & Mu, X. (2017). Use of double mass curves in hydrologic benefit evaluations. Hydrological Processes, 31(26), 4639-4646.

Gashaw, T., Tulu, T., Argaw, M., & Worqlul, A. W. (2018). Modeling the hydrological impacts of land use/land cover changes in the Andassa watershed, Blue Nile Basin, Ethiopia. Science of the Total Environment, 619, 1394-1408.

Gebru, T. A., & Tesfahunegn, G. B. (2020). GIS-based water balance components estimation in northern Ethiopia catchment. Soil and Tillage Research, 197, 104514.

Gelagay, H. S. (2016). RUSLE and SDR model-based sediment yield assessment in a GIS and remote sensing environment; a case study of Koga watershed, Upper Blue Nile Basin, Ethiopia. Hydrology: Current Research, 7, 239.

Gelagay, H. S., & Minale, A. S. (2016). Soil loss estimation using GIS and Remote sensing techniques: A case of Koga watershed, Northwestern Ethiopia. International Soil and Water Conservation Research, 4(2), 126-136.

Gizaw, D., & Kebede, M. (2019). Spatial and Temporal Distribution of Sediment Yield-Case Study Nashe, Blue Nile Basin, Ethiopia. Journal of Water Sustainability, 9(2), 23-34.

Green, W. H. (1911). Ampt. GA: Studies on soil physics. 1. Flow of air and water through soils. J. Agr. Sci, 4, 1-24.

Guse, B., Pfannerstill, M., & Fohrer, N. (2015). Dynamic modelling of land use change impacts on nitrate loads in rivers. Environmental Processes, 2(4), 575-592.

Gwenzi, W., & Nyamadzawo, G. (2014). Hydrological impacts of urbanization and urban roof water harvesting in water-limited catchments: a review. Environmental Processes, 1(4), 573-593.

Harris, A., Carr, A. S., & Dash, J. (2014). Remote sensing of vegetation cover dynamics and resilience across southern Africa. International Journal of Applied Earth Observation and Geoinformation, 28, 131-139. https://doi.org/10.1016/j.jag.2013.11.014

Healy, M., Newe, T., & Lewis, E. (2007). Efficiently securing data on a wireless sensor network. In Journal of Physics: Conference Series (Vol. 76, No. 1, p. 012063). IOP Publishing.

Huang, T. C., & Lo, K. F. A. (2015). Effects of land-use change on sediment and water yields in Yang Ming Shan National Park, Taiwan. Environments, 2(1), 32-42.

Hunink, J. E., Niadas, I. A., Antonaropoulos, P., Droogers, P., & De Vente, J. (2013). Targeting of intervention areas to reduce reservoir sedimentation in the Tana catchment (Kenya) using SWAT. Hydrological Sciences Journal, 58(3), 600-614.

Hussain, S., Mubeen, M., Ahmad, A., Akram, W., Hammad, H. M., Ali, M., ... & Nasim, W. (2019). Using GIS tools to detect the land use/land cover changes during forty years in Lodhran district of Pakistan. Environmental Science and Pollution Research, 1-17.

Intergovernmental Panel on Climate Change (2014). Climate change: Impacts, adaptation, and vulnerability. Part B: Regional aspects. In Contribution of Working Group II to the Fifth Assessment Report of the Intergovernmental Panel on Climate Change. Cambridge, United Kingdom and New York, NY, USA:and New York, NY, USA:

Jain, C. K., & Ram, D. (1997). Adsorption of lead and zinc on bed sediments of the river Kali. Water Research, 31(1), 154-162.

Jain, M. K., & Das, D. (2010). Estimation of sediment yield and areas of soil erosion and deposition for watershed prioritization using GIS and remote sensing. Water Resources Management, 24(10), 2091-2112

Jia, H., Ma, H., & Wei, M. (2011). Calculation of the minimum ecological water requirement of an urban river system and its deployment: A case study in Beijing central region. Ecological modeling, 222(17), 3271-3276.

Kaya, İ. A., & Görgün, E. K. (2020). Land use and land cover change monitoring in Bandırma (Turkey) using remote sensing and geographic information systems. Environmental Monitoring and Assessment, 192(7), 1-18.

Kefi, M., & Yoshino, K. (2011). Combination Approach to Assess Offsite Value of Soil Erosion Risk in Watersheds in Tunisia. Journal of International Environmental Application and Science, 6(4), 521.

Kirby, J. T., & Durrans, S. R. (2007). PnET-II3SL/SWAT: Modeling the combined effects of forests and agriculture on water availability. Journal of Hydrologic Engineering, 12(3), 319-326.

Kirpich, Z. P. (1940). Time of concentration of small agricultural watersheds. Civil engineering, 10(6), 362.

Kumar, N., Singh, S. K., Srivastava, P. K., & Narsimlu, B. (2017). SWAT Model calibration and uncertainty analysis for streamflow prediction of the Tons River Basin, India, using Sequential Uncertainty Fitting (SUFI-2) algorithm. Modeling Earth Systems and Environment, 3(1), 30.

Kumar, S., Mishra, A., & Raghuwanshi, N. S. (2015). Identification of critical erosion watersheds for control management in data-scarce conditions using the SWAT model. Journal of Hydrologic Engineering, 20(6), C4014008.

Li, R. M., Simons, D. B., & Stevens, M. A. (1976). Morphology of cobble streams in small watersheds. Journal of the Hydraulics Division, 102(8), 1101-1117.

Li, Y., & DeLiberty, T. (2020). Assessment of urban streamflow in historical wet and dry years using SWAT across Northwestern delaware. Environmental Processes, 7(2), 597-614.

Liu, Y., Wang, R., Guo, T., Engel, B. A., Flanagan, D. C., Lee, J. G., ... & Wallace, C. W. (2019). Evaluating efficiencies and cost-effectiveness of best management practices in improving agricultural water quality using integrated SWAT and cost evaluation tool. Journal of Hydrology, 577, 123965.

Lohani, A. K., Goel, N. K., & Bhatia, K. K. S. (2014). Improving real-time flood forecasting using a fuzzy inference system. Journal of Hydrology, 509, 25-41.

Loi, N. K., & Liem, N. D. (2012). Assessing Water discharge in Be River Basin, Vietnam using the SWAT model. In International SWAT Conference Proceedings (Vol. 414).

López-Ballesteros, A., Senent-Aparicio, J., Srinivasan, R., & Pérez-Sánchez, J. (2019). Assessing the Impact of Best Management Practices in a Highly Anthropogenic and Ungauged Watershed Using the SWAT Model: A Case Study in the El Beal Watershed (Southeast Spain). Agronomy, 9(10), 576.

Lu, H., Moran, C. J., & Prosser, I. P. (2006). Modelling sediment delivery ratio over the Murray Darling Basin. Environmental Modelling & Software, 21(9), 1297-1308.

Ma, D., Xu, Y. P., Xuan, W., Gu, H., Sun, Z., & Bai, Z. (2020). Do model parameters change under changing climate and land use upstream of the Lancang River Basin, China? Hydrological Sciences Journal, 65(11), 1894-1908.

Mahoney, D. T., Fox, J. F., & Al Aamery, N. (2018). Watershed erosion modeling using the probability of sediment connectivity in a gently rolling system. Journal of Hydrology, 561, 862-883.

Manjunatha, M. C., & Basavarajappa, H. T (2020). Mapping of Land units & its Change Detection Analysis in Chitradurga taluk of Karnataka State, India, using Geospatial Technology. International Advanced Research Journal in Science, Engineering & Technology, 7(7), 61-68.

Markhi, A., Laftouhi, N., Grusson, Y., & Soulaimani, A. (2019). Assessment of potential soil erosion and sediment yield in the semi-arid N′ basin (High Atlas, Morocco) using the SWAT model. Acta Geophysica, 67(1),263-272.

Mati, B. M. (2012). Soil and Water Conservation Structures for Smallholder Agriculture. Training Manual, 5, 60.

Meshram, S. G., Safari, M. J. S., Khosravi, K., & Meshram, C. (2020). Iterative classifier optimizer-based pace regression and random forest hybrid models for suspended sediment load prediction. Environmental Science and Pollution Research, 1-13.

Mohammadi, B., Guan, Y., Moazenzadeh, R., & Safari, M. J. S. (2021). Implementation of hybrid particle swarm optimization-differential evolution algorithms coupled with multi-layer perceptron for suspended sediment load estimation. Catena, 198, 105024.

Momm, H. G., Bingner, R. L., Emilaire, R., Garbrecht, J., Wells, R. R., & Kuhnle, R. A. (2017). Automated watershed subdivision for simulations using multi-objective optimization. Hydrological Sciences Journal, 62(10), 1564-1582.

Moriasi, D. N., Arnold, J. G., Van Liew, M. W., Bingner, R. L., Harmel, R. D., & Veith, T. L. (2007). Model evaluation guidelines for systematic quantification of accuracy in watershed simulations. Transactions of the ASABE, 50(3), 885-900.

Moss, B. (2008). Water pollution by agriculture. Philosophical Transactions of the Royal Society B: Biological Sciences, 363(1491), 659-666.

Mtibaa, S., Hotta, N., & Irie, M. (2018). Analysis of the efficacy and cost-effectiveness of best management practices for controlling sediment yield: a case study of the Joumine watershed, Tunisia. Science of the Total Environment, 616, 1-16.

Muleta, M. K., Nicklow, J. W., & Bekele, E. G. (2007). Sensitivity of a distributed watershed simulation model to spatial scale. Journal of Hydrologic Engineering, 12(2), 163-172.

Mutua, B. M., & Klik, A. (2006). Estimating spatial sediment delivery ratio on a large rural catchment. Journal of Spatial Hydrology, Vol.6, No.1

Namomsa, D. G., & Adugna, T. (2019). Swat Based Soil Erosion Modeling of Nashe, Blue Nile Basin, Ethiopia. Journal of Civil, Construction and Environmental Engineering, 4(1), 35.

Navin, M. S., & Agilandeeswari, L. (2019). Land use land cover change detection using k-means clustering and maximum likelihood classification method in the javadi hills, Tamil Nadu, India. International Journal of Engineering and Advanced Technology (IJEAT).

Ndhlovu, G. Z., & Woyessa, Y. E. (2020). Modeling impact of climate change on catchment water balance, Kabompo River in Zambezi River Basin. Journal of Hydrology: Regional Studies, 27, 100650.

N'Dri, W. K. C., Séverin, P., Jourda, J. P., & Kouamé, K. J. (2019). Application of SWAT to Estimate Water Balance in the Aghien Lagoon Basin, South-East of Côte d'Ivoire. International Journal of Science and Research, 8(10).

Neitsch, S. L., Arnold, J. G., Kiniry, J. R., & Williams, J. R. (2011). Soil and water assessment tool theoretical documentation version 2009. Texas Water Resources Institute.

Neitsch, S. L., Arnold, J. G., Kiniry, J. R., Williams, J. R., & King, K. W. (2005). Soil and water assessment tool theoretical documentation, version 2005. Temple, Tex.: USDA-ARS Grassland. Soil and Water Research Laboratory, 8.

Nilawar, A. P., & Waikar, M. L. (2019). Impacts of climate change on streamflow and sediment concentration under RCP 4.5 and 8.5: A case study in Purna river basin, India. Science of the total environment, 650, 2685-2696.

Noori, H., Karami, H., Farzin, S., Siadatmousavi, S. M., Mojaradi, B., & Kisi, O. (2018). Investigation of RS and GIS techniques on MPSIAC model to estimate soil erosion. Natural Hazards, 91(1), 221-238.

Otim, D., Smithers, J., Senzanje, A., & van Antwerpen, R. (2019). Design norms for soil and water conservation structures in the sugar industry of South Africa. Water SA, 45(1), 29-40.

Ouallali, A., Briak, H., Aassoumi, H., Beroho, M., Bouhsane, N., & Moukhchane, M. (2020). Hydrological foretelling uncertainty evaluation of water balance components and sediments yield using a multi-variable optimization approach in an external Rif's catchment. Morocco. Alexandria Engineering Journal, 59(2), 775-789.

Owolabi, S. T., Madi, K., & Kalumba, A. M. (2021). Comparative evaluation of spatio-temporal attributes of precipitation and streamflow in Buffalo and Tyume Catchments, Eastern Cape, South Africa. Environment, Development and Sustainability, 23, 4236-4251.

Park, Y. S., Kim, J., Kim, N. W., Kim, S. J., Jeon, J. H., Engel, B. A., ... & Lim, K. J. (2010). Development of new R, C and SDR modules for the SATEEC GIS system. Computers & Geosciences, 36(6), 726-734.

Pathak, S., Ojha, C. S. P., Shukla, A. K., & Garg, R. D. (2019). Assessment of Annual Water-Balance Models for Diverse Indian Watersheds. Journal of Sustainable Water in the Built Environment, 5(3), 04019002.

Patowary, S., Sarma, B., & Sarma, A. K. (2019). A Revision of OPTEMP-LS Model for Selecting Optimal EMP Combination for Minimizing Sediment and Water Yield from Hilly Urban Watersheds. Water Resources Management, 33(4), 1249-1264.

Pettorelli, N., Chauvenet, A. L., Duffy, J. P., Cornforth, W. A., Meillere, A., & Baillie, J. E. (2012). Tracking the effect of climate change on ecosystem functioning using protected areas: Africa as a case study. Ecological Indicators, 20, 269-276.

Pimentel, D., & Burgess, M. (2013). Soil erosion threatens food production. Agriculture, 3(3), 443-463.

Poesen, J. W., van Wesemael, B., Bunte, K., & Benet, A. S. (1998). Variation of rock fragment cover and size along semiarid hillslopes: a case-study from southeast Spain. Geomorphology, 23(2-4), 323-335.

Rahman, M. T. U., Tabassum, F., Rasheduzzaman, M., Saba, H., Sarkar, L., Ferdous, J., ... & Islam, A. Z. (2017). Temporal dynamics of land use/land cover change and its prediction using CA-ANN model for southwestern coastal Bangladesh. Environmental monitoring and assessment, 189(11), 1-18. https://doi.org/10.1007/s10661-017-6272-0

Rwanga, S. S., & Ndambuki, J. M. (2017). Accuracy assessment of land use/land cover classification using remote sensing and GIS. International Journal of Geosciences, 8(04), 611.

Rwanga, S. S., & Ndambuki, J. M. (2017). Approach to quantify groundwater recharge using gis based water balance model: a review. Int J Adv Agric Environ Eng (IJAAEE), 4, 1

Samimi, M., Mirchi, A., Moriasi, D., Ahn, S., Alian, S., Taghvaeian, S., & Sheng, Z. (2020). Modeling Arid/Semi-arid Irrigated Agricultural Watersheds with SWAT: Applications, Challenges, and Solution Strategies. Journal of Hydrology, 125418.

Sansare, D. A., & Mhaske, S. Y. (2020, June). Land-use change mapping and its impact on stormwater runoff using Remote sensing and GIS: a case study of Mumbai, India. In IOP Conference Series: Earth and Environmental Science (Vol. 500, No. 1, p. 012082). IOP Publishing.

Sarma, B., Sarma, A. K., Mahanta, C., & Singh, V. P. (2015). Optimal ecological management practices of controlling sediment yield and peak discharge from hilly urban areas. Journal of Hydrologic Engineering, 20(10), 04015005.

Setegn, S. G., Dargahi, B., Srinivasan, R., & Melesse, A. M. (2010). Modeling of Sediment Yield From Anjeni-Gauged Watershed, Ethiopia Using SWAT Model 1. JAWRA Journal of the American Water Resources Association, 46(3), 514-526.

Shawul, A. A., Chakma, S., & Melesse, A. M. (2019). The response of water balance components to land cover change based on hydrologic modeling and partial least squares regression (PLSR) analysis in the Upper Awash Basin. Journal of Hydrology: Regional Studies, 26, 100640.

Singh, A., Sarma, A. K., & Hack, J. (2020). Cost-Effective Optimization of Nature-Based Solutions for Reducing Urban Floods Considering Limited Space Availability. Environmental Processes, 7(1), 297-319.

Singh, R. K., Panda, R. K., Satapathy, K. K., & Ngachan, S. V. (2012). Runoff and sediment yield modelling for a treated hilly watershed in Eastern Himalaya using the water erosion prediction project model. Water resources management, 26(3), 643-665.

Song, X. P., Hansen, M. C., Stehman, S. V., Potapov, P. V., Tyukavina, A., Vermote, E. F., & Townshend, J. R. (2018). Author Correction: Global land change from 1982 to 2016: nature, 563(7732), E26-E26.

Strauch, M., Lima, J. E., Volk, M., Lorz, C., & Makeschin, F. (2013). The impact of Best Management Practices for simulated streamflow and sediment load in a Central Brazilian catchment. Journal of environmental management, 127, S24-S36.

Tadesse, W., Whitaker, S., Crosson, W., & Wilson, C. (2015). Assessing the impact of land-use land-cover change on stream water and sediment yields at a watershed level using SWAT—Open Journal of Modern Hydrology, 5(03), 68.

Thrasher, B., & Nemani, R. (2015). Nasa earth exchange global daily downscaled projections (nex-gddp). Van Vuuren DP, Edmonds J, Kainuma M, Riahi K, Thomson A, Hibbard K, Hurtt GC, Kram T, Krey V, Lamarque JF, et al. (2011): The representative concentration pathways: an overview. Climatic Change, 109(5).

Tomar, S., Saha, A., Kumari, M., & Somvanshi, S. (2017). Land use and land cover change monitoring of Surajpur Wetland, Uttar Pradesh: using GIS and remote sensing techniques. In 17th Esri India User Conference 2017 (pp. 19-20).

Touseef, M., Chen, L., Masud, T., Khan, A., Yang, K., Shahzad, A., ... & Wang, Y. (2020). Assessment of the Future Climate Change Projections on Streamflow Hydrology and Water Availability over Upper Xijiang River Basin, China. Applied Sciences, 10(11), 3671.

Tram, V. N. Q., Liem, N. D., & Loi, N. K. (2014). Assessing water availability in the Poko catchment using the SWAT model. Khon Kaen Agric. J, 42(2).

Treitz, P., & Rogan, J. (2004). Remote sensing for mapping and monitoring land-cover and land-use change-an an introduction. Progress in planning, 61(4), 269-279.

Tuppad, P., Kannan, N., Srinivasan, R., Rossi, C. G., & Arnold, J. G. (2010). Simulation of agricultural management alternatives for watershed protection. Water Resources Management, 24(12), 3115-3144.

U.S Department of Agriculture-Soil Conservation Service [USDA-SCS], United States Department of Agriculture – Soil Conservation Service. National Engineering Handbook, Sec. 4. Hydrology, 1979.

Ulke, A., Tayfur, G., & Ozkul, S. (2009). Predicting suspended sediment loads and missing data for Gediz River, Turkey. Journal of Hydrologic Engineering, 14(9), 954-965.

Uniyal, B., Jha, M. K., Verma, A. K., & Anebagilu, P. K. (2020). Identification of critical areas and evaluation of best management practices using SWAT for sustainable watershed management. Science of The Total Environment, 140737.

USDA-SCS (1979) United States Department of Agriculture-Soil Conservation Service. National Engineering Handbook, Sec 4. Hydrology

Van Griensven, A., & Meixner, T. (2006). Methods to quantify and identify the sources of uncertainty for river basin water quality models. Water Science and Technology, 53(1), 51-59.

Van Rompaey, A. J., Govers, G., & Puttemans, C. (2002). Modelling land use changes and their impact on soil erosion and sediment supply to rivers. Earth surface processes and landforms, 27(5), 481-494.

Vanoni, V. A. (1975). Sedimentation Engineering, Manuals Rep.Eng. Pract.,vol. 54. Am.Soc.of Civ.Eng., Reston, Va.

Vijith, H., & Dodge-Wan, D. (2020). Spatial and temporal characteristics of soil erosion and identification of source contributors of sediments in the tropical rainforest region of Borneo. Hydrological Sciences Journal, 65(16), 2797-2815.

Walling, D. E. (1983). The sediment delivery problem. Journal of hydrology, 65(1-3), 209-237.

Wang, L. L., Yao, W. Y., Tang, J. L., Wang, W. L., & Hou, X. X. (2018). Identifying the driving factors of sediment delivery ratio on individual flood events in a long-term monitoring headwater basin. Journal of Mountain Science, 15(8), 1825-1835.

Wang, Y., Bian, J., Lao, W., Zhao, Y., Hou, Z., & Sun, X. (2019). Assessing the impacts of best management practices on non-point source pollution considering cost-effectiveness in the source area of the Liao River, China. Water, 11(6), 1241.

Wei, X., Bailey, R. T., & Tasdighi, A. (2018). Using the SWAT model in intensively managed irrigated watersheds: model modification and application. Journal of Hydrologic Engineering, 23(10), 04018044.

Willams, J. R. (1975). Sediment-yield prediction with a universal equation using runoff energy factor. Present and prospective technology for predicting sediment yields and sources.

Winchell, M. F., Folle, S., Meals, D., Moore, J., Srinivasan, R., & Howe, E. A. (2015). Using SWAT for sub-field identification of phosphorus critical source areas in a saturation excess runoff region. Hydrological Sciences Journal, 60(5), 844-862.

Wischmeier, W. H., & Smith, D. D. (1978). Predicting rainfall erosion losses: a guide to conservation planning (No. 537). Department of Agriculture, Science, and Education Administration.

World Digital Soil Map (http://www.fao.org/geonetwork/srv/en/metadata) at the scale 1/5000000 for 2007 and (http://earthexplorer.usgs.gov/) SRTM (Shuttle Radar Topography Mission); Coordinated Regional Climate Downscaling Experiment (CORDEX) for Ethiopia was downloaded from (https://dataservices.gfzpotsdam.de/pik/showshort.php?id=escidoc:3124935); https://swat.tamu. edu/software/cmhyd/.

Woznicki, S. A., & Nejadhashemi, A. P. (2013). Spatial and temporal variabilities of sediment delivery ratio. Water resources management, 27(7), 2483-2499.

Wu, L., Yao, W., & Ma, X. (2018). Using the comprehensive governance degree to calibrate a piecewise sediment delivery ratio algorithm for dynamic sediment predictions: A case study in an ecological restoration watershed of northwest China. Journal of Hydrology, 564, 888-899.

Xu, Z. X., Pang, J. P., Liu, C. M., & Li, J. Y. (2009). Assessment of runoff and sediment yield in the Miyun Reservoir catchment by using SWAT model. Hydrological Processes: An International Journal, 23(25), 3619-3630.

Yuhai, W. X. B. (1999). Study on the methods of land uses dynamic change research [J]. Progress in geography, 1.

Zarris, D., Vlastara, M., & Panagoulia, D. (2011). Sediment delivery assessment for a transboundary Mediterranean catchment: The example of Nestos River catchment. Water Resources Management, 25(14), 3785-3803.

Zhou, Y., Xu, Y. J., Xiao, W., Wang, J., Huang, Y., & Yang, H. (2017). Climate change impacts on flow and suspended sediment yield in headwaters of high-latitude regions—A case study in China's far northeast. Water, 9(12), 966.

8. List of publications

- ✓ Negewo, T. F., & Sarma, A. K. (2021). Estimation of Water Yield under Baseline and Future Climate Change Scenarios in Genale Watershed, Genale Dawa River Basin, Ethiopia, Using SWAT Model. Journal of Hydrologic Engineering, 26(3), 05020051. DOI. (10.1061/(ASCE)HE.1943-5584.0002047).

- ✓ Negewo, T. F., & Sarma, A. K. (2021). Spatial and temporal variability evaluation of sediment yield and sub-basins/hydrologic response units prioritization on Genale Basin, Ethiopia. Journal of Hydrology, 603, 127190. DOI: https://doi.org/10.1016/j.jhydrol.2021.127190

- ✓ Negewo, T. F., & Sarma, A. K. (2021). Evaluation of Climate Change-Induced Impact on Streamflow and Sediment Yield of Genale Watershed, Ethiopia; "Global Warming and Climate Change" (ISBN 978-1-83968-612-2), (DOI: http://dx.doi.org/10.5772/intechopen.98515)

- ✓ Negewo, T. F., & Sarma, A. K. (In press). "Sustainable and Cost-Effective Management of Degradable Sub-Watersheds Using Nature-Based Ecological Management Practices (EMPs) for Genale River Basin, Ethiopia," Journal of Hydrologic Engineering-ASCE- ID.Ref.: Ms. No. HEENG-5722 (Under Review)

- ✓ Negewo, T. F., & Sarma, A. K. (In press). " Anthropogenic Land Use/Cover Change Detection Impacts on Hydrological Responses of Genale Catchment, Ethiopia," Hydrological Processes Journal - Manuscript ID: HYP-21-0928-Wiley (Under Review)

- ✓ Negewo, T. F., & Sarma, A. K. (In press). Assessment of Water Balance Components in the Genale River Basin, Ethiopia Using SWAT Model. HYDRO 2020; International Conference On "Hydraulics, Water Resources, and Coastal Engineering" (26-28 March, 2021). (Presented).